

63-3-4

403697

ASD-TDR-62-792  
VOL I

403 697

**AN EXPERIMENTAL INVESTIGATION OF THE  
SURFACE PRESSURE AND THE LAMINAR BOUNDARY  
LAYER ON A BLUNT FLAT PLATE IN HYPERSONIC FLOW**

**Vol I. Surface Pressure Distributions  
on a Blunted Flat Plate**

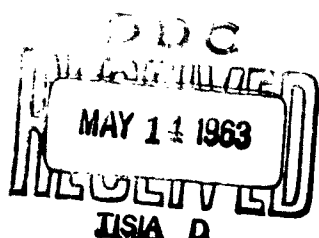
CATALOGED BY ASTIA  
AS AD 10.

TECHNICAL DOCUMENTARY REPORT NO. ASD-TDR-62-792, VOLUME I

March 1963

Flight Dynamics Laboratory  
Aeronautical Systems Division  
Air Force Systems Command  
Wright-Patterson Air Force Base, Ohio

Project No. 1366, Task No. 136606



(Prepared under Contract No. AF 33(616)-7827 by  
The Ohio State University, Columbus, Ohio;  
G. M. Gregorek, T. C. Nark, J. D. Lee, authors)

## **NOTICES**

**When Government drawings, specifications, or other data are used for any purpose other than in connection with a definitely related Government procurement operation, the United States Government thereby incurs no responsibility nor any obligation whatsoever; and the fact that the Government may have formulated, furnished, or in any way supplied the said drawings, specifications, or other data, is not to be regarded by implication or otherwise as in any manner licensing the holder or any other person or corporation, or conveying any rights or permission to manufacture, use, or sell any patented invention that may in any way be related thereto.**

**Qualified requesters may obtain copies of this report from the Armed Services Technical Information Agency, (ASTIA), Arlington Hall Station, Arlington 12, Virginia.**

**This report has been released to the Office of Technical Services, U.S. Department of Commerce, Washington 25, D.C., in stock quantities for sale to the general public.**

**Copies of this report should not be returned to the Aeronautical Systems Division unless return is required by security considerations, contractual obligations, or notice on a specific document.**

## FOREWORD

This report was prepared by the Aerodynamic Laboratory of the Ohio State University, Columbus, Ohio on Air Force Contract AF 33(616)-7827 under Task 136606 "Hypersonic Boundary Layer Properties" on Project No. 1366 "Aerodynamics and Flight Mechanics". This Task and Project are a part of Air Force System Command's Applied Research Program, 750A, "Mechanics of Flight". The work was administered under the direction of Flight Dynamics Laboratory, Aeronautical Systems Division. Mr. M. L. Buck and Captain H. Grubbs were project engineers for the Laboratory.

The study was initiated in January, 1961, and was completed in August, 1962. The final report is in two volumes: Volume I presents the surface pressure distributions on a blunted flat plate; Volume II presents the laminar boundary layer profiles on the flat plate.

This report concludes the work done by the Aerodynamic Laboratory on Contract AF 33(616)-7827.

## ABSTRACT

Pressures were measured over the surface of an unswept blunt flat plate having a cylindrical leading edge 1/2-inch in diameter under the following conditions:

M = 7	$7500 \leq Re_D \leq 20,600$	Angles-of-attack $15^\circ \leq \alpha \leq -15^\circ$
M = 10	$8300 \leq Re_D \leq 15,000$	
M = 12	$9000 \leq Re_D \leq 21,300$	
M = 14	$12700 \leq Re_D \leq 16,000$	

The flat plate was side-mounted in the ALOSU 12-inch continuous hypersonic wind tunnel. Separate tests were conducted with cylinders in order to obtain detailed data for the leading-edge. Stagnation temperatures were sufficiently high to eliminate condensation effects.

The leading-edge and cylinder pressure ratios were noted to be independent of both Mach number and Reynolds number. The flat plate pressure ratios show a small dependence on Mach number. Reynolds number effects on the plate pressure ratios were small except at the lower levels of Reynolds number where the interaction of the thickened boundary layer caused increases in pressure.

Boundary layer profiles, obtained during the same program, are reported in Volume II of this report.

This report has been reviewed and is approved.

*Philip P. Antonatos*  
PHILIP P. ANTONATOS  
Chief, Flight Branch  
Flight Dynamics Laboratory

## TABLE OF CONTENTS

<u>SECTION</u>		<u>PAGE</u>
I	INTRODUCTION	1
II	EXPERIMENTAL EQUIPMENT	2
	A. Test Facility	2
	B. Models	2
	C. Instrumentation	3
III	RESULTS	4
	A. Flat Plate Pressure Distributions	4
	B. Leading-Edge and Cylinder Pressures	5
	C. Temperature Distributions	5
IV	DISCUSSION OF RESULTS	6
	A. Effects of Mach and Reynolds Numbers on the Plate Pressures	6
	B. Independence of Leading-Edge Region from Mach and Reynolds Numbers	6
	C. Estimate of Errors	7
V	SUMMARY	9
	REFERENCES	10

### LIST OF TABLES

	Page
I Flat Plate Test Conditions	11
II Distributions of Pressure and Temperature on the Blunt Flat Plate at $M = 7$	12
III Distributions of Pressure and Temperature on the Blunt Flat Plate at $M = 10$	24
IV Distributions of Pressure and Temperature on the Blunt Flat Plate at $M = 12$	36
V Distribution of Pressure and Temperature on the Blunt Flat Plate at $M = 14$	53
VI Cylinder Test Conditions	61
VII Pressure Distributions on the Cylinders at $M = 10.5$	62
VIII Pressure Distributions on the Cylinders at $M = 12$	63
IX Pressure Distributions on the Cylinders at $M = 15$	63

## LIST OF FIGURES

Figure	Page
1 The Ohio State University 12-Inch Hypersonic Wind Tunnel Schematic	64
2 Flat Plate Dimensions	65
3 Flat Plate Orifice and Thermocouple Locations	66
4 The Completed Flat Plate Model	67
5 Model Installation	68
6 Cylinder Dimensions	69
7 The Cylinder	70
8 Inclinable Manometer Board	71
9 Nozzle Calibrations at Model Leading Edge	72
10 Co-ordinate Systems used for the Flat Plate and the Cylinder	73
11 Pressure Distribution over the Flat Plate $M = 7, Re_D = 7500$	74
12 Pressure Distribution over the Flat Plate $M = 7, Re_D = 20,600$	75
13 Pressure Distribution over the Flat Plate $M = 10, Re_D = 8,300$	76
14 Pressure Distribution over the Flat Plate $M = 10, Re_D = 15,000$	77
15 Pressure Distribution over the Flat Plate $M = 12, Re_D = 9000$	78
16 Pressure Distribution over the Flat Plate $M = 12, Re_D = 13,700$	79
17 Pressure Distribution over the Flat Plate $M = 12, Re_D = 21,300$	80
18 Pressure Distribution over the Flat Plate $M = 14, Re_D = 12,700$	81

Figure		Page
19	Pressure Distribution over the Flat Plate $M = 14, Re_D = 16,000$	82
20	Spanwise Pressure Distribution on the Flat Plate	83
21	Effect of Reynolds Number on Pressure Distribution	84
22	Effect of Mach Number on Pressure Distributions for $M = 7, 10, 12$	85
23	Effect of Mach Number on Pressure Distributions for $M = 10, 12, 14$	86
24	Tunnel Interference on Flat Plate Distributions	87
25	Pressure Distribution on the Nose of the Flat Plate $M = 7, Re_D = 7500$	88
26	Pressure Distribution on the Nose of the Flat Plate $M = 7, Re_D = 20,600$	89
27	Pressure Distribution on the Nose of the Flat Plate $M = 10, Re_D = 8300$	90
28	Pressure Distribution on the Nose of the Flat Plate $M = 10, Re_D = 15,000$	91
29	Pressure Distribution on the Nose of the Flat Plate $M = 12, Re_D = 9000$	92
30	Pressure Distribution on the Nose of the Flat Plate $M = 12, Re_D = 13,700$	93
31	Pressure Distribution on the Nose of the Flat Plate $M = 12, Re_D = 21,300$	94
32	Pressure Distribution on the Nose of the Flat Plate $M = 14, Re_D = 12,700$	95
33	Pressure Distribution on the Nose of the Flat Plate $M = 14, Re_D = 16,000$	96
34	Pressure Distribution about Cylinder $M = 10$	97
35	Pressure Distribution about Cylinder $M = 12$	98
36	Pressure Distribution about Cylinder $M = 15$	99

Figure		Page
37	Effect of Mach Number on Pressure Distribution about Cylinder, $Re_D = 11,000$	100
38	Effect of Mach Number on Pressure Distribution about a Cylinder, $Re_D = 4000$	101
39	Tunnel Interference on Cylinder Distributions	102
40	Typical Temperature Distribution on the Flat Plate	103
41	Comparison of Modified Creager Theory with Experiment	104

LIST OF SYMBOLS

Symbol		Dimension
$u$	Velocity	ft/sec
$D$	Diameter of hemicylinder	ft
$M$	Mach number	-----
$P$	Static Pressure	mm HG abs
$P_0$	Stagnation Pressure	lbs/in <sup>2</sup>
$P_{t2}$	Total pressure behind normal shock	mm HG abs
$Re_D$	Reynolds number (based on free stream conditions) = $\frac{\rho u D}{\mu}$	-----
$s$	Distance along surface from tip of model	ft
$s'$	Distance along surface from stagnation point	ft
$T_w$	Wall temperature	°R
$T_0$	Stagnation temperature	°R
$\alpha$	Angle-of-attack	Degrees
$\rho$	Density	Slugs/ft <sup>3</sup>
$\mu$	Viscosity	$\frac{lb \ sec}{ft^2}$
$\theta$	Peripheral angle on cylindrical surface	Degrees

## SECTION I

### INTRODUCTION

There is presently a great need for detailed information about the flow fields surrounding blunt bodies moving at hypersonic speeds. A variety of theoretical approaches have been proposed for the prediction of surface pressures, skin friction, heat transfer, and flow field temperature but experimental verification is lacking in many instances. This study was undertaken to provide information about the surface pressures and the nature of the boundary layer on an unswept blunt flat plate and the results are reported in two volumes.

The flat plate had a cylindrical leading edge 1/2-inch in diameter. It was side-mounted, fully spanning the semi-free jet of the wind tunnel in order to depress interference from the support and from the tunnel walls. Pressure orifices were arranged in three streamwise rows and thermocouples were embedded under the surface. No forced cooling was provided, but radiation and conduction maintained the model temperatures well below recovery temperature. In order to obtain more detailed information about the pressures on the leading edge, separate cylindrical models were also tested.

Experiments were conducted at nominal Mach numbers of 7, 10, 12, and 14 with the Reynolds number (based on the leading-edge diameter) ranging from 7500 to 21,300. Data were obtained at several angles-of-attack through the range  $\pm 15^\circ$ . Table I lists the test conditions in detail.

This part of the report (Volume I) deals with the pressure distributions obtained from the flat plate and the cylinder models. The facility, models and instrumentation are briefly described and the results from the many tests are tabulated. Representative data were selected and plotted to illustrate the effects of angle-of-attack, Mach number and Reynolds number on the pressure distributions.

Volume II describes the boundary layer surveys, taken at three streamwise stations on the plate by means of a pitot probe and a sonic-pneumatic total temperature probe.

-----  
Manuscript released by authors 17 August 1962 for publication  
as an ASD Technical Documentary Report.

ASD-TDR-62-792, Vol. I

## SECTION II

### EXPERIMENTAL EQUIPMENT

#### A. Test Facilities

The major portion of this investigation was conducted in the ALOSU 12-inch hypersonic wind tunnel which is described in some detail in references 1 and 2. This is a continuous-flow, free-jet tunnel utilizing an electric resistance-type air heater which can deliver stagnation temperatures to  $2800^{\circ}\text{R}$ . Axisymmetric contoured nozzles are used for nominal flow Mach numbers of 6, 7, 8, 10, 12 and 14. A diagram of the facility is presented in Figure 1.

For some of the leading-edge data, tests of a small cylinder model were conducted in a four-inch hypersonic tunnel. Except for size, the configuration of this tunnel and its capabilities are essentially the same as that of the larger tunnel.

#### B. Models

The flat plate model was constructed from stainless steel. Static pressure orifices of 0.060" diameter, were arranged along three parallel streamwise rows so that any departure from two-dimensional flow could be ascertained. For reference purposes, two rows of chromel-alumel thermocouples were located on either side of the centerline to measure surface temperatures. Plate dimensions are given in Figure 2; the locations of the orifices and of the thermocouples are shown on the diagram of Figure 3. A photograph of the model after initial testing, Figure 4, indicates the surface discoloration due to the elevated temperatures of the tests. It should be pointed out that although plate temperatures reached  $800^{\circ}\text{F}$  during some tests and the surface discolored, the smoothness of the surface was not altered, nor was any distortion of the plate observed.

Figure 5 shows the flat plate mounted in the wind tunnel test chamber, seen from the nozzle end. The model is surrounded by a cylindrical "scoop", leading into the diffuser; this arrangement was found by initial tests to be most favorable in depressing tunnel interference, especially at large angle-of-attack. For the same reason, small wedges were added to the ends of the plate. During the starting and shut-down procedures, the model was retracted from the jet through a slot in the scoop. For changes in angle-of-attack,

the model could be rotated about its leading edge without stopping the tunnel flow.

The cylinder models were also fabricated from stainless steel; the basic dimensions of the cylinders are given in Figure 6. These models, which fully spanned the jet, could be rotated about their axes to obtain detailed pressure distributions and were retracted from the jet to ease tunnel starts. Photographs of the two models are shown in Figure 7.

### C. Instrumentation

Pressure data from the flat plate were obtained on three inclinable manometer boards of the type shown in Figure 8. Each board consisted of eighteen U-tubes containing Dow Corning No. 200 Silicone Fluid. One side of each U-tube was connected by tubing to a model pressure orifice; the other side was coupled, through a manifold, to a vacuum pump which held the back pressure to 1 to 2 microns of mercury. To determine the reference levels of each tube, to degas and to leak check the measuring system, the two legs of the U-tube could be connected together. High reading accuracy was maintained by properly matching the slope of the boards with the pressure levels to be measured. The manometer system required an average time of 10 minutes to stabilize; however, as the plate temperature required a period of the same order to stabilize, this response was not considered excessive.

The pressure distributions on the cylinders were sensed with a variable reluctance, differential pressure transducer. For these tests, the cylinder attitude indicator and the pressure transducer were connected to the analogue computer of the laboratory for direct on-line reduction and plotting.

The tunnel supply conditions were measured by means of standard wind tunnel instrumentation, i.e., a thermocouple with a Brown Recorder for stagnation temperature and a Bourdon-type pressure gage for stagnation pressure. The Mach number at the model leading edge for each test condition was determined by an impact probe calibration. With the model retracted, a single pitot probe was traversed across the nozzle while its pressure and position were plotted. Real air corrections, although generally small, were made when reducing this pressure data to Mach number distributions; typical calibrations are plotted in Figure 9.

## SECTION III

### RESULTS

#### A. Flat Plate Pressure Distributions

Plate pressures and the associated surface temperatures measured during the test program have been tabulated and some typical data plotted to illustrate trends. Table I indicates the test conditions for the series; Table II through V contain the surface pressures, ratioed to the stagnation point pressure. It should be noted from Figure 10, that the distance  $S$  is the surface distance measured from the front of the model leading edge and does not coincide with the distance from the stagnation point,  $S'$ , except at an angle-of-attack of zero. As described below, wind tunnel interference effects were noted in a number of cases; this influenced data has been deleted from the record and only that data considered valid are tabulated.

Typical plots of the measurements from the model centerline taps are presented in Figures 11 through 19, indicating the trend of the pressures with angle-of-attack. Note that only  $\alpha = 0^\circ$  and  $\alpha = +10^\circ$  are shown. Figure 20 is representative of data from the three rows of orifices and indicates that the flow was essentially two dimensional; the greatest deviation, for  $\alpha = 10^\circ$  compression, is less than 1% of the impact pressure. The typical dependence upon Reynolds number at a fixed Mach number is shown in Figure 21. Figures 22 and 23 illustrate the small dependence upon stream Mach numbers when conditions downstream of the normal shock were held constant.

Data presented in Figure 24 is typical of  $t'$ , tunnel-interference found at low Reynolds numbers and at angle-of-attack. Apparently, bow shock interaction with the tunnel boundary layer or an opening of the model wake (or, in some cases, a combination of both effects) produced a rise in the model pressures and a departure from two-dimensional flow. The point of deviation progressed forward as angle-of-attack was increased and as Reynolds number was decreased, eventually leading to a collapse of the tunnel flow. Comparisons indicate that the measurements were valid up to the point of minimum pressure; data downstream of this point have been deleted from the tabulated results.

## B. Leading Edge and Cylinder Pressures

A number of pressure orifices were installed around the leading edge of the flat plate but it was felt that more detailed information should be obtained from that region. Accordingly, these data were supplemented by obtaining pressure measurements from two cylinder models. One cylinder had a diameter of 1/2-inch, the same as the plate leading edge, and was tested in the 12-inch tunnel. The other, having a diameter of 0.2 inch, was tested in the 4-inch tunnel. Thus, it was possible to obtain pressure data over a wide range of Reynolds and Mach numbers and to examine the influence of body geometry. In addition, backside pressures were also obtained from the cylinders.

Results from these measurements are plotted in Figures 25 through 39; it should be noted that the correlations are with the dimensionless surface distance to the stagnation point,  $S'/D$ , as the abscissa. Figures 25 through 33 show the pressure ratios from the leading edge of the flat plate while those from the cylinders are presented in Figures 34, 35 and 36 and in Tables VI through IX. Repeated data in Figures 37 and 38 show the influence of Mach number.

During some of these tests, tunnel interference produced an opening of the wake, with the backside pressures being increased; Figure 39 illustrates the typical observed effect.

## C. Temperature Distribution

Tabulated values of the record temperatures are presented in Tables II to V for the flat plate and in Table VI for the cylinders. A typical flat plate temperature distribution is shown in Figure 40. As the measurements of wall temperature obtained from the two rows of thermocouples differed by less than 10°F, the plotted values are averaged temperature readings. The surface temperatures of the cylinders ranged from 750°F to 1500°F, depending upon test conditions, but within +15°F around the cylinder in a particular test; hence, the cylinder may be considered as essentially an isothermal body at the temperature presented in the table.

## SECTION IV

### DISCUSSION OF RESULTS

#### A. Effect of Mach and Reynolds Numbers on the Plate Pressures

Whenever possible, the tunnel test conditions were chosen such that the stagnation temperature,  $T_0$ , and the stagnation pressure behind the normal shock,  $P_{t2}$ , would be repeated at different stream Mach numbers. In this manner, there should be a near-similarity of flows over the model, including the boundary layer, as the model temperatures were also nearly repeated at such conditions. Comparisons like those in Figures 22 and 23 will then permit the small effects of stream Mach number to be separated.

In Figure 22, the influence of Mach number on the pressure distributions at  $M = 7, 10$ , and  $12$  is shown for a total pressure behind the normal shock of approximately  $45$  mm Hg. The surface pressures are observed to decrease as Mach number increases from  $7$  to  $12$ . Figure 23 is a similar plot for  $M = 10, 12$ , and  $14$  at impact pressures close to  $25$  mm Hg. At this pressure level, the distributions do not show the Mach number trend of the previous figure; the  $M = 14$  data are above the  $M = 12$  pressures. However, at this low level of Reynolds number, viscous interaction is quite evident and the discrepancy may be due to the fact that the nose pressures were not exactly duplicated; further testing seems advisable to resolve the apparent disagreement.

While testing in a nozzle of given nominal Mach number, the stream Mach number was different at each Reynolds number because of changes in the boundary layer thickness on the nozzle walls. These changes in Mach number, of the order of 1%, were too small to produce any significant effects on the pressures, as may be noted from Figure 22. Hence, the increase in pressures observed on the plate with stagnation pressure, in Figure 21, can be interpreted as being caused only by Reynolds number, i.e., by viscous interaction. This same figure also indicates that the data obtained at the high Reynolds number is very close to the inviscid distributions.

#### B. Independence of Leading-Edge Region from Mach and Reynolds Numbers

The data taken from the cylinders show an independence from both stream Mach number and Reynolds number, in the range tested. In Reference 4, an empirical expression is

given which adequately describes the pressure distribution about cylinders in supersonic flow. A modification of this expression to the form

$$\frac{P}{P_{t_2}} = 0.320 + 0.455 \cos\theta + 0.195 \cos 2\theta + 0.035 \cos 3\theta - 0.005 \cos 4\theta \quad (1)$$

applies to all the data obtained on the cylinders in the present test series with a maximum deviation of 2.5%.

Equation (1) has been plotted with the data of the leading-edge region, Figures 25 to 33; the agreement is excellent, even when the model is pitched through its angle-of-attack range. The close agreement between the cylinder data and the plate leading edge data, besides revealing its independence to Mach and Reynolds number, indicate no effect of the afterbody on the nose region. For example the pressure measured at the shoulder when the model is pitched to  $15^\circ$  on the expansion side, corresponds to the cylinder data at  $\theta = 105^\circ$ . Similarly, on the compression side, the leading-edge distribution follows the cylinder data closely until the departure due to the plate angle-of-attack. Therefore, Equation (1) may be used to describe the leading edge region of the cylindrical-nosed flat plate with excellent accuracy over the wide range of Mach number and Reynolds number examined in this study.

### C. Estimate of Errors

In an experimental program, an estimate of the possible errors in the data is required. The wide range of pressures measured in the study, from 80.00 to 0.30 mm of mercury, make a percentage estimate of error difficult. However, the standard manometer techniques used during the tests should produce data accurate to within 1% at pressure levels down to 2.00 mm Hg abs. Below this pressure, a more realistic estimate of the errors may be obtained by assuming a relatively constant error of  $\pm .025$  mm Hg. This value is felt to be appropriate, despite the care used in the manometry--e.g., copper pressure leads, silver soldered joints, inclined boards, long stabilization periods, periodic leak checks, etc. Hence, the percentage error of the pressure on the plate may vary from less than 1% near the nose to almost 10% near the trailing edge and/or at high expansion angles.

The temperature measurements on the plate have a maximum possible error of  $\pm 10^{\circ}\text{R}$ ; therefore, as surface temperatures varied from  $750^{\circ}\text{R}$  to  $1500^{\circ}\text{R}$ , the maximum percentage errors ranged between  $1\frac{1}{3}\%$  and  $2\frac{1}{3}\%$ .

The wind tunnel test conditions were determined from the laboratory instruments, which are estimated to give the following maximum possible errors:

$$P_0 \quad \pm 0.25\%$$

$$T_0 \quad \pm 0.50\%$$

$$M \quad \pm 0.50\%$$

$$\alpha \quad \pm 0.1^{\circ}$$

## SECTION V

### SUMMARY

A series of tests has been conducted at nominal Mach numbers of 7, 10, 12 and 14 on a flat plate having a cylindrical leading-edge at several angles-of-attack ranging through  $\pm 15^\circ$  for several Reynolds numbers. The results of the tests are summarized by the following comments:

- (1) Wind tunnel interference occasionally limited the data validity at angles-of-attack. The interference effects were confined near the trailing edge and the data ahead of the influenced region were valid. These data are presented in tabular form while typical parts are plotted.
- (2) The spanwise distribution of the three rows of streamwise taps indicated two-dimensional flow, the pressure variation across the span being less than 1% of the impact pressure at the nose.
- (3) When the wall temperatures and the conditions behind the normal shock are matched, the plate distributions are found to be only slightly influenced by Mach number, the trend being towards lowered pressure ratios with increasing Mach number.
- (4) At a given Mach number, the pressure ratios increased with decreasing Reynolds number, indicating some viscous interaction effects were encountered.
- (5) Pressures on the leading edge of the plate and on the cylinders were found to be independent of Mach number and Reynolds number. In both cases, pressure distributions were accurately described by an empirical relation, Equation 1.
- (6) As this investigation was solely of an experimental nature, no attempt was made to correlate the results with the available theories. However, an extensive program, based on the modified Creager method of Reference 5, is being carried out by the Flight Dynamics Laboratory of the Aeronautical System Division. A preliminary result of the program, showing the excellent agreement of the theory with the experimental data is presented in Figure 41.

REFERENCES

1. Gregorek, G. M., Nark, T. C., and Lee, J. D., An Experimental Investigation of the Surface Pressure and the Laminar Boundary Layer on a Blunt Plate in Hypersonic Flow: Volume II ASD-TDR-62-792, September, 1962
2. Thomas, R. E., and Lee, J. D., The Ohio State University 12-inch Hypersonic Wind Tunnel, TN(AOSU)559-2; The Ohio State University Research Foundation, Technical Report to WADC on Contract AF 33(616)-5593, July, 1959
3. Lee, J. D., Axisymmetric Nozzles for Hypersonic Flows TN(AOSU)459-1; The Ohio State University Research Foundation, Technical Report to WADC on Contract AF 33(616)-5593, July, 1959
4. Tewfik, O. K., and Giedt, W. H., Heat Transfer, Recovery Factor and Pressure Distributions Around a Cylinder Normal to a Supersonic Rarefied Airstream - Part I, Experimental Data, University of California Tech Report HE-150-162, January, 1959
5. Buck, M. L., and McLaughlin, E. J., An Aerodynamic Prediction Technique for Hypersonic Winged Re-entry Vehicles - Part I - Analysis. Flight Dynamics Laboratory ASRMDF TM-62-5, February, 1962

TABLE I  
Flat Plate Test Conditions

Cond.	Mach No.	$P_o$ PSIA	$T_o$ $^{\circ}$ R	$R_{eD}$	$P_{tq}$ mm Hg
A	6.96	58.7	2060	7,500	44.6
B	7.01	104.7	1560	20,600	79.4
C	9.85	164.7	2060	8,300	26.0
D	9.95	306.7	2060	15,000	46.2
E	12.16	339.7	2090	9,000	19.8
F	12.20	514.7	2060	13,700	29.7
G	12.28	814.7	2060	21,300	45.5
H	14.2	714.7	1910	12,700	19.9
I	14.28	914.7	1910	16,000	24.8

TABLE II

Distributions of Pressure and Temperature  
on the Blunt Flat Plate at  $M = 7$

## Condition A

 $M = 6.96$  $R_e_D = 7500$  $P_{t_0} = 44.6 \text{ mm Hg}$  $\alpha = 0^\circ$ 

S/D	L	C	R	Temp. $\sim 0^\circ\text{F}$	
				P/P_{t_0}	L
0.26	.871	--	--		
0	--	1.000	--		
0.26	.816	--	--		
0.52	--	--	.428		
0.79	--	.142	--		
1.29	.094	--	.096		
1.79	--	.083	--		
3.79	.063	--	.065		
4.79	--	.056	--		
6.29	.050	--	.049		
6.79	--	.047	--		
8.79	.042	.041	.042		
11.29	.035	.038	.034		
13.79	.031	.034	.030		
16.29	.027	.031	.027		
18.79	.026	.028	.025		
21.29	--	.027	.022		
22.79	--	.024	--		
23.79	.020	.023	.020		

Temperature Recorder Incorporated  
on the Test

TABLE II (CONTINUED)  
Condition A

$\alpha = 5^\circ$  Exp

S/D	L	C	R	Temp. ~ °F	
				P/P <sub>t<sub>0</sub></sub>	L
0.26	1.005	--	--		---
0	--	1.088	--		---
0.26	.756	--	--		---
0.52	--	--	.358		---
0.79	--	.111	--		---
1.29	.071	--	--	857	---
1.79	--	.061	--		---
3.79	.045	--	.047	710	722
4.79	--	.038	--		---
6.29	.036	--	.036	630	645
6.79	--	.034	--		---
8.79	.030	.029	.029	600	590
11.29	.024	.026	.025	568	580
13.79	.021	.023	.020	549	556
16.29	.019	.021	.017	530	---
18.79	.017	.019	.017	520	527
21.29	--	.017	.015	515	520
22.79	--	.015	--		---
23.79	.014	.014	.012		---

TABLE II (CONTINUED)

Condition A

 $\alpha = 10^0$  Exp

S/D	P/P <sub>t<sub>2</sub></sub>			Temp. ~ °F	
	L	C	R	L	R
0.26	.953	--	--	---	---
0	--	.968	--	---	---
0.26	.679	--	--	---	---
0.52	--	--	.297	---	---
0.79	--	.089	--	---	---
1.29	.054	--	.055	878	---
1.79	--	.046	--	---	---
3.79	.034	--	.035	743	752
4.79	--	.031	--	---	---
6.29	.026	--	.026	680	690
6.79	--	.023	--	---	---
8.79	.022	.021	.022	641	651
11.29	.017	.017	.017	615	624
13.79	.015	.015	.014	597	607
16.29	.014	.014	.012	589	---
18.79	.013	.013	.011	599	597
21.29	--	.012	.011	600	604
22.79	--	.010	--	---	---

TABLE II (CONTINUED)

Condition A

 $\alpha = 15^{\circ}$  Exp

S/D	P/P <sub>t<sub>0</sub></sub>	L	C	R	L	R	Temp. ~ °F
0.26	.984	--	--	--	---	---	
0	--	.964	--	--	---	---	
0.26	.602	--	--	--	---	---	
0.52	--	--	.238	--	---	---	
0.79	--	.071	--	--	---	---	
1.29	.041	--	.041	--	637	---	
1.79	--	.035	--	--	---	---	
3.79	.026	--	.026	--	777	772	
4.79	--	.021	--	--	---	---	
6.29	.020	--	.019	--	699	711	
6.79	--	.018	--	--	---	---	
8.79	.013	.015	.016	--	664	674	
11.29	.014	.013	.013	--	640	650	
13.79	.013	.011	.011	--	587	637	
16.29	--	--	--	--	623	---	
18.79	--	--	--	--	629	640	
21.29	--	--	--	--	542	650	

TABLE II (CONTINUED)

Condition A

 $\alpha = 5^\circ$  Comp

S/D	P/P <sub>ext</sub>			Temp. ~ °F	
	L	C	R	L	R
0.26	.805	--	--	---	---
0	--	.657	--	---	---
0.26	.673	--	--	---	---
0.52	--	--	.504	---	---
0.79	--	.177	--	---	---
1.29	.122	--	.126	101	---
1.79	--	.107	--	---	---
3.79	.064	--	.086	77	732
4.79	--	.061	--	---	---
6.29	.069	--	.068	715	722
6.79	--	.064	--	---	---
8.79	.060	.059	.059	640	655
11.29	.053	.054	.052	653	660
13.79	.048	.050	.047	641	642
16.29	.044	.046	.043	630	---
18.79	.041	.044	.040	624	627
21.29	--	.042	.038	612	616
22.79	--	.040	--	---	---
23.79	.035	.035	.033	---	---

TABLE II (CONTINUED)

Condition A

 $\alpha = 10^{\circ}$  Comp

S/D	P/P <sub>t<sub>0</sub></sub>			Temp ~ °F	
	L	C	R	L	R
0.26	.744	--	--	---	---
0	--	.985	--	---	---
0.26	.920	--	--	---	---
0.52	--	--	.581	---	---
0.79	--	.219	--	---	---
1.29	.159	--	.163	911	---
1.79	--	.137	--	---	---
2.79	--	--	--	---	---
3.79	.114	--	.115	783	784
4.79	--	.102	--	---	---
6.29	.097	--	.097	724	730
6.79	--	.092	--	---	---
8.79	.088	.087	.088	686	693
11.29	.081	.084	.079	665	668
13.79	.075	.080	.074	650	650
16.29	.073	.077	.070	640	---
18.79	.070	.075	.068	631	635
21.29	--	.072	.067	620	625
22.79	--	.071	--	---	---
23.79	.065		.063	---	---

TABLE II (CONTINUED)

## Condition B

 $M = 7.01$  $R_{eD} = 20,600$  $P_{t_2} = 79.4 \text{ mm Hg}$  $\alpha = 0^\circ$  $P/P_{t_2}$ Temp.  $\sim {}^\circ F$ 

S/D	L	C	R	L	R
0.26	--	--	--	---	---
0	--	1.00	--	---	---
0.26	--	--	--	---	---
0.52	--	--	.405	---	---
0.79	--	.125	--	---	---
1.29	.086	--	.087	697	---
1.79	--	.076	--	---	---
3.79	.059	--	.060	599	604
4.79	--	.055	--	---	---
6.29	.041	--	.046	547	553
6.79	--	.043	--	---	---
8.79	.038	.038	.039	508	519
11.29	.034	.034	.027	487	497
13.79	.029	.031	.022	469	479
16.29	.025	.029	.025	457	---
18.79	.024	.026	.023	448	458
21.29	--	.024	.022	440	449
22.79	--	.023	--	---	---
23.79	.019	.022	.018	---	---

TABLE II (CONTINUED)  
Condition B

$\alpha = 10^6$  Exp

S/D	P/P <sub>t<sub>0</sub></sub>			Temp. ~ °F	
	L	C	R	L	R
0.26	--	--	--	---	---
0	--	.989	--	---	---
0.26	--	--	--	---	---
0.52	--	--	.282	---	---
0.79	--	.079	--	---	---
1.29	.048	--	.048	712	---
1.79	--	.043	--	---	---
3.79	.032	--	.032	624	629
4.79	--	.027	--	---	---
6.29	.024	--	.025	579	584
6.79	--	.022	--	---	---
8.79	.020	.019	.020	551	557
11.29	.016	.017	.017	533	535
13.79	.014	.015	.013	519	520
16.29	.012	.013	.012	514	---
18.79	.011	.012	.010	508	508
21.29	--	.011	.010	502	502
22.79	--	.010	--	---	---
23.79	--	--	--	---	---

TABLE II (CONTINUED)

Condition B

 $\alpha = 10^\circ$  Comp

S/D	$P/P_{t_0}$			Temp. ~ °F	
	L	C	R	L	R
0.26	--	--	--	---	---
0	--	.989	--	---	---
0.26	--	--	--	---	---
0.52	--	--	.569	---	---
0.79	--	.202	--	---	---
1.29	.149	--	.152	727	---
1.79	--	.132	--	---	---
3.79	.108	--	.109	651	651
4.79	--	.097	--	---	---
6.29	.092	--	.093	610	610
6.79	--	.087	--	---	---
8.79	.084	.082	.083	584	588
11.29	.078	.078	.076	568	568
13.79	.073	.075	.068	559	558
16.29	.069	.074	.067	549	---
18.79	.067	.072	.065	544	544
21.29	--	.069	.061	537	538
22.79	--	--	--	---	---
23.79	.060	.065	.057	---	---

TABLE II (CONTINUED)  
Condition B

$\alpha = 5^\circ$  Exp

S/D	L	$P/P_{t_2}$		Temp. ~ °F	
		C	R	L	R
0.26	--	--	--	---	---
0	--	.995	--	---	---
0.26	--	--	--	---	---
0.52	--	--	.339	---	---
0.79	--	.099	--	---	---
1.29	.064	--	.065	702	---
1.79	--	.057	--	---	---
3.79	.043	--	.044	617	619
4.79	--	.037	--	---	---
6.29	.033	--	.033	568	571
6.79	--	.031	--	---	---
8.79	.027	.027	.027	539	543
11.29	.023	.023	.022	518	520
13.79	.020	.021	.019	507	508
16.29	.017	.019	.016	497	---
18.79	.015	.017	.015	489	491
21.29	--	.016	.014	487	488
22.79	--	.015	--	---	---
23.79	.012	.013	.012	---	---

TABLE II (CONTINUED)

Condition B

 $\alpha = 5^\circ$  Comp

S/D	P/P <sub>t<sub>a</sub></sub>			Temp. ~ °F	
	L	C	R	L	R
0.26	--	--	--	---	---
0	--	.995	--	---	---
0.26	--	--	--	---	---
0.52	--	--	.481	---	---
0.79	--	.164	--	---	---
1.29	.113	--	.115	726	---
1.79	--	.100	--	---	---
3.79	.078	--	.079	643	644
4.79	--	.069	--	---	---
6.29	.064	--	.064	599	602
6.79	--	.060	--	---	---
8.79	.055	.055	.055	576	579
11.29	.049	.051	.048	560	560
13.79	.045	.047	.044	550	550
16.29	.041	.045	.040	543	---
18.79	.039	.042	.038	538	538
21.29	--	.040	.035	532	532
22.79	--	.039	--	---	---
23.79	.033	.036	.032	---	---

TABLE II (CONTINUED)

Condition B

 $\alpha = 15^\circ$  Exp

S/D	$P/P_{t_0}$			Temp. ~ °F	
	L	C	R	L	R
0.26	--	--	--	---	---
0	--	.966	--	---	---
0.26	--	--	--	---	---
0.52	--	--	.234	---	---
0.79	--	.063	--	---	---
1.29	.036	--	.036	711	---
1.79	--	.031	--	---	---
3.79	.023	--	.024	632	636
4.79	--	.021	--	---	---
6.29	.018	--	.018	589	598
6.79	--	.017	--	---	---
8.79	.014	.014	.015	565	568
11.29	.013	.012	.012	548	549
13.79	.012	.011	.010	537	538
16.29	.012	.010	.009	533	---
18.79	--	--	--	537	537
21.29	--	--	--	548	548
22.79	--	--	--	---	---
23.79	--	--	--	---	---

TABLE III

Distributions of Pressure and Temperature  
on the Blunt Flat Plate at  $M = 10$

## Condition C

 $M = 9.85$  $Re_D = 8,300$  $P_{t_2} = 26 \text{ mm Hg}$  $\alpha = 0^\circ$ 

S/D	$P/P_{t_2}$			Temp. $\sim {}^\circ F$	
	L	C	R	L	R
0.26	.882	--	--	---	---
0	--	1.00	--	---	---
0.26	.804	--	--	---	---
0.52	--	--	.150	---	---
0.79	--	.139	--	---	---
1.29	.093	--	.092	791	---
1.79	--	.075	--	---	---
3.79	.057	--	.056	665	673
4.79	--	.047	--	---	---
6.29	.043	--	.042	601	611
6.79	--	.041	--	---	---
8.79	.036	.035	.034	559	569
11.29	.028	.031	.028	551	554
13.79	.023	.027	.024	512	519
16.29	.021	.023	.020	501	---
18.79	--	--	--	491	486
21.29	--	.020	.019	487	487
22.79	--	.017	--	---	---
23.79	--	--	--	---	---

TABLE III (CONTINUED)  
Condition C

$\alpha = 5^\circ$  Comp

S/D	$P/P_{t_2}$			Temp. ~°F	
	L	C	R	L	R
0.26	.803	--	--	---	---
0	--	.997	--	---	---
0.26	.860	--	--	---	---
0.52	--	--	.493	---	---
0.79	--	.174	--	---	---
1.29	.123	--	.121	805	---
1.79	--	.100	--	---	---
3.79	.078	--	.077	691	690
4.79	--	.064	--	---	---
6.29	.060	--	.058	630	632
6.79	--	.056	--	---	---
8.79	.051	.052	.048	563	599
11.29	.043	.045	.042	551	562
13.79	.038	.041	.038	549	550
16.29	.036	.038	.033	534	---
18.79	--	--	--	528	530
21.29	--	.034	.032	518	520
22.79	--	.031	--	---	---
23.79	.029	.028	.028	---	---

TABLE III (CONTINUED)  
Condition C

$\alpha = 10^{\circ}$  Comp

S/D	$P/P_{t_0}$			Temp. ~ °F	
	L	C	R	L	R
0.26	.728	--	--	---	---
0	--	.983	--	---	---
0.26	.908	--	--	---	---
0.52	--	--	.300	---	---
0.79	--	.217	--	---	---
1.29	.156	--	.156	814	---
1.79	--	.131	--	---	---
3.79	.091	--	.089	698	702
4.79	--	.091	--	---	---
6.29	.086	--	.085	639	641
6.79	--	.081	--	---	---
8.79	.078	.077	.074	601	609
11.29	.071	.071	.068	575	576
13.79	.066	.069	.066	560	562
16.29	--	--	--	555	---
18.79	--	--	--	542	550
21.29	--	--	--	530	542
22.79	--	--	--	---	---
23.79	--	--	--	---	---

TABLE III (CONTINUED)

Condition C

 $\alpha = 5^\circ \text{ Exp}$ 

S/D	L	P/P <sub>t<sub>0</sub></sub>		Temp. ~ °F	
		C	R	L	R
0.26	1.340	--	--	---	---
0	--	.997	--	---	---
0.26	.737	--	--	---	---
0.52	--	--	.348	---	---
0.79	--	.110	--	---	---
1.29	.073	--	.070	783	---
1.79	--	.060	--	---	---
3.79	.042	--	.042	658	671
4.79	--	.035	--	---	---
6.29	.031	--	.025	591	601
6.79	--	.029	--	---	---
8.79	.018	.025	.024	550	560
11.29	.021	.022	.020	521	524
13.79	.016	.018	.017	502	509
16.29	.014	.016	.014	489	---
18.79	.014	.014	.012	481	487
21.29	--	--	--	481	479
22.79	--	--	--	---	---
23.79	.011	.011	.011	---	---

TABLE III (CONTINUED)  
Condition C

$a = 10^9$  Exp

S/D	$P/P_{t_0}$			Temp. ~ °F	
	L	C	R	L	R
0.26	.947	--	--	---	---
0	--	.993	--	---	---
0.26	.666	--	--	---	---
0.52	--	--	.287	---	---
0.79	--	.081	--	---	---
1.29	.054	--	.053	763	---
1.79	--	.042	--	---	---
3.79	.032	--	.029	631	643
4.79	--	.027	--	---	---
6.29	.024	--	.024	611	623
6.79	--	.021	--	---	---
8.79	.018	.018	.018	513	527
11.29	.015	.016	.014	482	491
13.79	.012	.013	.011	461	473
16.29	.011	.011	.011	451	---
18.79	--	--	--	443	451
21.29	--	--	--	450	449
22.79	--	--	--	---	---
23.79	--	--	--	---	---

TABLE III (CONTINUED)  
Condition C

$\alpha = 15^\circ$  Exp

S/D	P/P <sub>t<sub>2</sub></sub>			Temp. ~ °F	
	L	C	R	L	R
0.26	.988	--	--	---	---
0	--	.969	--	---	---
0.26	.591	--	--	---	---
0.52	--	--	.236	---	---
0.79	--	.067	--	---	---
1.29	.041	--	.039	722	---
1.79	--	.031	--	---	---
3.79	.022	--	.022	573	591
4.79	--	.018	--	---	---
6.29	.018	--	.018	491	511
6.79	--	.015	--	---	---
8.79	.014	.014	.014	432	451
11.29	.013	.011	.013	419	410
13.79	--	--	--	400	414
16.29	--	--	--	391	---
18.79	--	--	--	391	402
21.29	--	--	--	388	413
22.79	--	--	--	---	---
23.79	--	--	--	---	---

TABLE III (CONTINUED)

## Condition D

 $M = 9.95$  $R_{eD} = 15,000$  $P_{t_2} = 46.2 \text{ mm Hg}$  $\alpha = 0^\circ$ 

S/D	$P/P_{t_2}$			Temp. $\sim {}^\circ F$	
	L	C	R	L	R
0.26	.861	--	--	---	---
0	--	1.00	--	---	---
0.26	.791	--	--	---	---
0.52	--	--	.410	---	---
0.79	--	.131	--	---	---
1.29	.089	--	.088	885	---
1.79	--	.074	--	---	---
3.79	.056	--	.055	750	754
4.79	--	.047	--	---	---
6.29	.042	--	.040	683	690
6.79	--	.039	--	---	---
8.79	.034	.034	.033	642	650
11.29	.028	.031	.020	619	618
13.79	.024	.026	.023	603	603
16.29	.021	.023	.020	592	---
18.79	.019	.021	.018	583	583
21.29	--	.021	.017	575	575
22.79	--	.019	--	---	---
23.79	.015	.017	.015	---	---

TABLE III (CONTINUED)

 $\alpha = 5^\circ$  Comp

S/D	P/P <sub>ts</sub>			Temp. ~ °F	
	L	C	R	L	R
0.26	.913	--	--	---	---
0	--	.998	--	---	---
0.26	.847	--	--	---	---
0.52	--	--	.486	---	---
0.79	--	.167	--	---	---
1.29	.116	--	.116	892	---
1.79	--	.099	--	---	---
3.79	.075	--	.076	757	762
4.79	--	.065	--	---	---
6.29	.058	--	.058	693	698
6.79	--	.055	--	---	---
8.79	.049	.049	.047	651	661
11.29	.043	.045	.041	626	627
13.79	.038	.040	.035	610	610
16.29	.035	.037	.033	605	---
18.79	.032	.035	.030	590	599
21.29	--	.033	.028	584	582
22.79	--	.031	--	---	---
23.79	.026	.028	.024	---	---

TABLE III (CONTINUED)

 $\alpha = 10^9$  Comp

S/D	$P/P_{t_0}$			Temp. ~ °F	
	L	C	R	L	R
0.26	.724	--	--	---	---
0	--	.988	--	---	---
0.26	.897	--	--	---	---
0.52	--	--	.560	---	---
0.79	--	.204	--	---	---
1.29	.149	--	.149	834	---
1.79	--	.128	--	---	---
3.79	.101	--	.101	744	751
4.79	--	.088	--	---	---
6.29	.083	--	.081	684	692
6.79	--	.079	--	---	---
8.79	.073	.073	.071	648	654
11.29	.067	.069	.064	623	623
13.79	.063	.066	.058	---	611
16.29	.060	.063	.056	---	---
18.79	.058	.060	.055	---	---
21.29	--	.058	.055	---	---
22.79	--	--	--	---	---
23.79	.053	.053	.055	---	---

TABLE III (CONTINUED)  
Condition D

$\alpha = 15^\circ \text{ Exp}$

S/D	P/P <sub>t<sub>2</sub></sub>			Temp. ~°F	
	L	C	R	L	R
0.26	.801	--	--	---	---
0	--	.994	--	---	---
0.26	.587	--	--	---	---
0.52	--	--	.225	---	---
0.79	--	.062	--	---	---
1.29	.037	--	.036	795	---
1.79	--	.029	--	---	---
3.79	.022	--	.022	682	693
4.79	--	.018	--	---	---
6.29	.016	--	.015	599	613
6.79	--	.015	--	---	---
8.79	.013	.013	.013	544	555
11.29	.010	.011	.010	505	528
13.79	.008	.009	.008	481	492
16.29	.009	.008	.007	470	---
18.79	--	--	--	471	479
21.29	--	--	--	489	493
22.79	--	--	--	---	---
23.79	--	--	--	---	---

TABLE III (CONTINUED)

Condition D

 $\alpha = 5^\circ$  Exp

S/D	P/P <sub>t<sub>2</sub></sub>			Temp. ~ °F	
	L	C	R	L	R
0.26	.885	--	--	---	---
0	--	1.006	--	---	---
0.26	.730	--	--	---	---
0.52	--	--	.340	---	---
0.79	--	.104	--	---	---
1.29	.067	--	.066	879	---
1.79	--	.056	--	---	---
3.79	.041	--	.042	742	752
4.79	--	.034	--	---	---
6.29	.031	--	.029	674	683
6.79	--	.028	--	---	---
8.79	.025	.024	.024	634	642
11.29	.020	.021	.019	610	612
13.79	.017	.017	.016	593	594
16.29	.015	.016	.013	587	---
18.79	.012	.014	.012	572	581
21.29	--	.014	.010	563	564
22.79	--	.009	--	---	---
23.79	--	--	--	---	---

TABLE III (CONTINUED)  
Condition D

$\alpha = 10^6$  Exp

S/D	$P/P_{t_2}$			Temp. ~ °F	
	L	C	R	L	R
0.26	.920	--	--	---	---
0	--	1.000	--	---	---
0.26	.661	--	--	---	---
0.52	--	--	.280	---	---
0.79	--	.081	--	---	---
1.29	.050	--	.049	819	---
1.79	--	.041	--	---	---
3.79	.031	--	.030	714	724
4.79	--	.025	--	---	---
6.29	.023	--	.021	654	661
6.79	--	.021	--	---	---
8.79	.018	.017	.016	610	618
11.29	.014	.016	.013	582	587
13.79	.011	.012	.011	561	571
16.29	.010	.010	.009	553	---
18.79	.009	.010	.008	549	551
21.29	--	.010	.008	540	542
22.79	--	.009	--	---	---
23.79	.008	.008	.008	---	---

TABLE IV

Distributions of Pressure and Temperature  
on the Blunt Flat Plate at  $M = 12$

Condition E

 $M = 12.16$  $Re_D = 9,000$  $P_{t_2} = 19.8 \text{ mm Hg}$  $\alpha = 0^\circ$ 

$x/d$	$P/P_{t_2}$			Temp. $\sim {}^\circ F$	
	L	C	R	L	R
0.26	.866	--	--	---	---
0	--	1.000	--	---	---
0.26	.809	--	--	---	---
0.52	--	--	.413	---	---
0.79	--	.138	--	---	---
1.29	.092	--	.093	762	757
1.79	--	.075	--	---	---
3.79	.058	--	.056	639	650
4.79	--	.047	--	---	---
6.29	.041	--	.043	579	590
6.79	--	.041	--	---	---
8.79	.034	.036	.034	538	550
11.29	.034	.032	.030	514	524
13.79	.025	.025	.026	497	503
16.29	.022	.022	.027	483	---
18.79	.020	--	.020	472	480
21.29	--	--	--	---	---
22.79	--	--	--	---	---
23.79	--	--	--	---	---

TABLE IV (CONTINUED)  
Condition E

$\alpha = 5^\circ$  Exp

x/d	$P/P_{t_0}$			Temp. ~ °F	
	L	C	R	L	R
0.26	.919	--	--	---	---
0	--	1.000	--	---	---
0.26	.742	--	--	---	---
0.52	--	--	.346	---	---
0.79	--	.110	--	---	---
1.29	.073	--	.073	---	---
1.79	--	.058	--	---	---
3.79	.043	--	.043	---	---
4.79	--	.034	--	---	---
6.29	.030	--	.032	---	---
6.79	--	.030	--	---	---
8.79	.026	.025	.026	---	---
11.29	.023	.023	.038	---	---
13.79	.017	.015	.017	---	---
16.29	.015	.014	.015	---	---
18.79	.015	.014	.012	---	---
21.29	--	.017	.014	---	---
22.79	--	.012	--	---	---
23.79	--	--	--	---	---

Temperature  
On this Test  
Recorder Inoperative

TABLE IV (CONTINUED)

## Condition F

 $M = 12$  $R_{eD} = 13,700$  $P_{t_2} = 29.7 \text{ mm Hg}$  $\alpha = 0^\circ$ 

$x/d$	$P/P_{t_2}$			Temp. $\sim {}^\circ\text{F}$	
	L	C	R	L	R
0.26	.875	--	--	---	---
0	--	1.000	--	---	---
0.26	.813	--	--	---	---
0.52	--	--	.404	---	---
0.79	--	.135	--	---	---
1.29	.086	--	.085	797	---
1.79	--	.072	--	---	---
3.79	.054	--	.054	687	702
4.79	--	.045	--	---	---
6.29	.040	--	.040	633	646
6.79	--	.035	--	---	---
8.79	.032	.032	.029	599	610
11.29	.026	.028	.025	578	588
13.79	.021	.025	.020	563	570
16.29	.020	.022	.018	552	---
18.79	.018	.020	.017	548	553
21.29	--	.018	.017	546	548
22.79	--	.017	--	---	---
23.79	.014	.017	.014	---	---

TABLE IV (CONTINUED)

Condition F

 $\alpha = 10^{\circ}$  Exp

x/d	$P/P_{t_0}$			Temp. ~ °F	
	L	C	R	L	R
0.26	.955	--	--	---	---
0	--	.983	--	---	---
0.26	.665	--	--	---	---
0.52	--	--	.283	---	---
0.79	--	.085	--	---	---
1.29	.047	--	.064	765	761
1.79	--	.036	--	---	---
3.79	.032	--	.032	658	670
4.79	--	.026	--	---	---
6.29	.023	--	.025	602	614
6.79	--	.023	--	---	---
8.79	.021	.019	.019	570	580
11.29	.017	.017	.015	550	558
13.79	.015	.012	.013	539	549
16.29	--	.010	.012	528	---

TABLE IV (CONTINUED)  
Condition F

$\alpha = 5^\circ$  Comp

x/d	$P/P_{t_0}$			Temp. ~ °F	
	L	C	R	L	R
0.26	.805	--	--	---	---
0	--	.994	--	---	---
0.26	.875	--	--	---	---
0.52	--	--	.471	---	---
0.79	--	.166	--	---	---
1.29	.109	--	.109	836	819
1.79	--	.090	--	---	---
3.79	.072	--	.072	708	715
4.79	--	.059	--	---	---
6.29	--	--	.053	652	660
6.79	--	.049	--	---	---
8.79	.044	.044	.044	618	625
11.29	.038	.038	.037	598	600
13.79	.034	.037	.034	583	585
16.29	.032	.0418	.032	570	---
18.79	.032	.032	.032	566	569
21.29	--	.026	.029	559	559
22.79	--	.028	--	---	---
23.79	.028	.025	.029	---	---

TABLE IV (CONTINUED)  
Condition F

$\alpha = 10^6$  Comp

x/d	$P/P_{t_2}$			Temp. ~ °F	
	L	C	R	L	R
0.26	.731	--	--	---	---
0	--	.978	--	---	---
0.26	.924	--	--	---	---
0.52	--	--	.554	---	---
0.79	--	.212	--	---	---
1.29	.143	--	.143	807	800
1.79	--	.120	--	---	---
3.79	.096	--	.097	675	683
4.79	--	.081	--	---	---
6.29	.076	--	.078	610	618
6.79	--	.072	--	---	---
8.79	.068	.067	.065	565	578
11.29	.061	.062	.059	537	546
13.79	--	--	--	517	520
16.29	--	--	--	500	---
18.79	--	--	--	484	489
21.29	--	--	--	475	479
22.79	--	--	--	---	---
23.79	--	--	--	---	---

TABLE IV (CONTINUED)

Condition F

 $\alpha = 15^\circ \text{ Comp}$ 

x/d	P/P <sub>t<sub>a</sub></sub>			Temp. ~ °F		Temperature Recorder Inoperative on this Test
	L	C	R	L	R	
0.26	.652	--	--	--	--	
0	--	.948	--	--	--	
0.26	.964	--	--	--	--	
0.52	--	--	.633	--	--	
0.79	--	.259	--	--	--	
1.29	.182	--	.184	--	--	
1.79	--	.158	--	--	--	
3.79	.138	--	.140	--	--	
4.79	--	.126	--	--	--	
6.29	.144	--	.143	--	--	
6.79	--	.165	--	--	--	

TABLE IV (CONTINUED)

Condition F

 $\alpha = 15^\circ$  Exp

x/d	P/P <sub>t<sub>2</sub></sub>			Temp. ~°F	
	L	C	R	L	R
0.26	.983	--	--	---	---
0	--	.945	--	---	---
0.26	.568	--	--	---	---
0.52	--	--	.221	---	---
0.79	--	.058	--	---	---
1.29	.037	--	.046	824	---
1.79	--	.031	--	---	---
3.79	.017	--	.022	710	727
4.79	--	.020	--	---	---
6.29	.014	--	.019	657	673
6.79	--	.013	--	---	---
8.79	.011	.011	.013	628	643
11.29	.011	--	.014	614	628
13.79	--	--	--	612	622

TABLE IV (CONTINUED)  
Condition F

$\alpha = 5^\circ \text{ Exp}$

x/d	$P/P_{t_2}$			Temp. ~ °F	
	L	C	R	L	R
0.26	.921	--	--	--	--
0	--	.996	--	--	--
0.26	.738	--	--	--	--
0.52	--	--	.333	--	--
0.79	--	.103	--	--	--
1.29	.065	--	.064	--	--
1.79	--	.053	--	--	--
3.79	.040	--	.041	--	--
4.79	--	.032	--	--	--
6.29	.028	--	.028	--	--
6.79	--	.026	--	--	--
8.79	.022	.023	.022	--	--
11.29	.019	.019	.029	--	--
13.79	.018	.020	.014	--	--
16.29	.015	.018	.017	--	--
18.79	.014	.014	.014	--	--

Temperature  
on This Test  
Reproducibility

TABLE IV (CONTINUED)

Condition F

 $\alpha = 10^0$  Exp

x/d	P/P <sub>t<sub>2</sub></sub>			Temp. ~ °F	
	L	C	R	L	R
0.26	.962	--	--	---	---
0	--	.986	--	---	---
0.26	.660	--	--	---	---
0.52	--	--	.277	---	---
0.79	--	.082	--	---	---
1.29	.049	--	.049	804	800
1.79	--	.040	--	---	---
3.79	.031	--	.029	677	686
4.79	--	.025	--	---	---
6.29	.019	--	.022	616	628
6.79	--	.019	--	---	---
8.79	.016	.017	.016	579	588
11.29	.014	.013	.014	551	560
13.79	.012	.012	.011	536	545
16.29	.012	.011	.011	525	---
18.79	.011	.009	.008	517	523
21.29	--	--	--	511	518

TABLE IV (CONTINUED)

## Condition G

 $M = 12.28$  $R_{eD} = 21,300$  $P_{t_a} = 45.5 \text{ mm Hg}$  $\alpha = 0^\circ$ 

s/d	$P/P_{t_a}$			Temp. $\sim {}^\circ F$	
	L	C	R	L	R
0.26	.882	--	--	---	---
0	--	1.00	--	---	---
0.26	.806	--	--	---	---
0.52	--	--	.397	---	---
0.79	--	.126	--	---	---
1.29	.082	--	.082	857	859
1.79	--	.069	--	---	---
3.79	.052	--	.053	721	738
4.79	--	.043	--	---	---
6.29	.038	--	.039	656	670
6.79	--	.035	--	---	---
8.79	.031	.031	.030	611	625
11.29	.025	.025	.024	580	598
13.79	.021	.023	.020	560	568
16.29	.018	.021	.018	543	---
18.79	--	--	--	535	540
21.29	--	--	--	524	528

TABLE IV (CONTINUED)

Condition G

 $\alpha = 5^\circ$  Comp

s/d	P/P <sub>t<sub>2</sub></sub>			Temp. ~ °F	
	L	C	R	L	R
0.26	.819	--	--	---	---
0	--	1.002	--	---	---
0.26	.879	--	--	---	---
0.52	--	--	.473	---	---
0.79	--	.160	--	---	---
1.29	.106	--	.107	862	862
1.79	--	.091	--	---	---
3.79	.070	--	.070	722	742
4.79	--	.059	--	---	---
6.29	.053	--	.053	658	672
6.79	--	.049	--	---	---
8.79	.044	.044	.043	615	630
11.29	.038	.038	.037	588	597
13.79	.034	.037	.032	567	575
16.29	.033	.037	.030	550	---
18.79	.030	.030	.028	540	548
21.29	--	.026	.026	530	537
22.79	--	.024	--	---	---
23.79	.023	.023	.022	---	---

TABLE IV (CONTINUED)  
Condition G

$\alpha = 10^6$  Comp

s/d	P/P <sub>t<sub>2</sub></sub>			Temp. ~°F	
	L	C	R	L	R
0.26	.747	--	--	---	---
0	--	.988	--	---	---
0.26	.946	--	--	---	---
0.52	--	--	.553	---	---
0.79	--	.203	--	---	---
1.29	.139	--	.141	868	845
1.79	--	.115	--	---	---
3.79	.096	--	.096	716	730
4.79	--	.082	--	---	---
6.29	.077	--	.077	650	660
6.79	--	.072	--	---	---
8.79	.067	.066	.066	600	612
11.29	.061	.062	.060	569	579
13.79	--	--	--	549	552
16.29	--	--	--	530	---
18.79	--	--	--	521	526
21.29	--	--	--	511	518

TABLE IV (CONTINUED)

Condition G

 $\alpha = 15^\circ \text{ Comp}$ 

s/d	L	C	R	Temp. ~ °F	
				L	R
0.26	.645	--	--	---	---
0	--	.940	--	---	---
0.26	.976	--	--	---	---
0.52	--	--	.617	---	---
0.79	--	.248	--	---	---
1.29	.176	--	.176	---	---
1.79	--	.153	--	---	---
3.79	.129	--	.127	---	---
4.79	--	.112	--	---	---
6.29	.111	--	.111	---	---
6.79	--	.113	--	---	---
8.79	.105	.113	.105	---	---
11.29	.116	.127	.125	---	---

Temperature  
on the  
Recorder  
before  
Impression

TABLE IV (CONTINUED)

Condition G

 $\alpha = 15^\circ \text{ Exp}$ 

s/d	P/P <sub>t<sub>2</sub></sub>			Temp. ~ °F	
	L	C	R	L	R
0.26	.968	--	--	---	---
0	--	.924	--	---	---
0.26	.560	--	--	---	---
0.52	--	--	.224	---	---
0.79	--	.060	--	---	---
1.29	.083	--	.035	859	860
1.79	--	.028	--	---	---
3.79	.021	--	.022	737	756
4.79	--	.019	--	---	---
6.29	.014	--	.015	680	699
6.79	--	.013	--	---	---
8.79	.011	.011	.011	650	665
11.29	.010	.009	.010	630	644
13.79	--	--	--	620	631
16.29	--	--	--	620	---
18.79	--	--	--	630	640
21.29	--	--	--	650	651

TABLE IV (CONTINUED)  
Condition G

$\alpha = 5^\circ \text{ Exp}$

s/d	$P/P_{t_0}$			Temp. $\sim 0^\circ \text{F}$	
	L	C	R	L	R
0.26	.926	--	--	---	---
0	--	.972	--	---	---
0.26	.727	--	--	---	---
0.52	--	--	.330	---	---
0.79	--	.254	--	---	---
1.29	.071	--	.062	---	---
1.79	--	.051	--	---	---
3.79	.038	--	.039	---	---
4.79	--	.031	--	---	---
6.29	.027	--	.028	---	---
6.79	--	.025	--	---	---
8.79	.021	.022	.020	---	---
11.29	.018	.017	.017	---	---
13.79	.014	.016	.013	---	---
16.29	.013	.013	.012	---	---
18.79	.011	.012	.010	---	---
21.29	--	.012	.092	---	---
22.79	--	.010	--	---	---

Temperature Recorder Inoperative  
on this Test

TABLE IV (CONTINUED)  
Condition G

$\alpha = 10^0$  Exp

s/d	$P/P_{t_a}$			Temp. ~ °F	
	L	C	R	L	R
0.26	.956	--	--	---	---
0	--	.956	--	---	---
0.26	.647	--	--	---	---
0.52	--	--	.273	---	---
0.79	--	--	--	---	---
1.29	.046	--	.047	869	870
1.79	--	.038	--	---	---
3.79	.028	--	.029	745	763
4.79	--	.023	--	---	---
6.29	.019	--	.020	690	703
6.79	--	.018	--	---	---
8.79	.016	.016	.015	660	670
11.29	.012	.012	.012	641	650
13.79	.012	.011	.009	630	635
16.29	.009	.009	.009	620	---
18.79	--	--	--	615	620
21.29	--	.008	--	610	615

TABLE V

Distributions of Pressure and Temperature  
on the Blunt Flat Plate at  $M = 14$

## Condition H

 $M = 14.2$  $R_{eD} = 12,700$  $P_{t_2} = 19.9 \text{ mm Hg}$  $\alpha = 0^\circ$ 

s/d	L	C	R	Temp. $\sim {}^{\circ}\text{F}$		Temperature Recorder Inoperative on this Test
				L	R	
0.26	1.364	--	--			
0	--	1.000	--			
0.26	.782	--	--			
0.52	--	--	.399			
0.79	--	1.365	--			
1.29	.093	--	.094			
1.79	--	.074	--			
3.79	.057	--	.057			
4.79	--	.049	--			
6.29	.044	--	.042			
6.79	--	.042	--			
8.79	.036	.037	.034			
11.29	.031	.034	.029			
13.79	.027	.030	.027			
16.29	.024	.026	.022			
18.79	.023	.024	.020			
21.29	--	.023	.021			
22.79	--	.023	--			
23.79	.020	.020	.019			

TABLE V (CONTINUED)  
Condition H

$\alpha = 5^\circ$  Comp

s/d	L	C	R	Temp. ~°F		Temperature Recorder Inoperative on this Test
				L	R	
0.26	1.466	--	--			
0	--	.999	--			
0.26	.831	--	--			
0.52	--	--	.474			
0.79	--	.171	--			
1.29	.121	--	.124			
1.79	--	.098	--			
3.79	.078	--	.077			
4.79	--	.066	--			
6.29	.062	--	.059			
6.79	--	.060	--			
8.79	.053	.053	.049			
11.29	.047	.048	.047			
13.79	.042	.045	.043			

TABLE V (CONTINUED)  
Condition H

$\alpha = 5^\circ \text{ Exp}$

x/d	P/P <sub>t<sub>2</sub></sub>			Temp. ~ °F		Temperature Recorder Inoperative on this Test
	L	C	R	L	R	
0.26	1.579	--	--			
0	--	1.003	--			
0.26	.734	--	--			
0.52	--	--	.339			
0.79	--	.117	--			
1.29	.072	--	.072			
1.79	--	.056	--			
3.79	.044	--	.045			
4.79	--	.038	--			
6.29	.034	--	.033			
6.79	--	.033	--			
8.79	.027	.027	.025			
11.29	.023	.025	.039			
13.79	.019	.021	.019			
16.29	.017	.018	.015			
18.79	.017	.016	.014			

TABLE V (CONTINUED)

## Condition I

 $M = 14.28$  $Re_D = 16,000$  $P_{t_2} = 24.8 \text{ mm Hg}$  $\alpha = 0^\circ$ 

s/d	$P/P_{t_2}$			Temp. $\sim {}^{\circ}\text{F}$	
	L	C	R	L	R
0.26	.943	--	--	---	---
0	--	1.000	--	---	---
0.26	.796	--	--	---	---
0.52	--	--	.374	---	---
0.79	--	.125	--	---	---
1.29	.089	--	.092	665	---
1.79	--	.070	--	---	---
3.79	.053	--	.053	503	521
4.79	--	.047	--	---	---
6.29	.040	--	.039	409	427
6.79	--	.040	--	---	---
8.79	.033	.036	.031	340	360
11.29	.027	.031	.027	298	316
13.79	.024	.021	.024	266	279
16.29	.021	.024	.023	245	---
18.79	.020	.020	.017	232	245
21.29	--	.019	.016	225	232
22.79	--	.016	--	---	---

TABLE V (CONTINUED)

Condition I

 $\alpha = 5^\circ$  Comp

s/d	$P/P_{t_0}$			Temp. $\sim {}^{\circ}\text{F}$	
	L	C	R	L	R
0.26	.965	--	--	---	---
0	--	.996	--	---	---
0.26	.846	--	--	---	---
0.52	--	--	.450	---	---
0.79	--	.159	--	---	---
1.29	.115	--	.118	720	---
1.79	--	.096	--	---	---
3.79	.074	--	.071	574	582
4.79	--	.064	--	---	---
6.29	.056	--	.055	491	500
6.79	--	.056	--	---	---
8.79	.044	.036	.046	430	445
11.29	.042	.044	.040	390	400
13.79	.036	.034	.037	359	369

TABLE V (CONTINUED)  
Condition I

$\alpha = 10^6$  Comp

s/d	P/P <sub>t<sub>2</sub></sub>			Temp. ~ °F	
	L	C	R	L	R
0.26	.944	--	--	---	---
0	--	.981	--	---	---
0.26	.904	--	--	---	---
0.52	--	--	.529	---	---
0.79	--	.204	--	---	---
1.29	.163	--	.171	762	---
1.79	--	.130	--	---	---
3.79	.100	--	.097	628	634
4.79	--	.067	--	---	---
6.29	.084	--	.080	558	562
6.79	--	.081	--	---	---
8.79	.074	.077	.074	504	518
11.29	.072	.072	.071	472	481
13.79	.068	.067	.069	450	453

TABLE V (CONTINUED)  
Condition I

$\alpha = 5^\circ$  Exp

s/d	$P/P_{t_2}$			Temp. ~ °F	
	L	C	R	L	R
0.26	1.119	--	--	---	---
0	--	1.000	--	---	---
0.26	.741	--	--	---	---
0.52	--	--	.317	---	---
0.79	--	.142	--	---	---
1.29	.068	--	.069	754	---
1.79	--	.055	--	---	---
3.79	.043	--	.040	630	640
4.79	--	.034	--	---	---
6.29	.030	--	.030	566	572
6.79	--	.030	--	---	---
8.79	.015	.024	.024	521	530
11.29	.033	.022	.034	492	500
13.79	.017	.016	.017	472	480
16.29	.016	.017	.016	460	---
18.79	.015	.015	.014	450	452

TABLE V (CONTINUED)  
Condition I

$\alpha = 10^0$  Exp

s/d	$P/P_{t_3}$			Temp. $\sim {}^\circ F$	
	L	C	R	L	R
0.26	1.17	--	--	---	---
0	--	.992	--	---	---
0.26	.684	--	--	---	---
0.52	--	--	.269	---	---
0.79	--	.051	--	---	---
1.29	.052	--	.055	761	---
1.79	--	.042	--	---	---
3.79	.031	--	.030	639	648
4.79	--	.027	--	---	---
6.29	.022	--	.022	577	586
6.79	--	.024	--	---	---
8.79	.017	.018	.015	538	543
11.29	--	--	--	510	519
13.79	--	--	--	492	500
16.29	--	--	--	481	---
18.79	--	--	--	474	480
21.29	--	--	--	470	476

TABLE VI  
Cylinder Test Conditions

Condition	Mach No.	P <sub>o</sub> psia	T <sub>o</sub> °R	T <sub>w</sub> °F	P(0) mm/Hg	R <sub>eD</sub>
A	10.45	117	1960	735	14.06	1,905
B	10.61	150	1860	690	16.94	3,130
C	10.37	190	1965	820	23.50	3,770
D	10.71	150	1460	505	16.82	4,120
E	10.60	400	1470	570	46.87	11,142
F	10.86	600	1080	300	63.74	22,797
G	11.76	250	1960	715	17.27	3,418
H	12.11	303	1965	720	18.20	3,758
J	12.37	790	1970	920	42.94	9,140
K	12.10	362	1975	725	30.40	11,000
L	14.44	875	2450	1050	21.40	4,564
M	15.37	1485	1810	810	28.47	9,072
N	15.00	1495	1700	730	32.70	10,768

TABLE VII  
Pressure Distributions on the Cylinders at  $M_\infty = 10.5$

Condition	A	B	C	D	E	F
$M_\infty$	10.45	10.61	10.37	10.71	10.60	10.86
$R_{eD}$	1,905	3,130	3,770	4,120	11,142	22,797
$\theta$	$P(\theta)/P(0)$					
0	1.000	1.000	1.000	1.000	1.000	1.000
5	0.992	0.997	-	0.996	0.996	-
10	-	-	0.976	0.984	0.981	0.989
15	0.946	0.951	-	0.962	0.953	-
20	-	-	0.908	0.920	0.916	0.928
25	0.849	0.870	-	0.874	0.866	-
30	-	-	0.805	0.813	0.814	0.825
35	0.738	0.746	-	0.753	-	-
40	-	-	0.670	0.681	0.682	0.695
45	0.602	0.606	-	0.612	-	-
50	-	-	0.519	0.528	0.519	0.537
55	0.457	0.458	-	0.462	-	-
60	-	-	0.381	0.388	0.371	0.372
65	0.323	0.319	-	0.327	-	-
70	-	-	0.260	0.272	0.247	0.247
75	0.223	0.221	-	0.227	-	-
80	-	-	0.179	0.184	0.164	0.160
85	0.142	0.143	-	0.149	0.128	-
90	-	-	0.122	0.120	0.104	0.099
95	0.089	0.092	-	0.097	0.083	-
100	-	-	0.086	0.076	0.067	0.063
105	0.054	0.056	-	0.061	0.055	-
110	-	-	0.067	0.048	0.045	0.041
115	0.033	0.034	-	0.038	0.038	-
120	-	-	0.057	0.030	0.034	0.029
125	0.022	0.023	-	0.026	0.031	-
130	-	-	0.052	0.021	0.029	0.0228
135	0.017	0.020	-	0.020	0.0277	-
140	-	-	0.0503	0.019	0.0274	0.0221
145	0.017	0.020	-	0.020	0.0276	-
150	-	-	0.0505	0.021	0.028	0.024
155	0.020	0.021	-	0.023	0.029	-
160	-	-	0.053	0.025	0.031	0.025
165	0.024	0.027	-	0.026	0.032	-
170	-	-	0.055	0.028	0.032	0.026
175	0.026	0.027	-	0.029	0.033	-
180	-	-	0.055	-	0.033	0.027

TABLE VIII

Pressure Distributions on  
Cylinders at  $M = 12$

Condition	G	H	J	K
$M_\infty$	11.76	12.11	12.37	12.10
$R_{ep}$	3,418	3,758	9,140	11,000
$\theta$	$P(\theta)/P(0)$			
0	1.000	1.000	1.000	1.000
5	-	0.995	0.999	1.000
10	0.982	0.985	0.988	0.990
15	-	0.970	0.966	0.970
20	0.926	0.951	0.936	0.937
25	-	0.923	0.893	0.888
30	0.827	0.858	0.845	-
35	-	0.783	-	0.768
40	0.706	0.699	0.723	-
45	-	0.618	-	0.622
50	6.561	-	0.572	-
55	-	0.451	-	0.465
60	0.420	-	0.420	-
65	-	0.315	-	0.331
70	0.294	-	0.287	-
75	-	0.211	-	0.224
80	0.188	-	0.194	0.184
85	-	0.139	-	0.150
90	0.122	-	0.125	0.118
95	-	0.089	-	0.095
100	0.078	-	0.073	0.076
105	-	0.061	0.056	0.058
110	0.049	-	0.044	0.044
115	-	0.044	0.034	0.036
120	0.031	-	0.026	-
125	-	0.037	0.019	0.021
130	0.021	0.034	0.015	-
135	-	0.033	0.012	0.018
140	0.016	0.032	0.010	-
145	-	0.030	0.009	0.013
150	0.014	0.029	0.010	-
155	-	0.030	0.011	0.016
160	0.015	-	0.012	-
165	-	0.031	0.014	0.018
170	0.017	-	0.016	0.020
175	-	0.033	0.017	-
180	0.018	-	0.018	-

TABLE IX

Pressure Distributions on  
Cylinders at  $M = 15$

L	M	N
14.44	15.37	15.00
4,564	9,072	10,768
$\theta$	$P(\theta)/P(0)$	
0	1.000	1.000
5	0.994	0.998
10	0.978	0.984
15	0.952	0.953
20	0.918	0.920
25	0.875	0.870
30	0.828	0.822
35	-	-
40	0.705	0.691
45	-	-
50	0.574	0.538
55	-	-
60	0.445	0.395
65	-	-
70	0.326	0.268
75	-	-
80	0.238	0.186
85	-	-
90	0.159	0.122
95	-	-
100	0.101	0.080
105	0.089	-
110	0.075	0.051
115	0.064	-
120	0.059	0.031
125	0.0587	-
130	0.0534	0.022
135	0.062	0.021
140	0.065	0.020
145	-	0.021
150	0.073	0.022
155	0.024	-
160	0.084	0.027
165	0.086	-
170	0.091	0.030
175	-	-
180	0.093	0.032

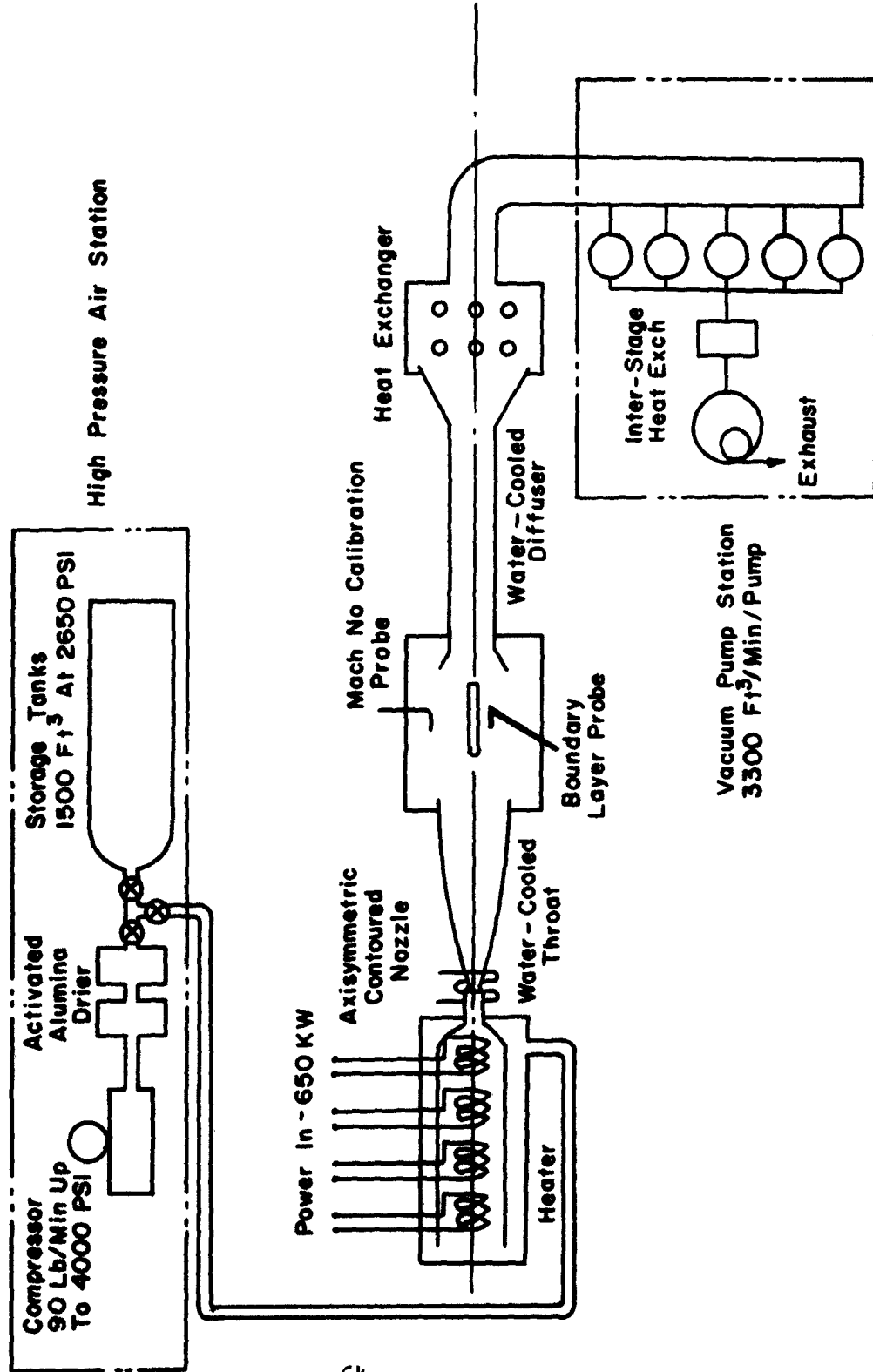
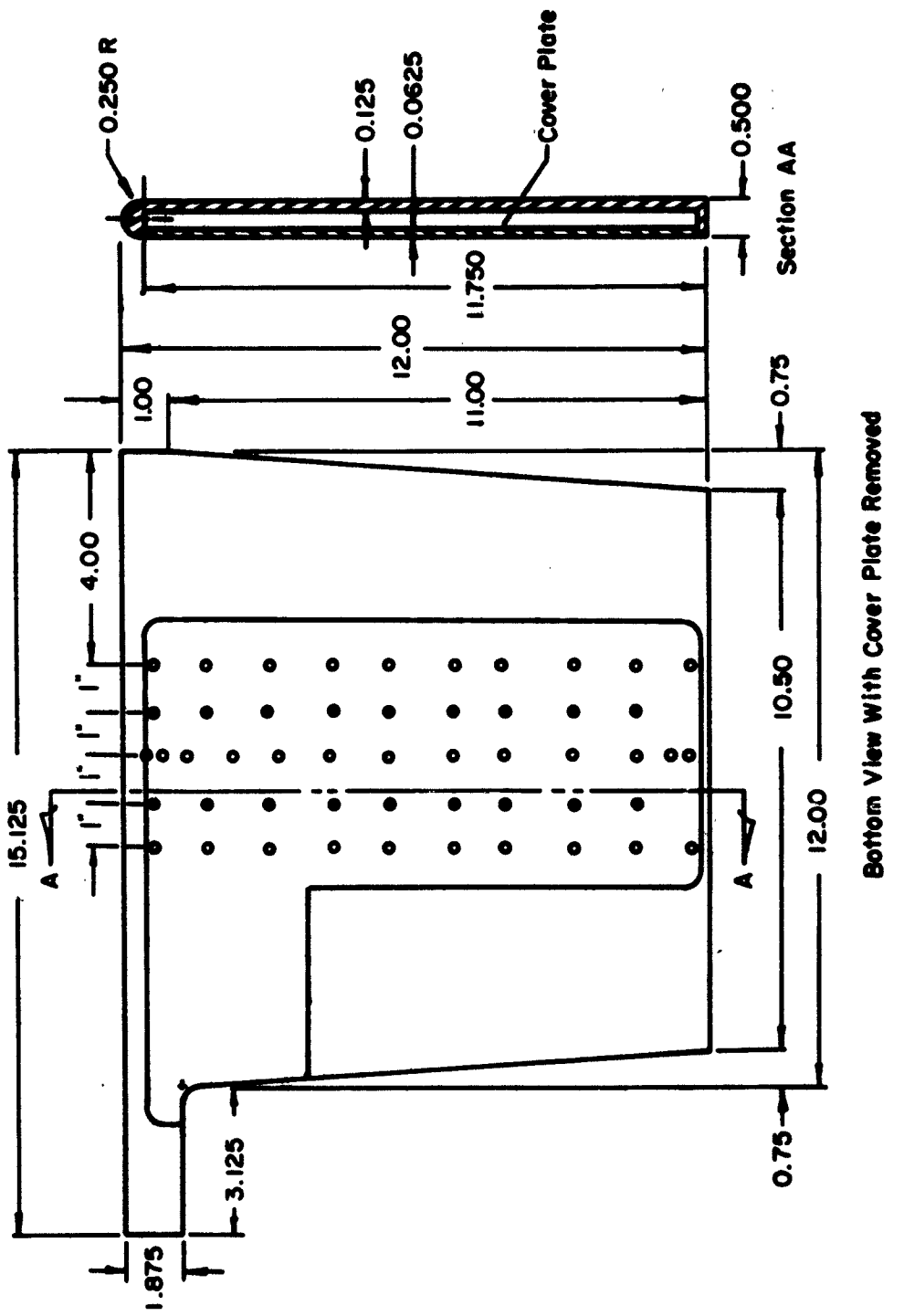


Figure 1 The Ohio State University 12 Inch Hypersonic Wind Tunnel Schematic



### **Bottom View With Cover Plate Removed**

**Figure 2** Flat Plate Dimensions

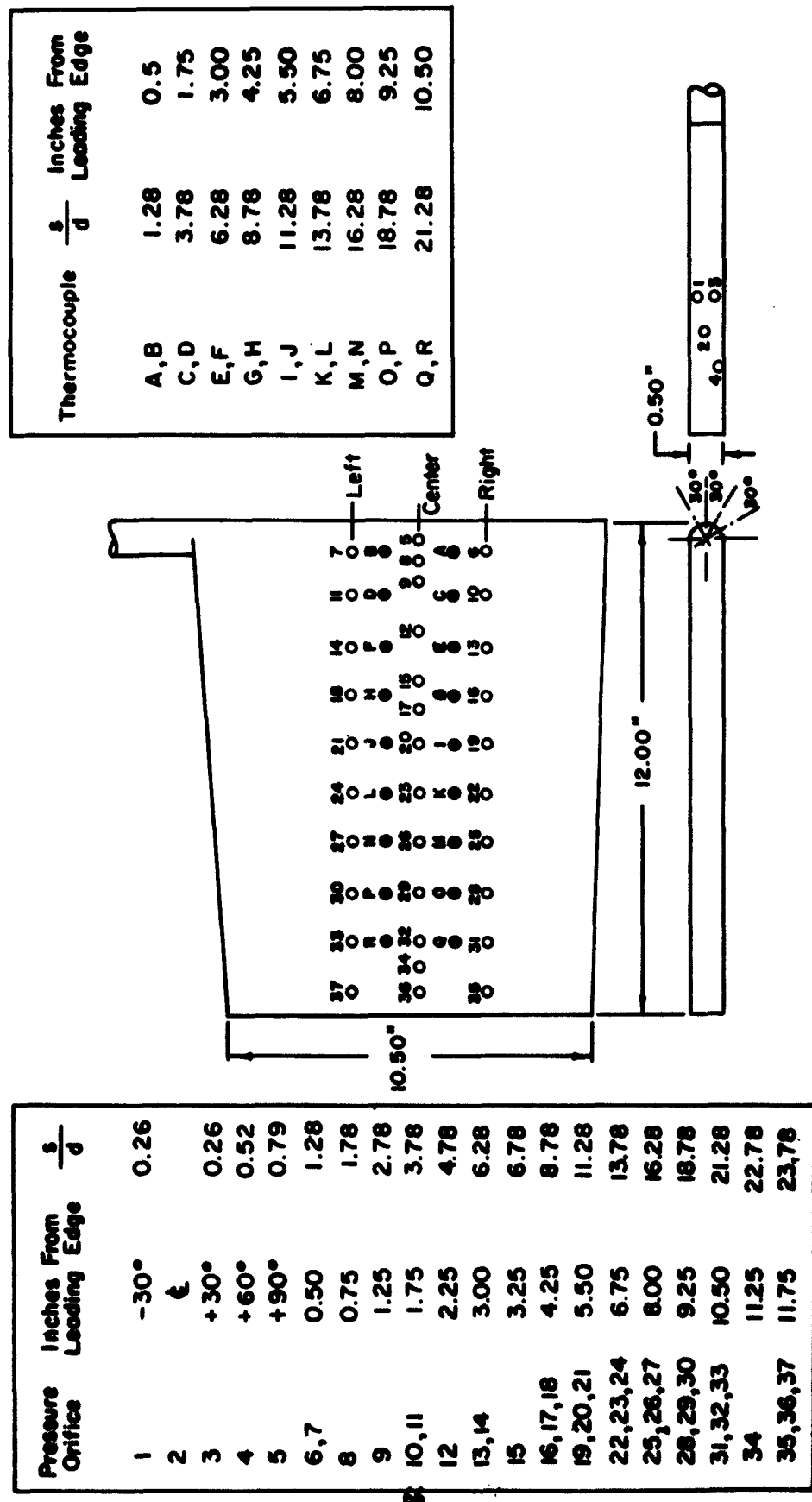
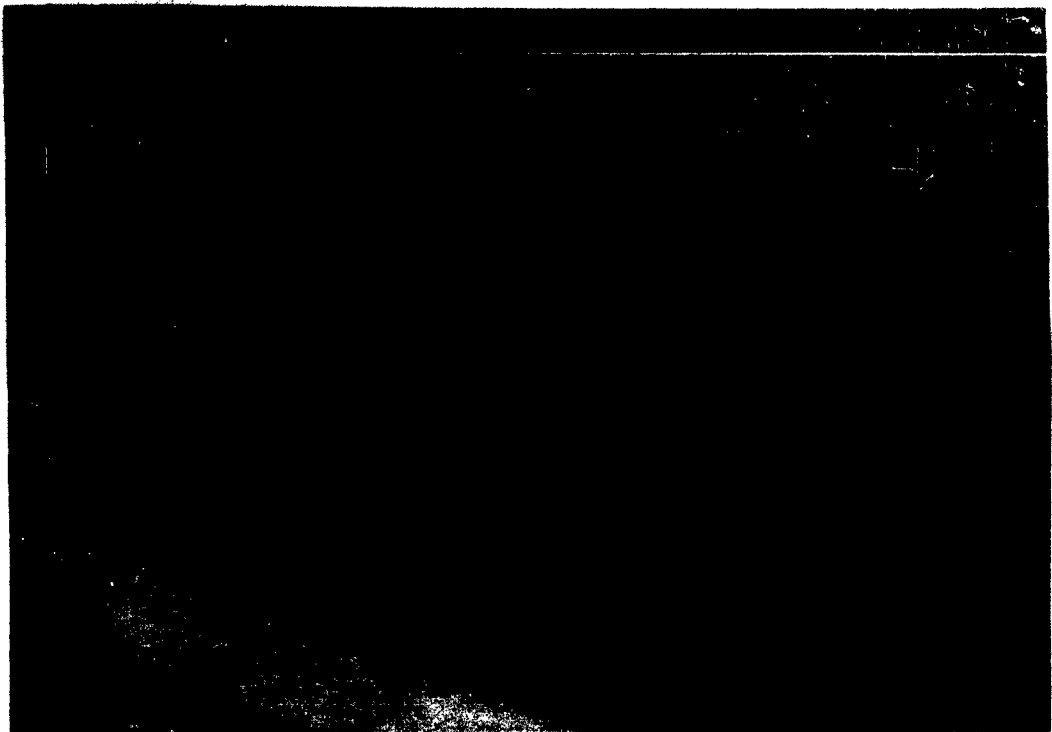
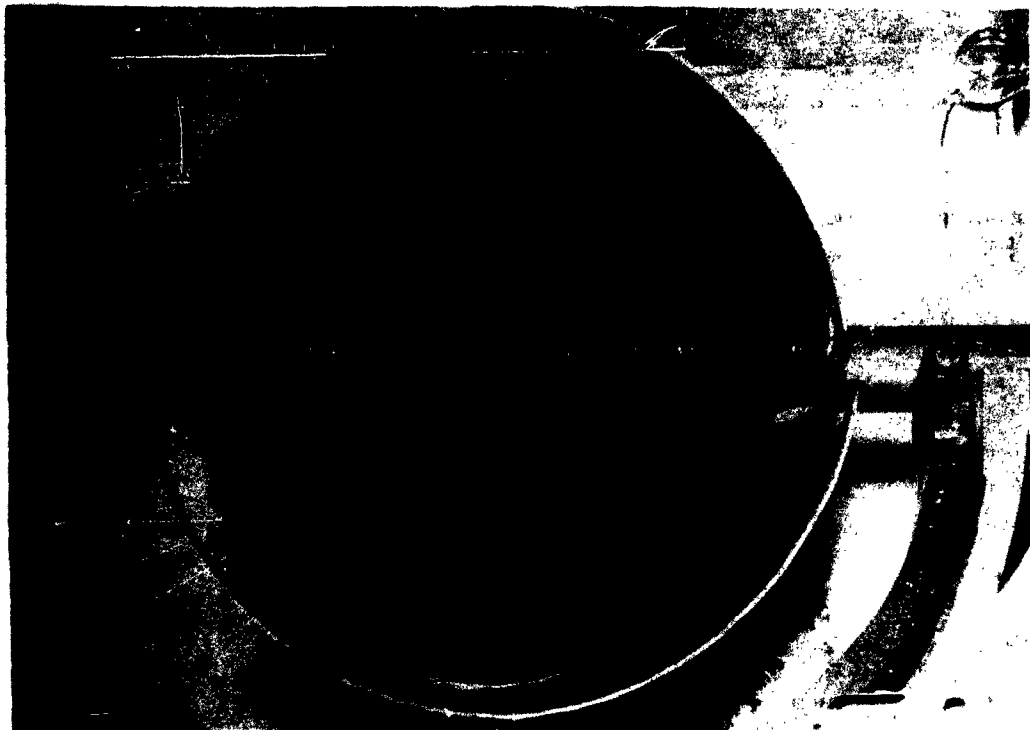


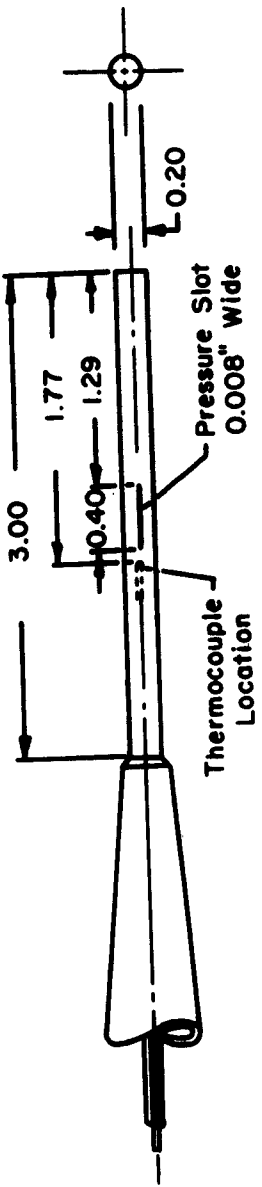
Figure 3 Flat Plate Orifice And Thermocouple Locations



**Figure 4 The Completed Flat Plate Model**



**Figure 5 Model Installation**



0.20" O.D. Cylinder Model

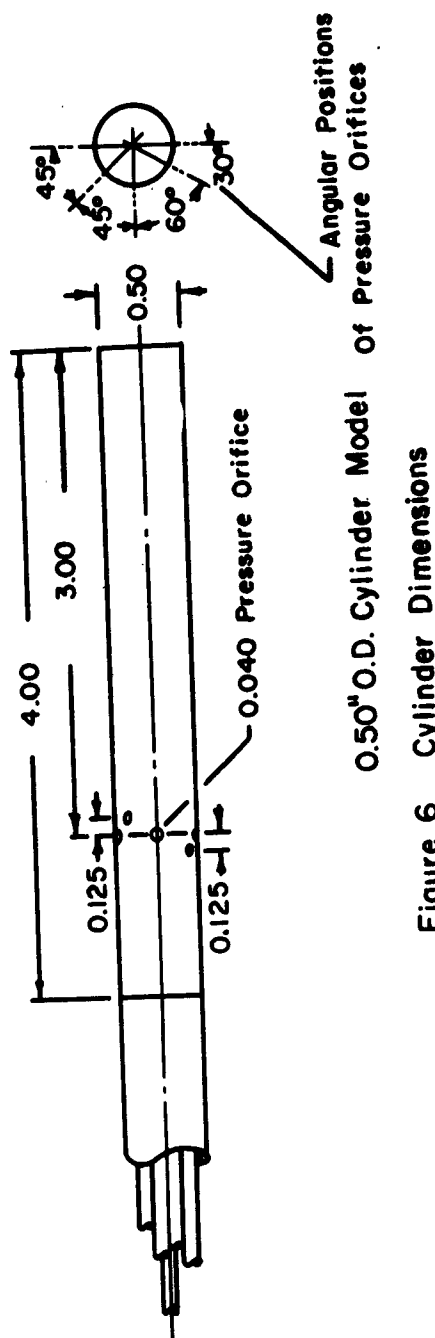
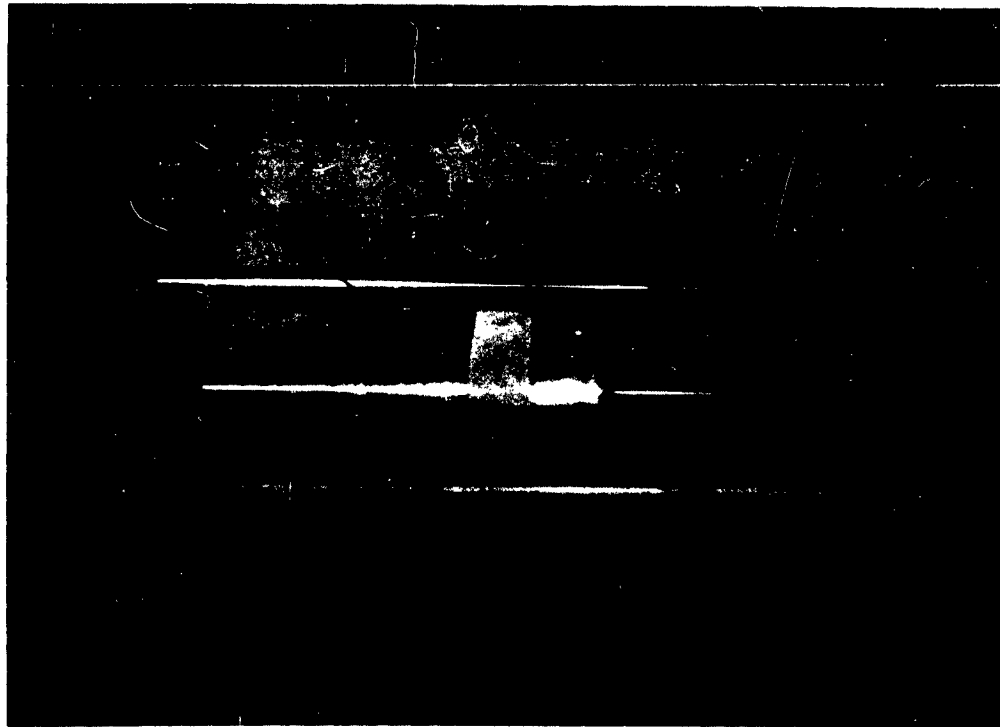
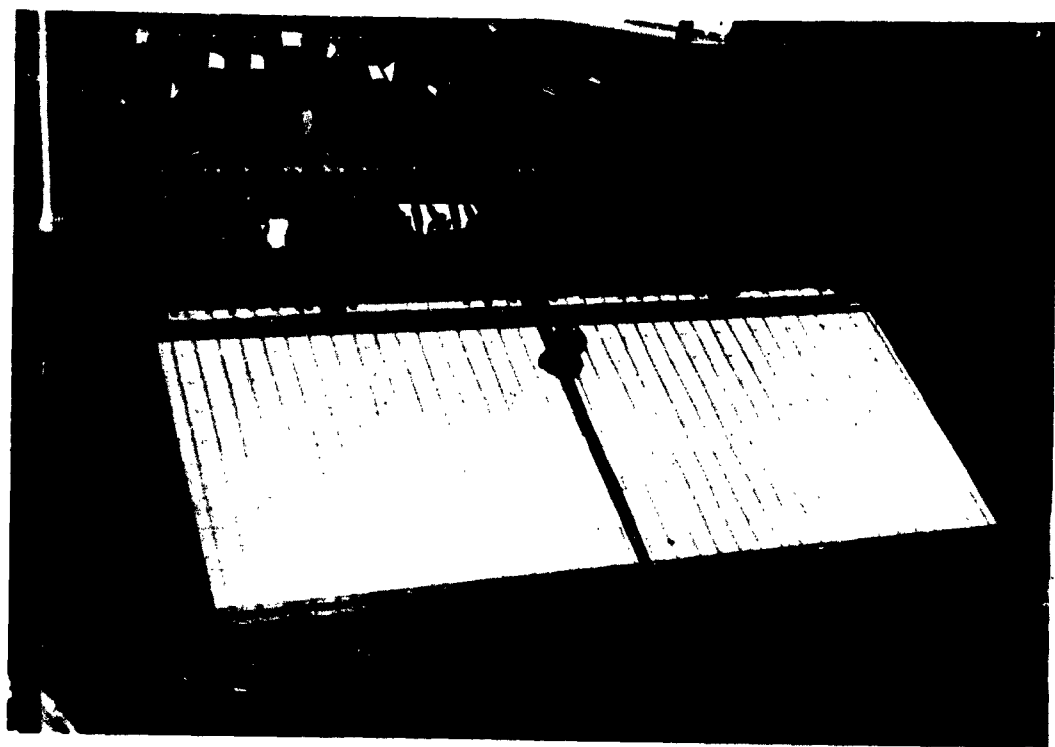


Figure 6 Cylinder Dimensions



**Figure 7   The Cylinders**



**Figure 8 Inclinable Manometer Board**

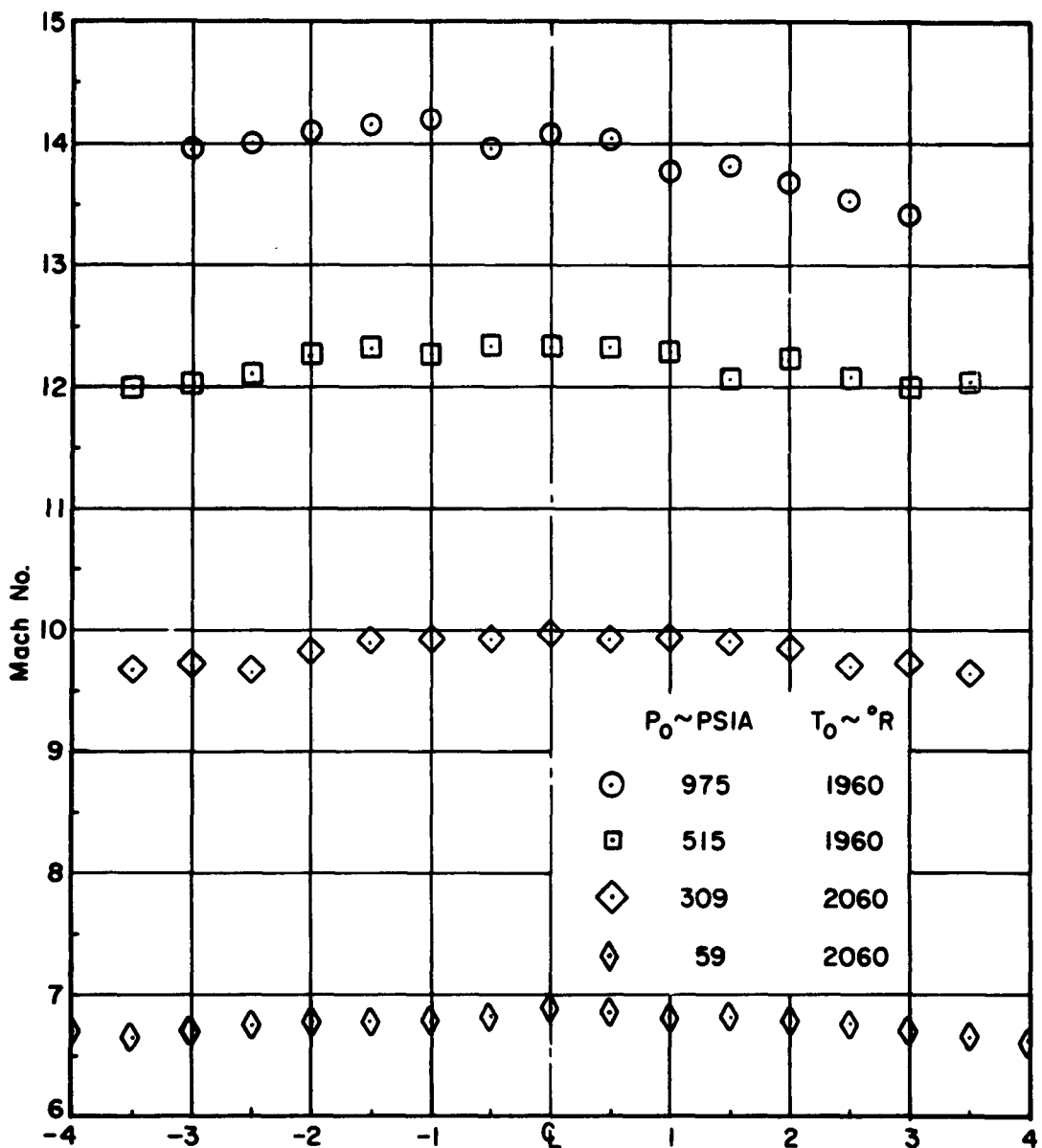


Figure 9 Nozzle Calibrations At Model Leading Edge

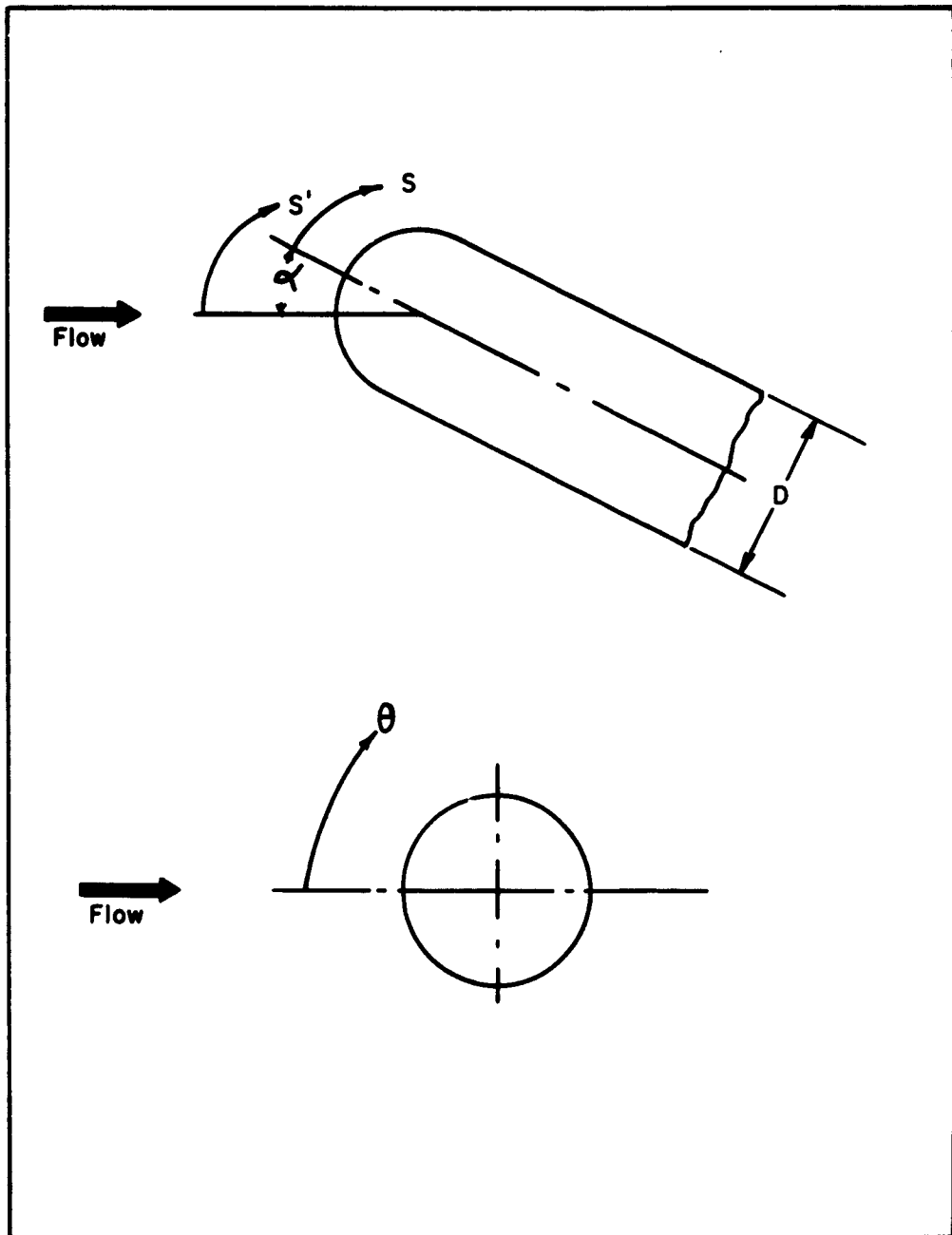


Figure 10 Coordinate Systems Used For The Flat Plate  
And The Cylinder

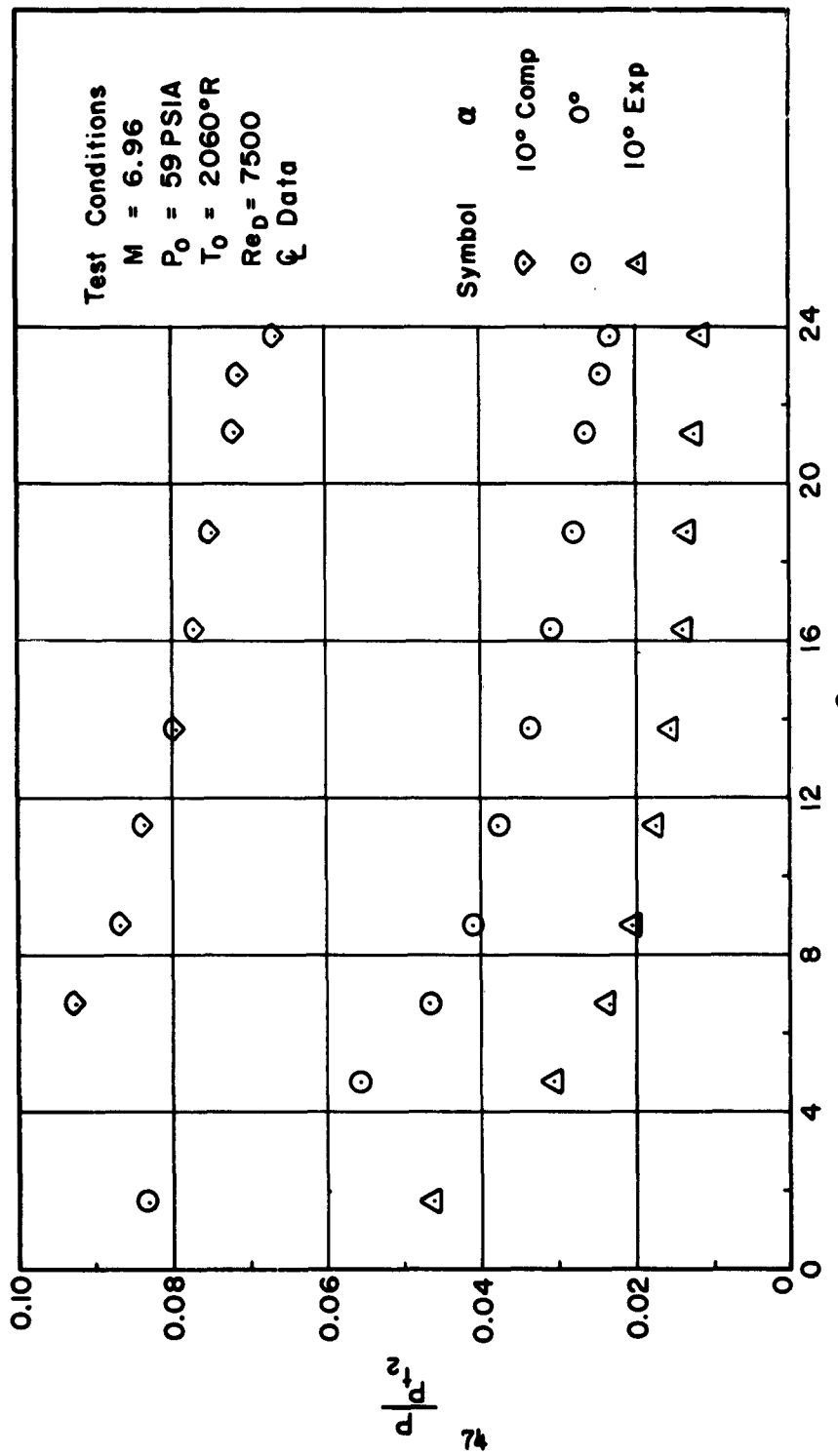


Figure 11 Pressure Distribution Over The Flat Plate —  $M = 7$ ,  $Re_D = 7500$

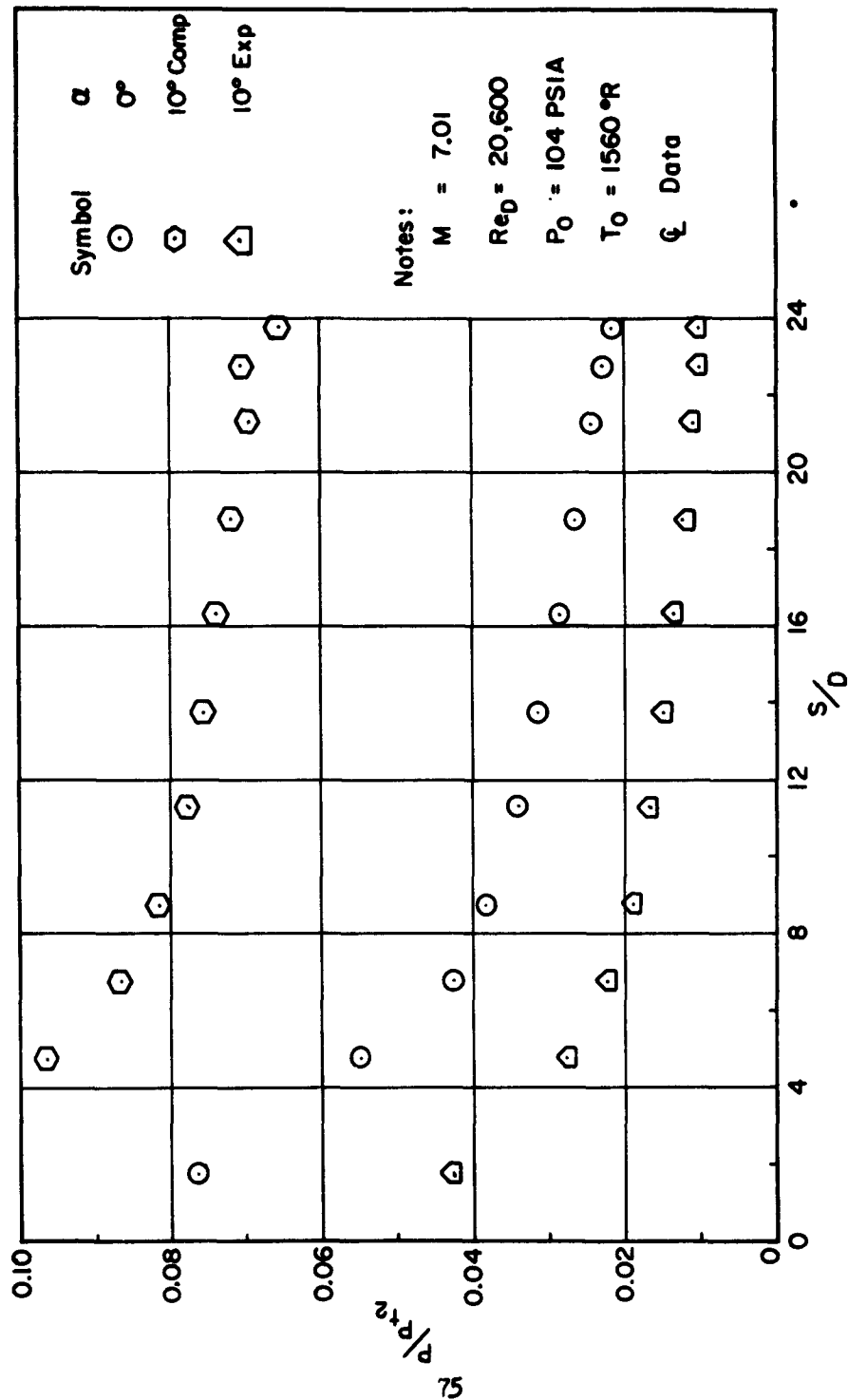


Figure 12 Pressure Distribution Over The Flat Plate-M = 7 ,  $Re_D = 20,600$

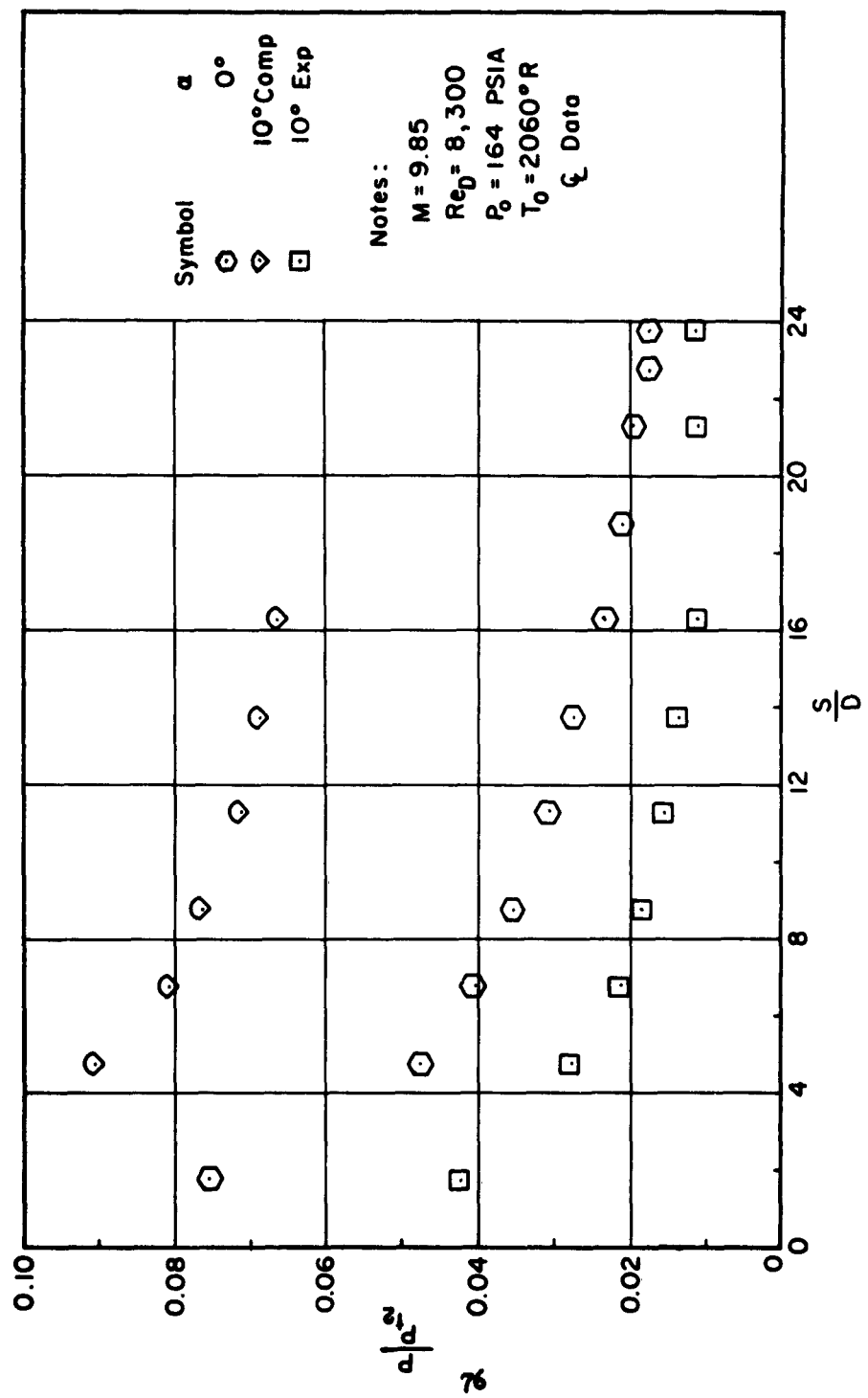


Figure 13 Pressure Distribution Over The Flat Plate —  $M = 10$ ,  $Re_0 = 8,300$

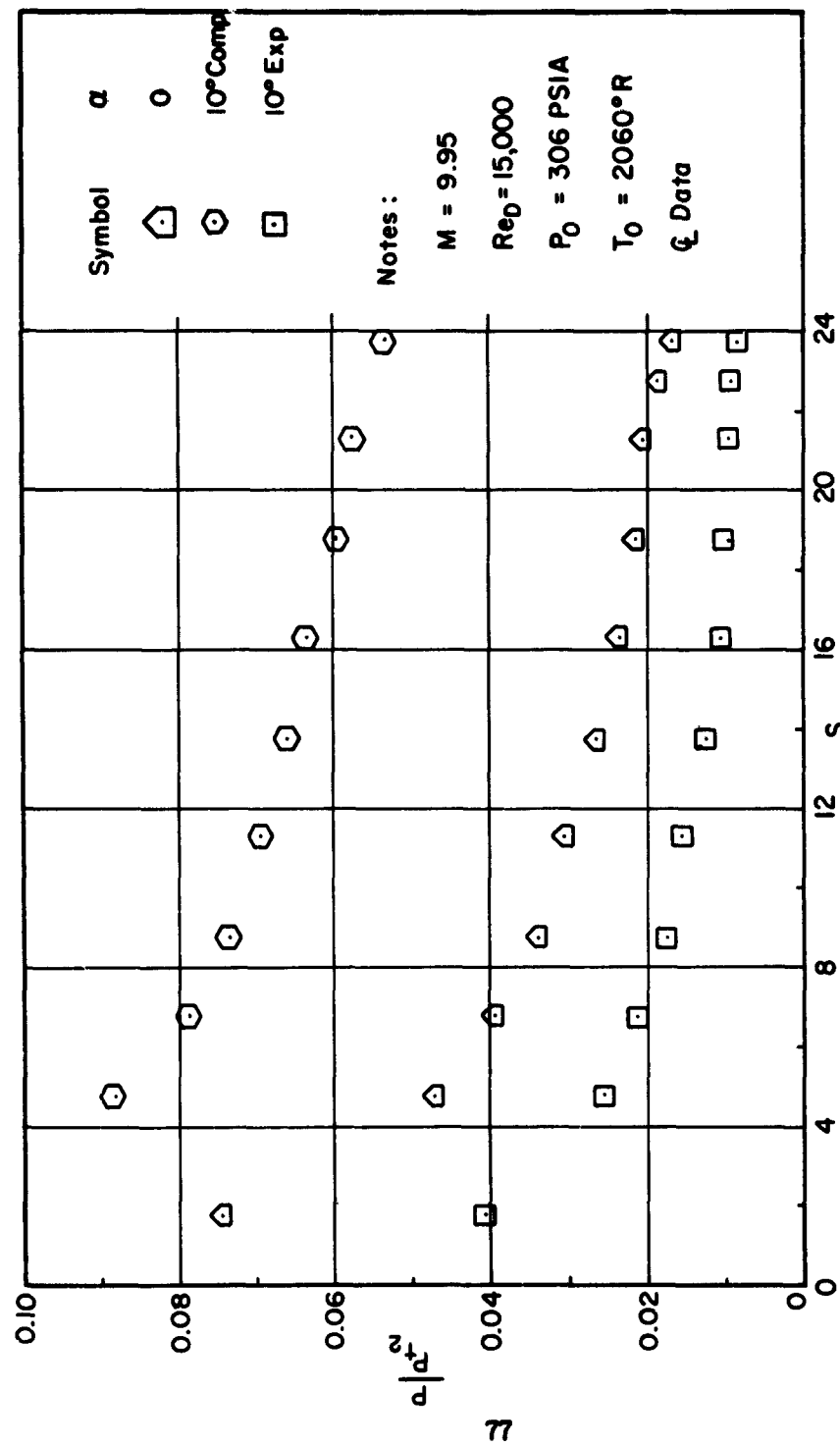


Figure 14 Pressure Distribution Over The Flat Plate —  $M = 10$ ,  $Re_D = 15,000$

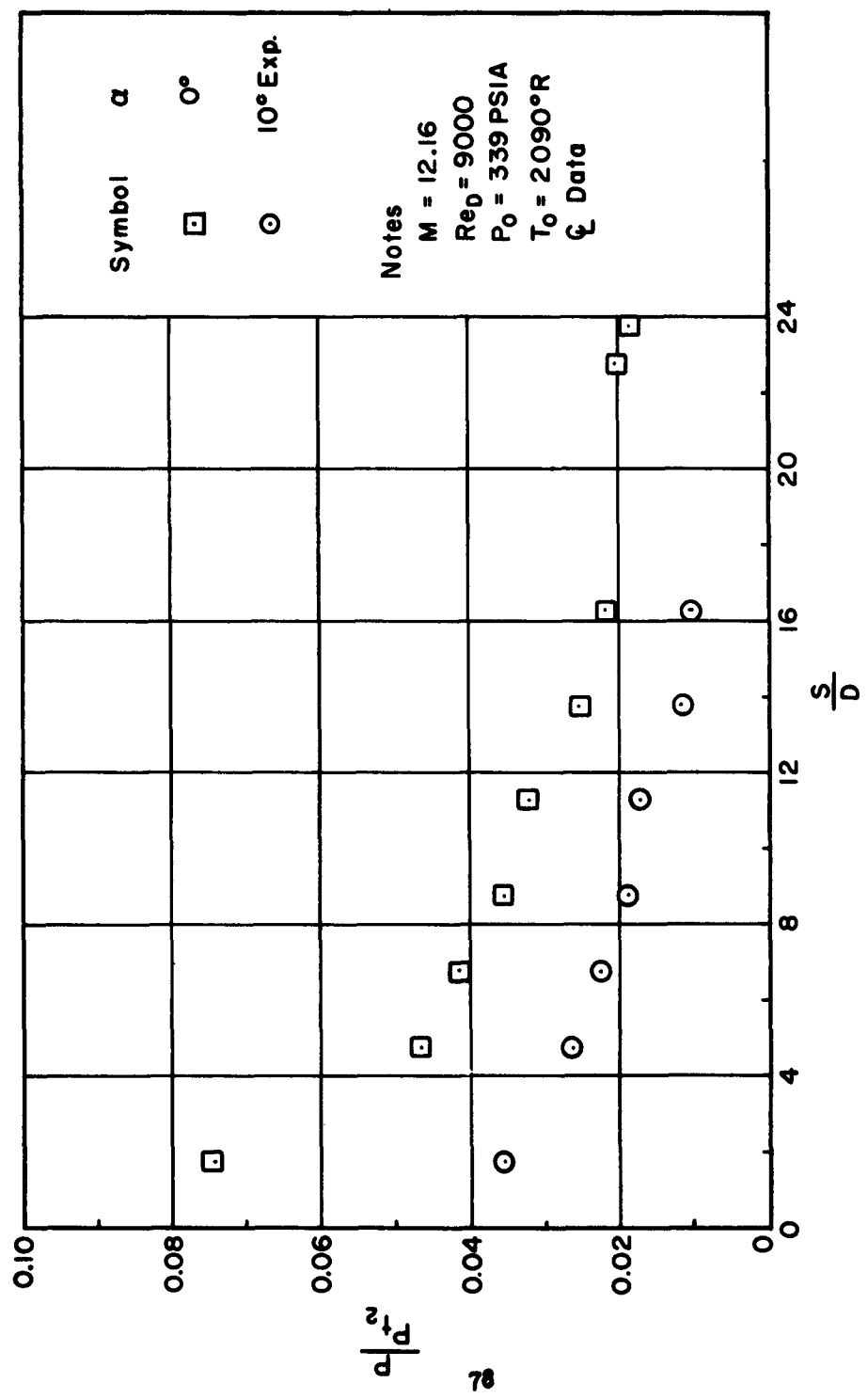


Figure 15 Pressure Distribution Over The Flat Plate —  $M = 12$ ,  $Re_D = 9000$

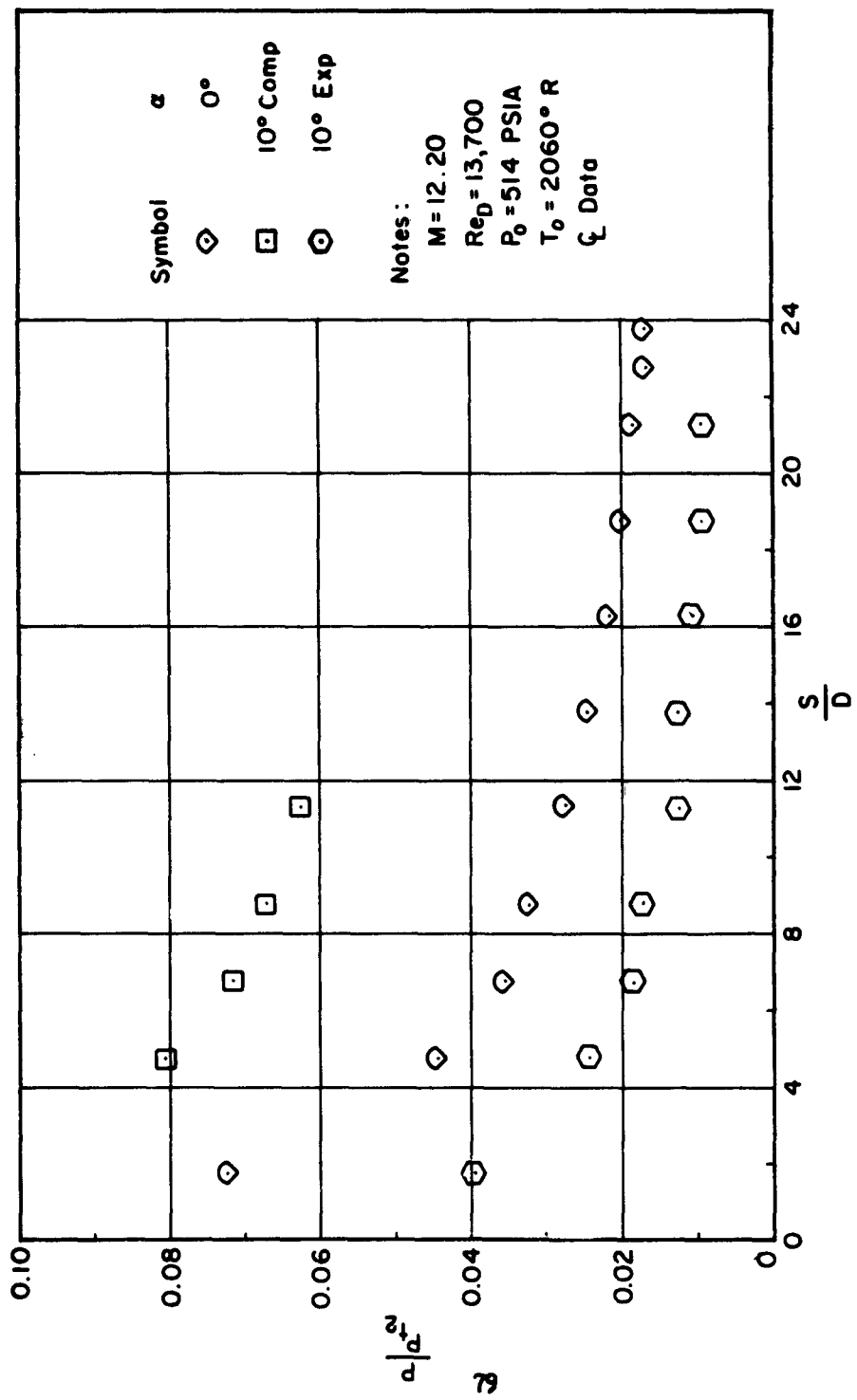


Figure 16 Pressure Distribution Over The Flat Plate —  $M = 12$ ,  $Re_D = 13,700$

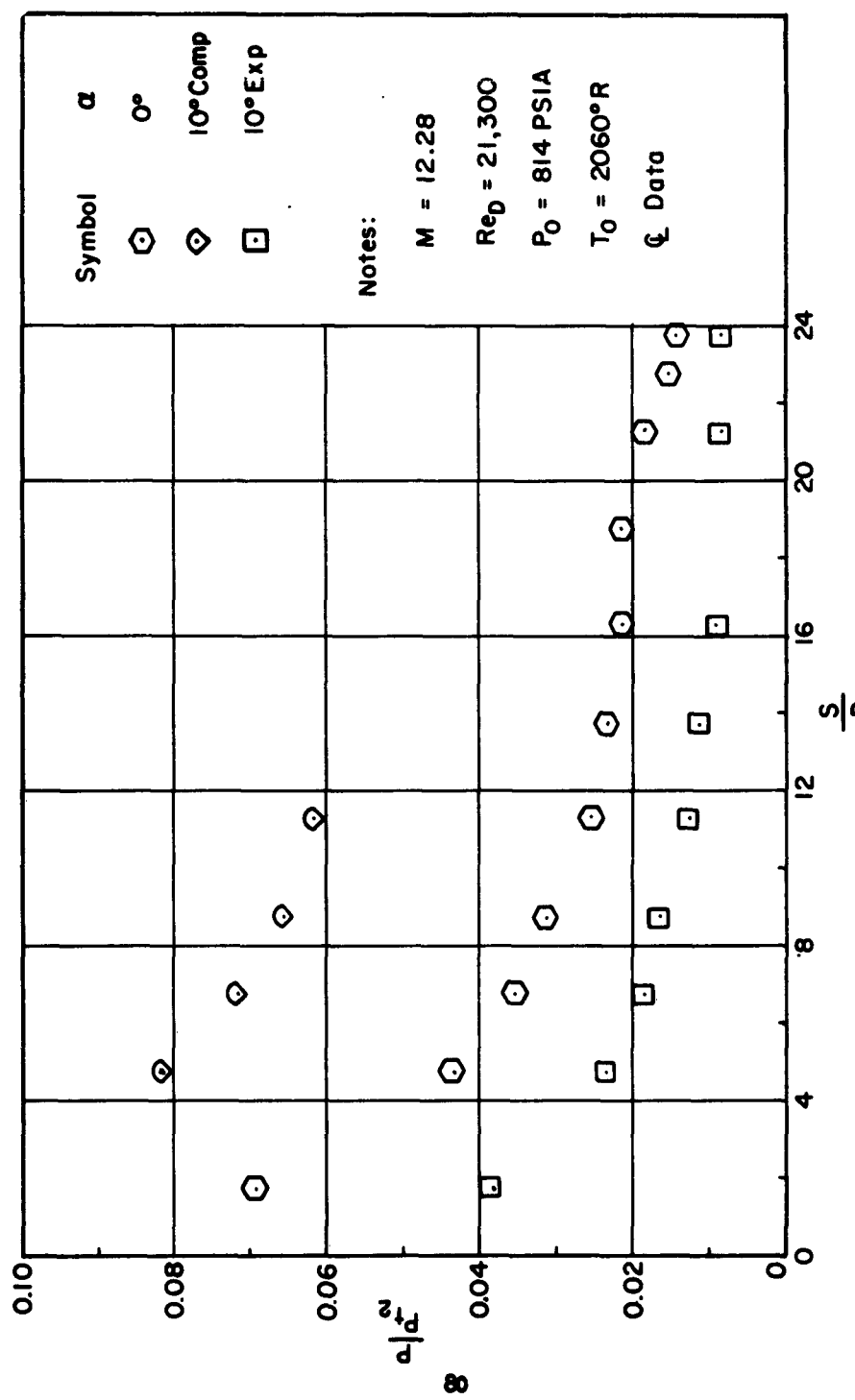


Figure 17 Pressure Distribution Over The Flat Plate —  $M = 12$ ,  $Re_D = 21,300$

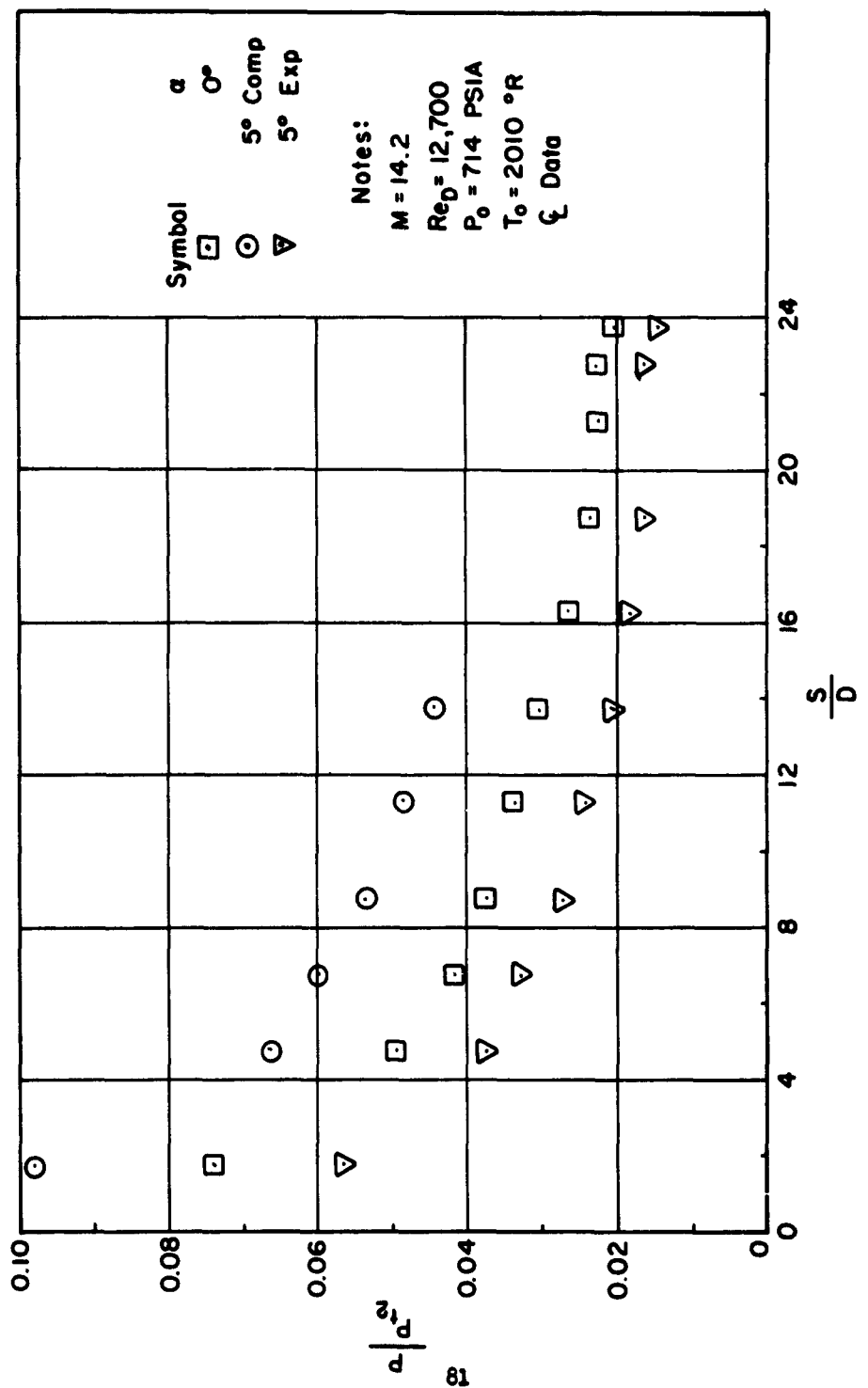


Figure 18 Pressure Distribution Over The Flat Plate —  $M = 14$  ,  $Re_D = 12,700$

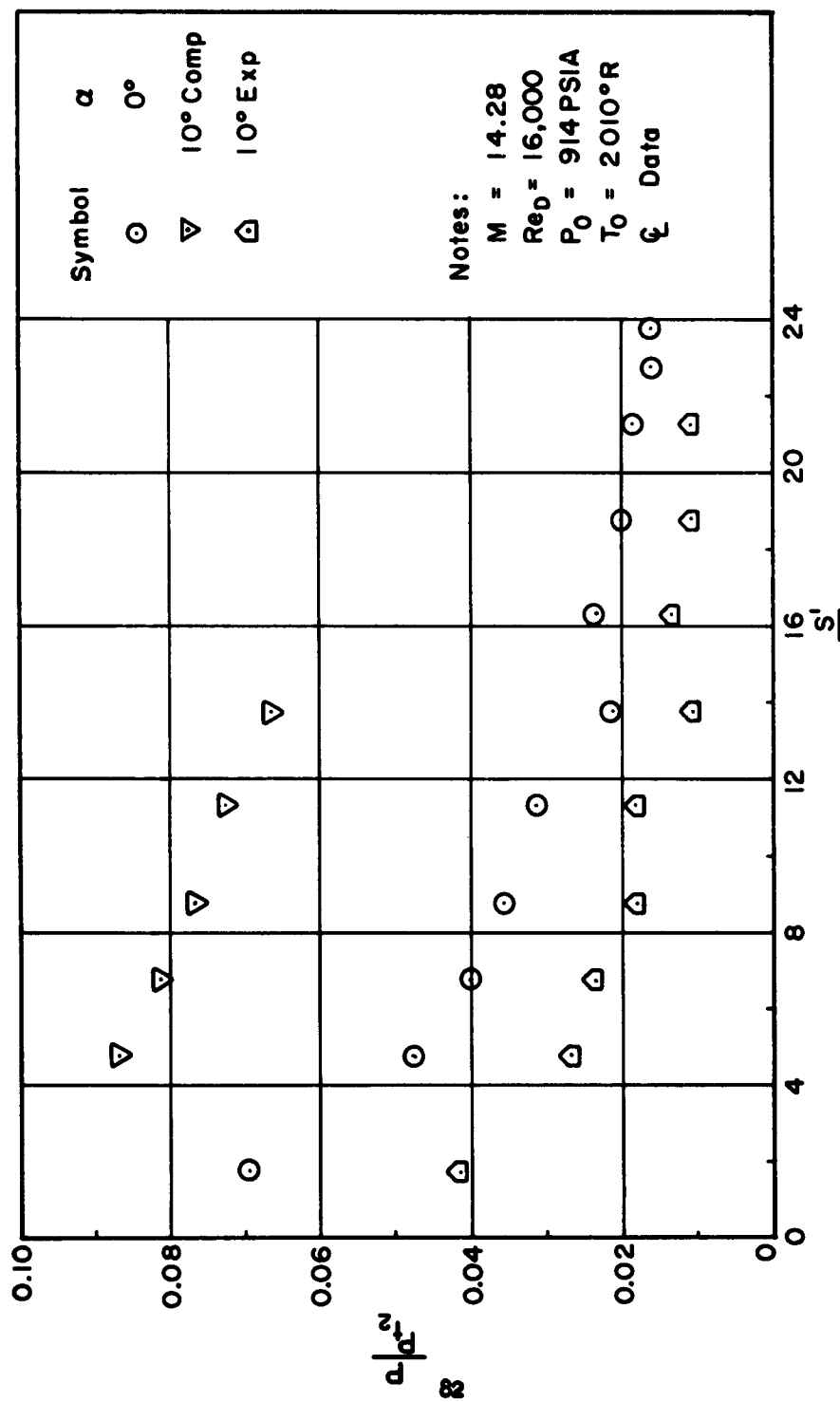


Figure 19 Pressure Distribution Over The Flat Plate— $M = 14$ ,  $Re_D = 16,000$

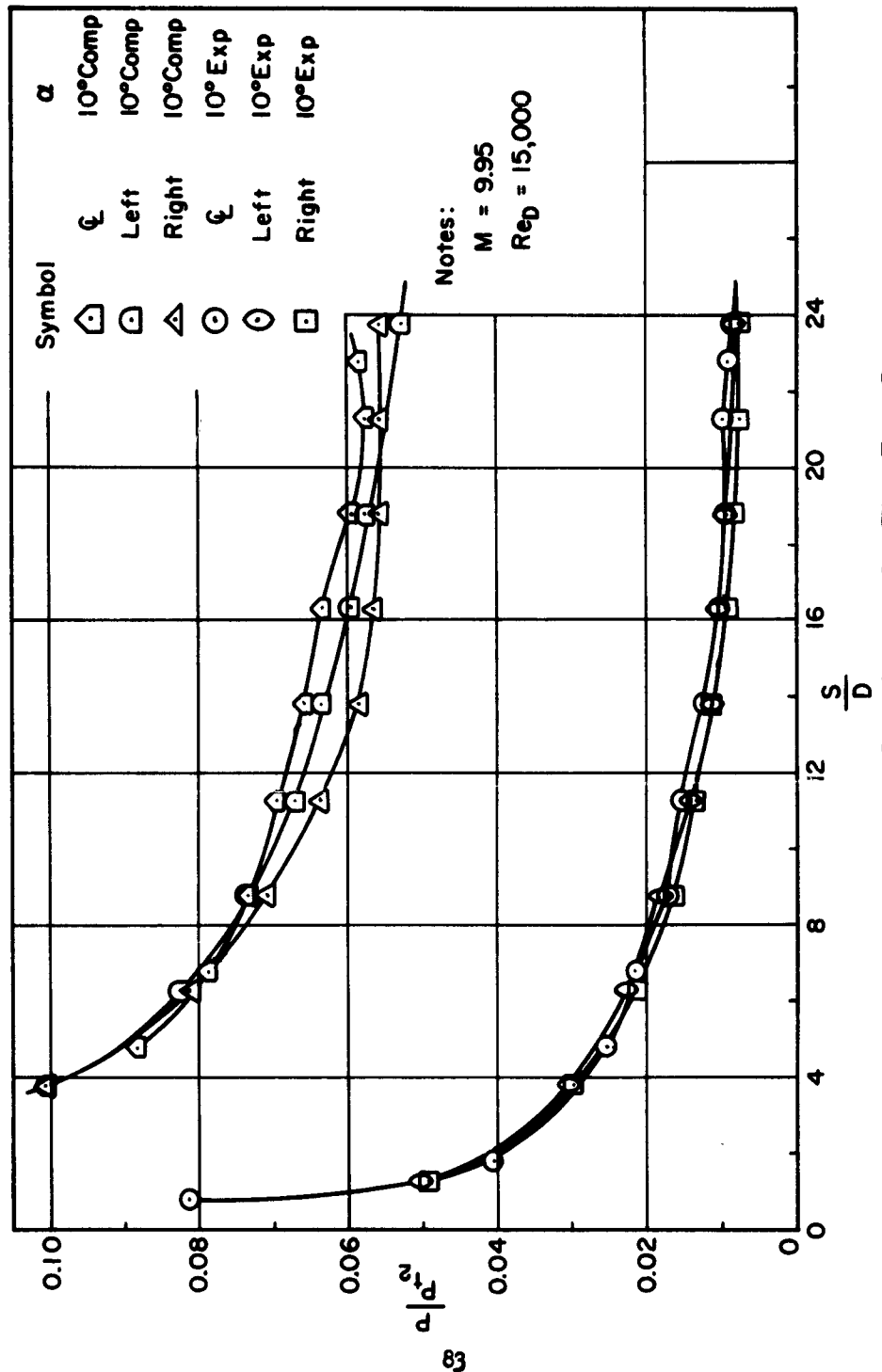


Figure 20 Spanwise Pressure Distribution On The Flat Plate

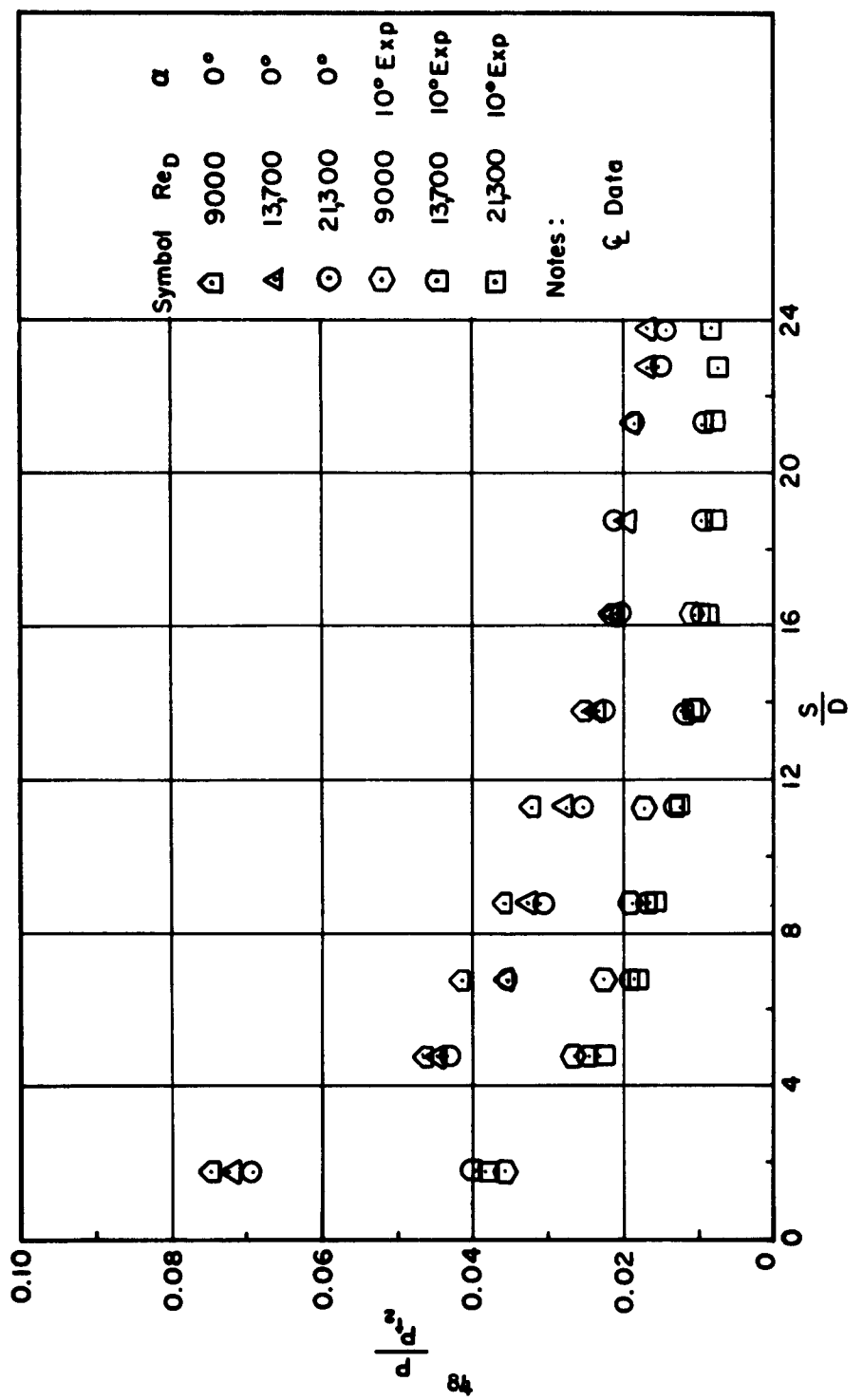


Figure 2| Effect Of Reynolds Number On Pressure Distribution

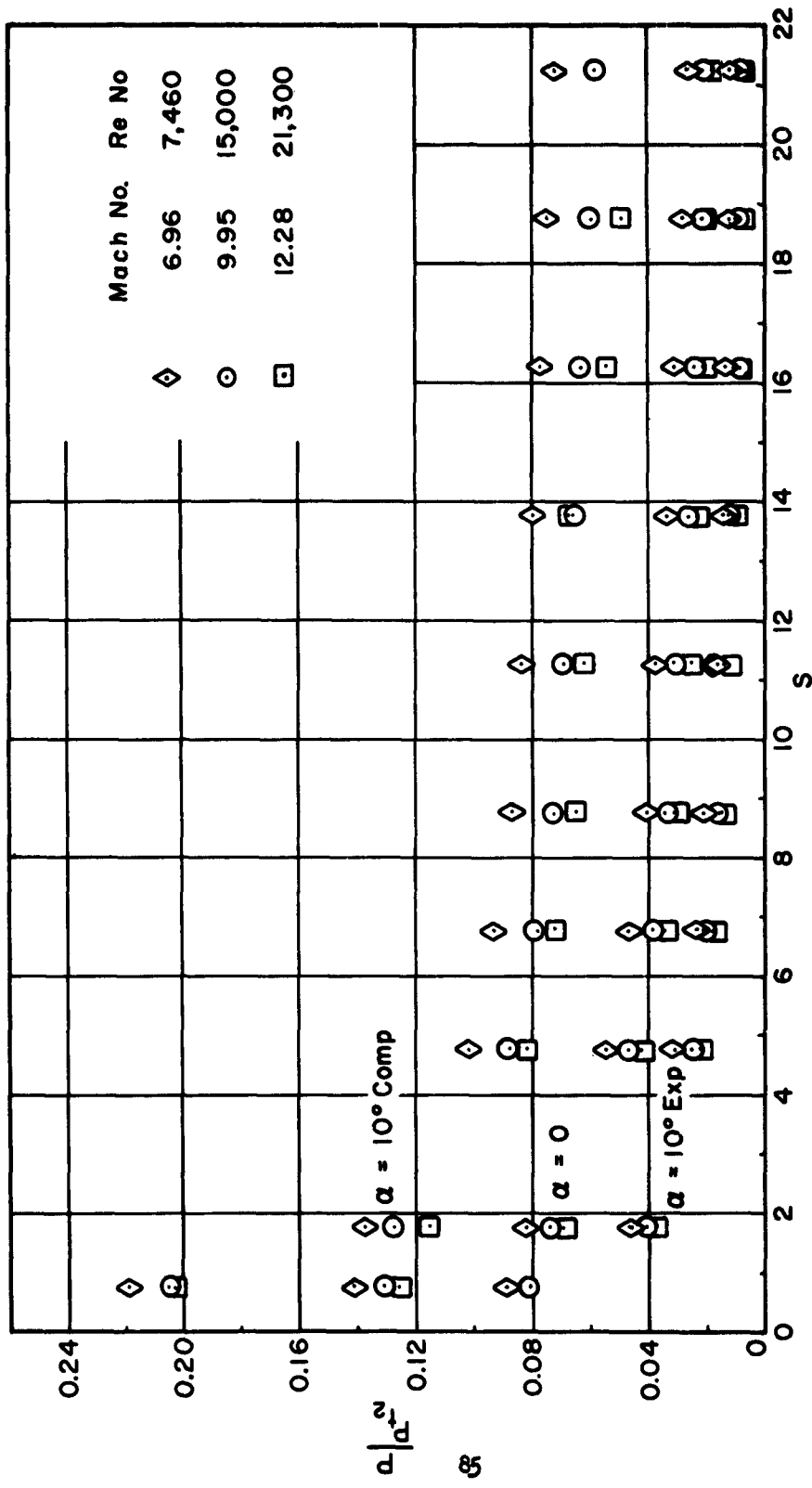


Figure 22 Effect Of Mach Number On Pressure Distributions For  $M = 7, 10, 12$

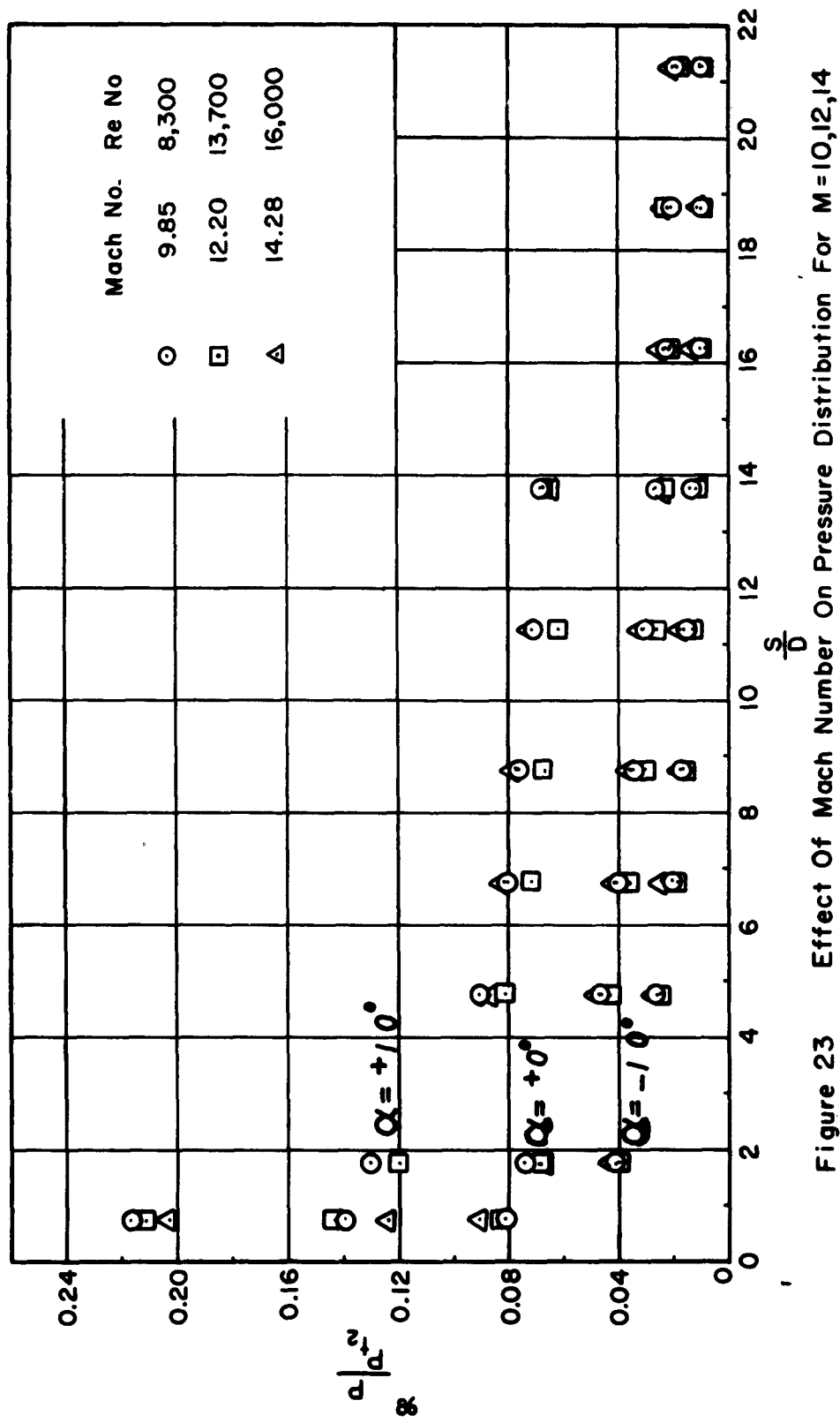


Figure 23 Effect Of Mach Number On Pressure Distribution For  $M=10,12,14$

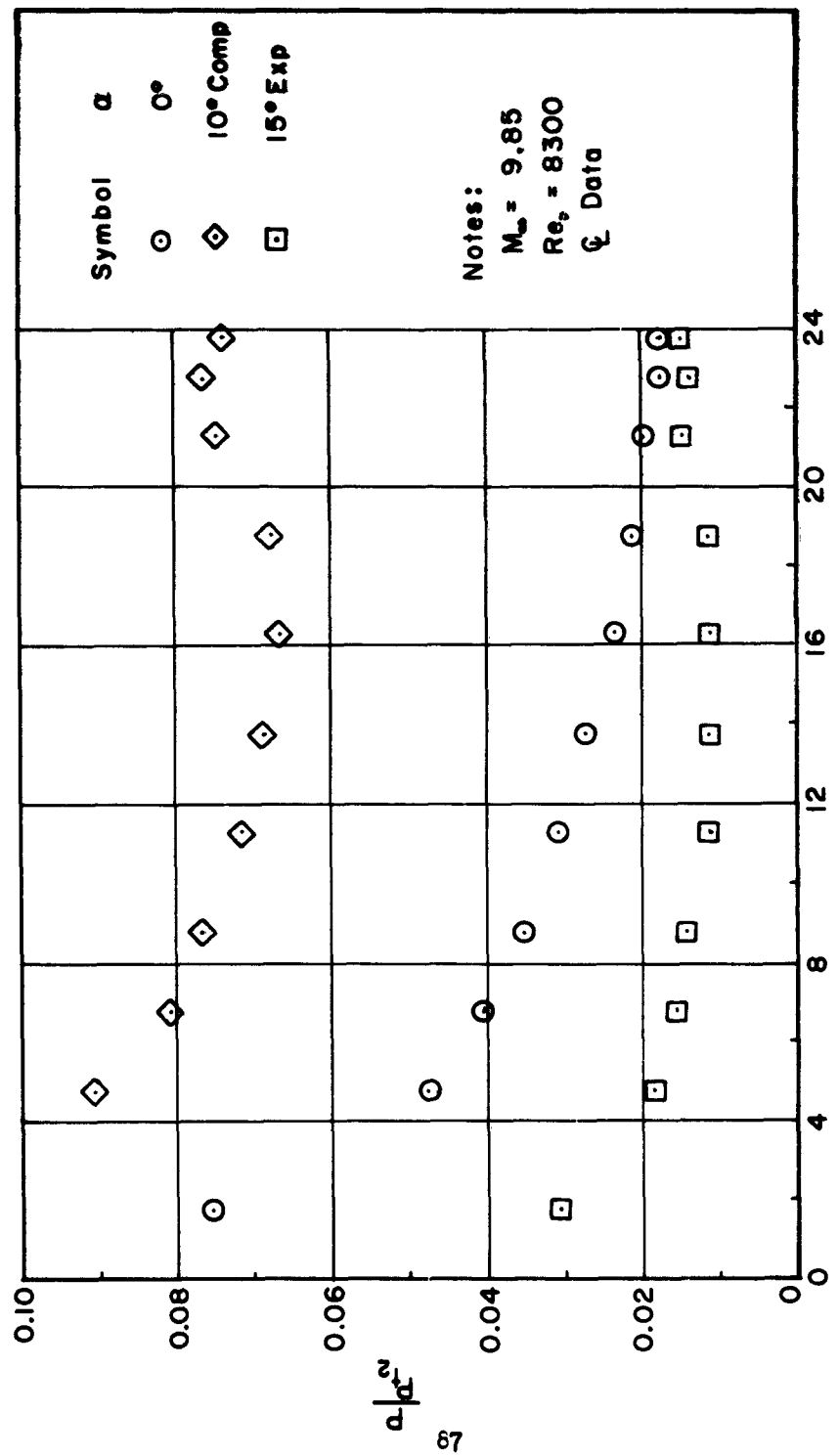


Figure 24 Tunnel Interference On Flat Plate Distribution

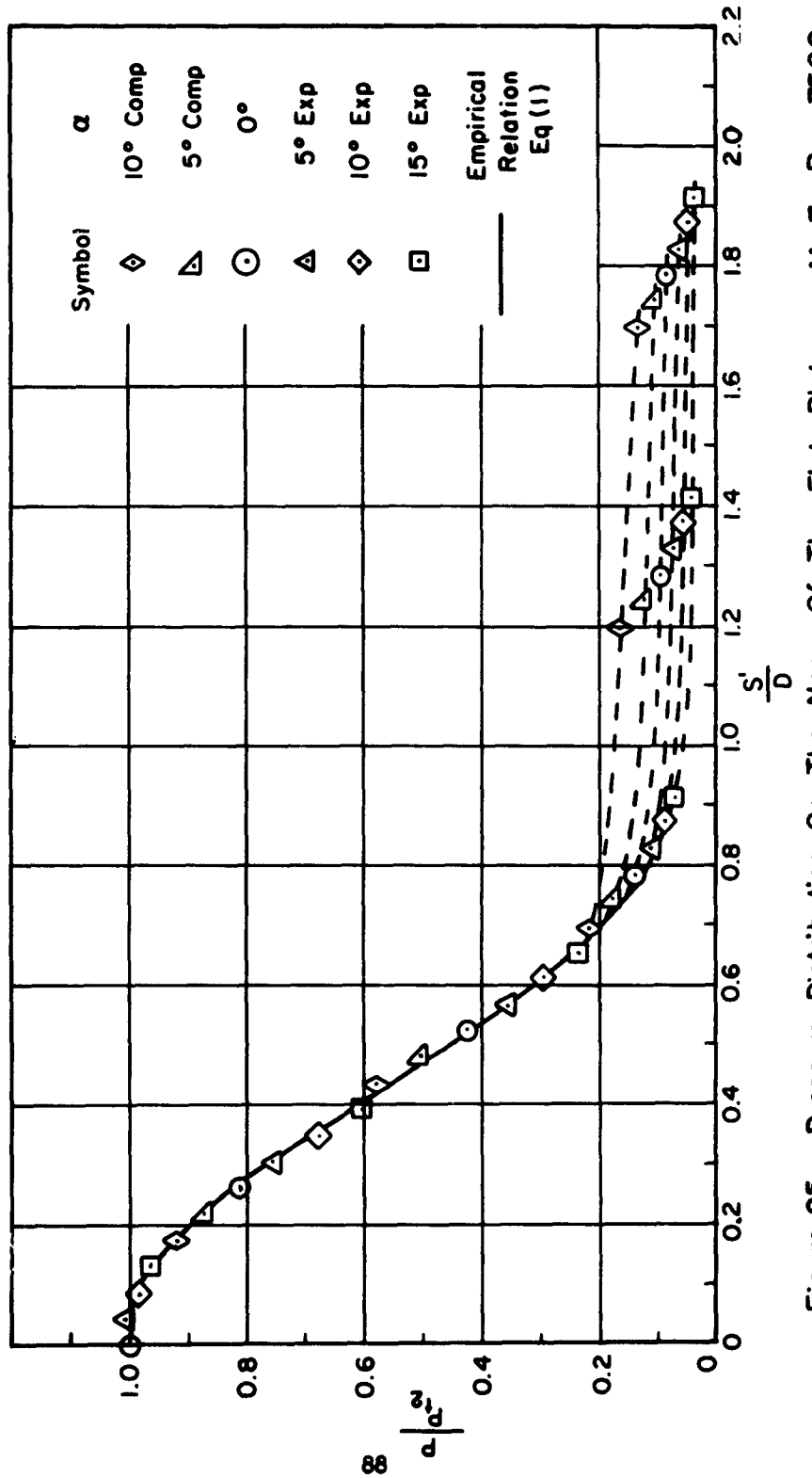


Figure 25 Pressure Distribution On The Nose Of The Flat Plate —  $M = 7$ ,  $Re_D = 7500$

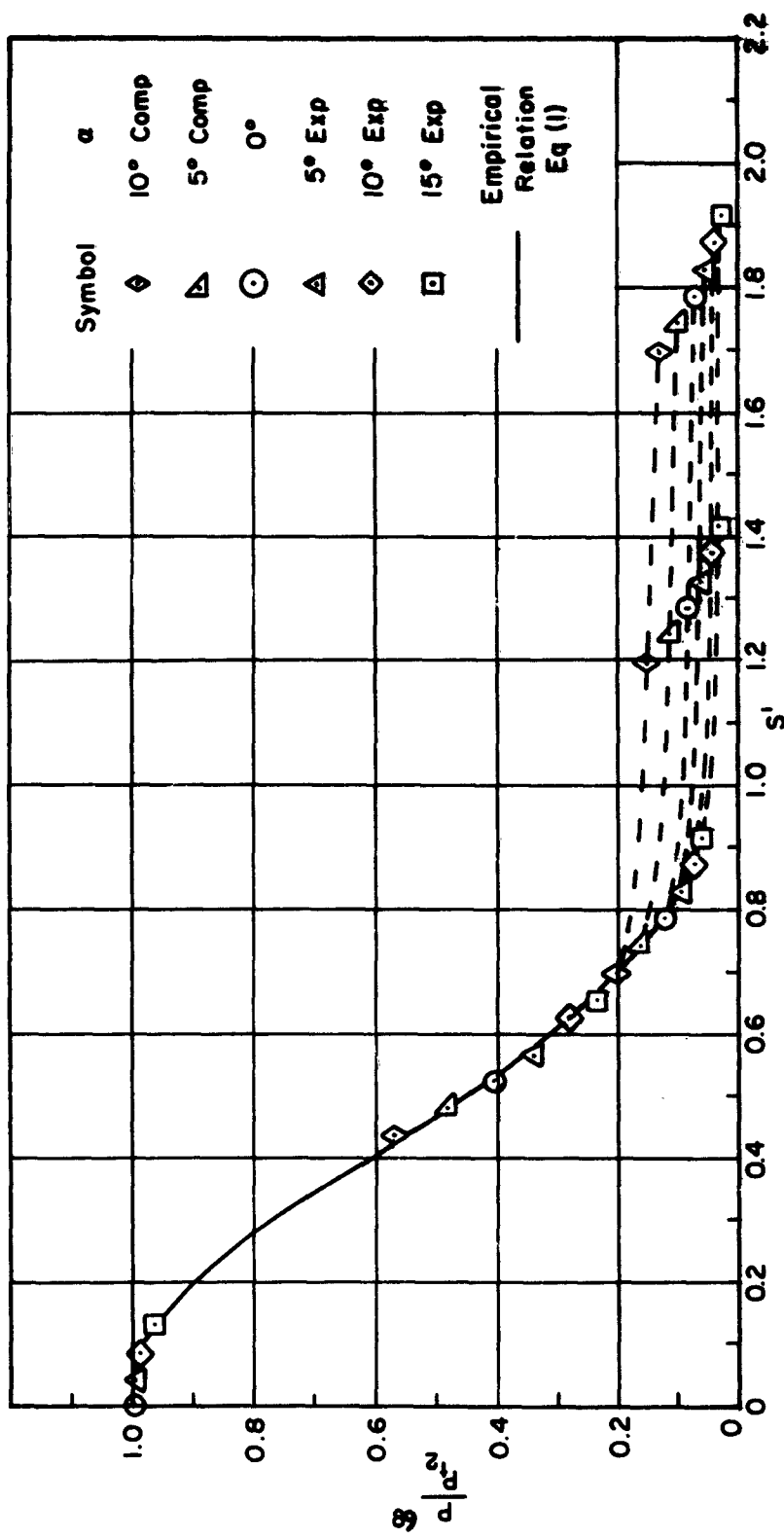


Figure 26 Pressure Distribution On The Nose Of The Flat Plate —  $M = 7$ ,  $Re_0 = 20,600$

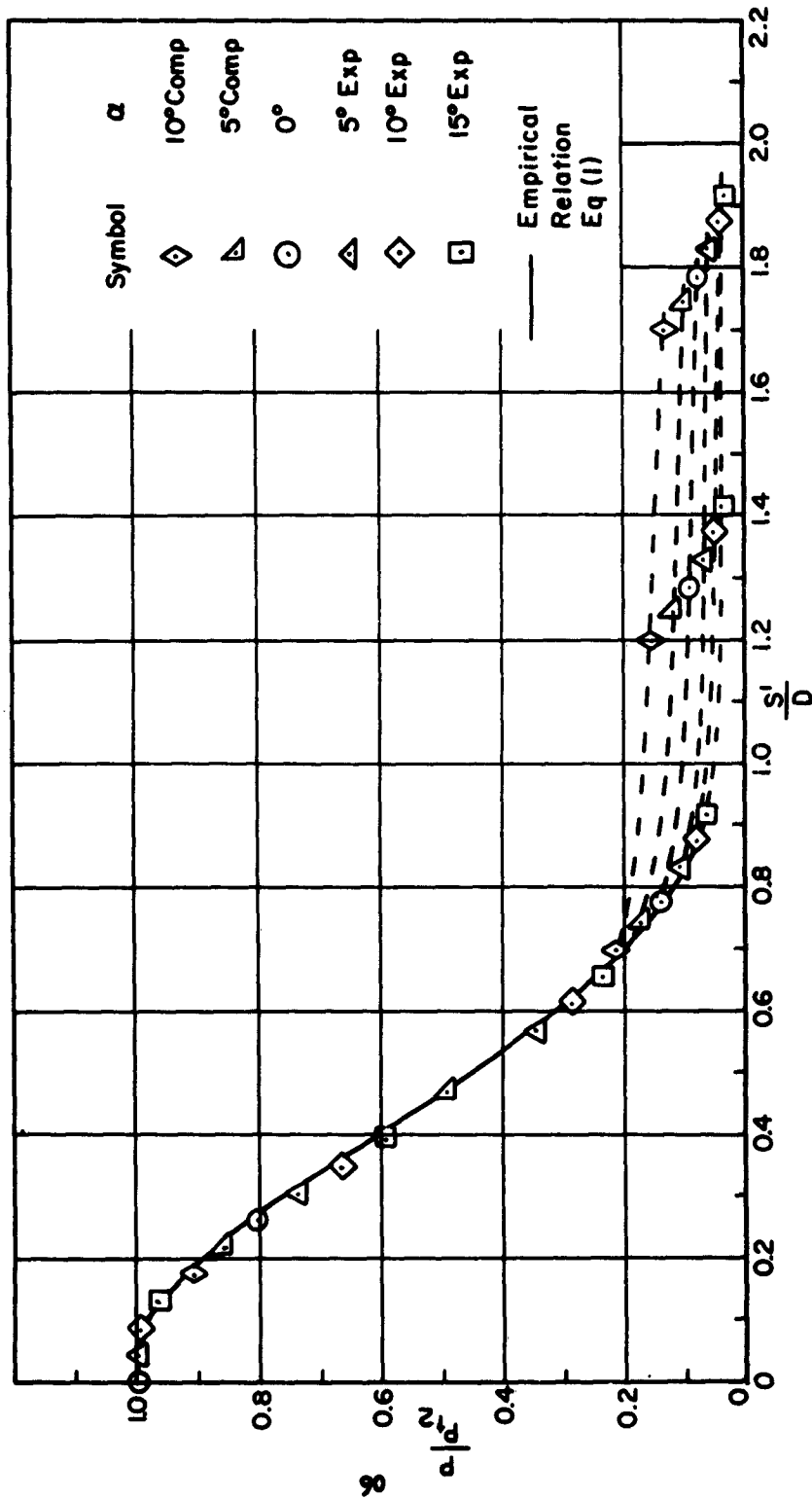


Figure 27 Pressure Distribution On The Nose Of The Flat Plate —  $M = 10$ ,  $Re = 8300$

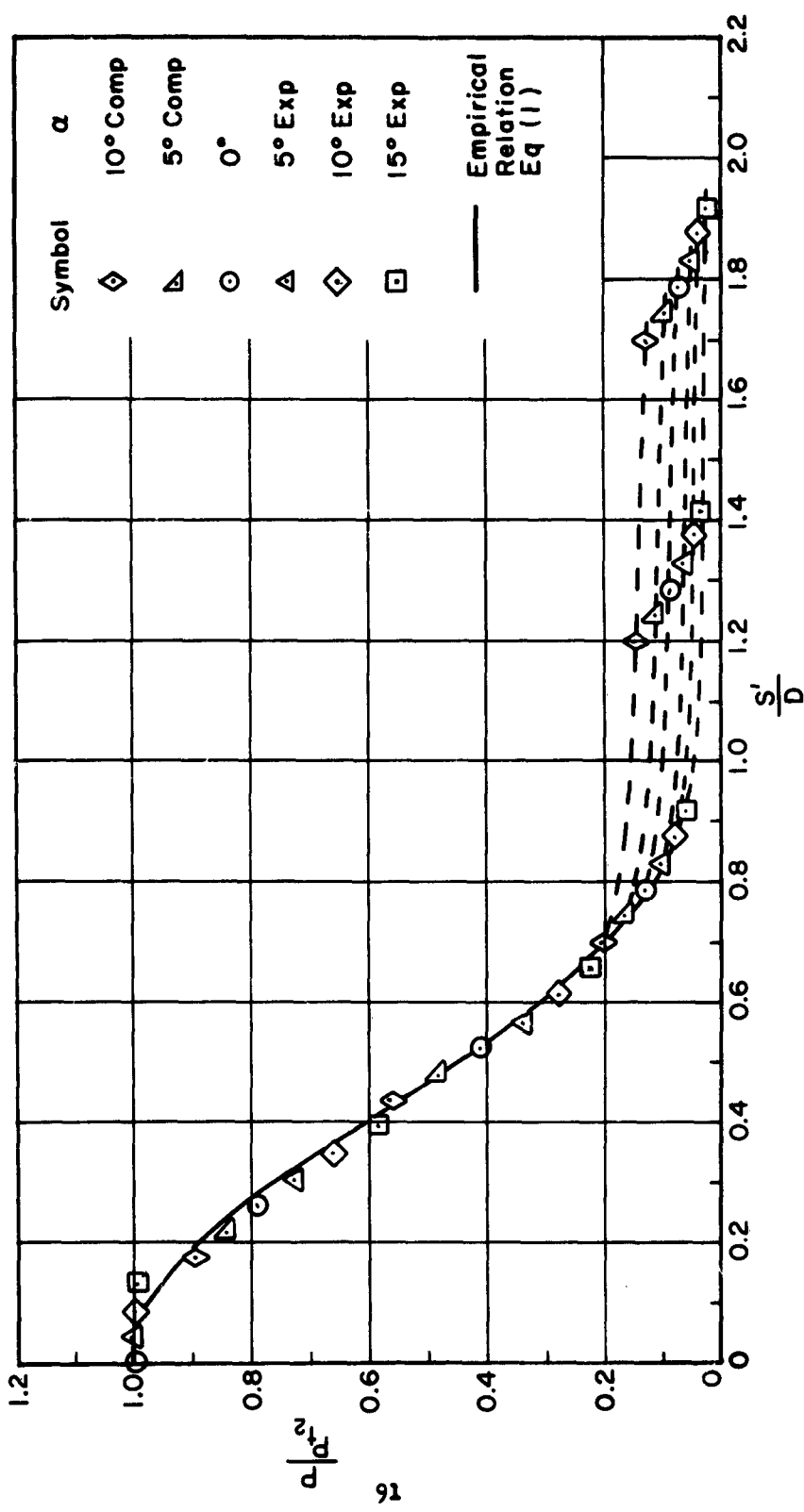


Figure 28 Pressure Distribution On The Nose Of The Flat Plate— $M = 10, Re_D = 15,000$

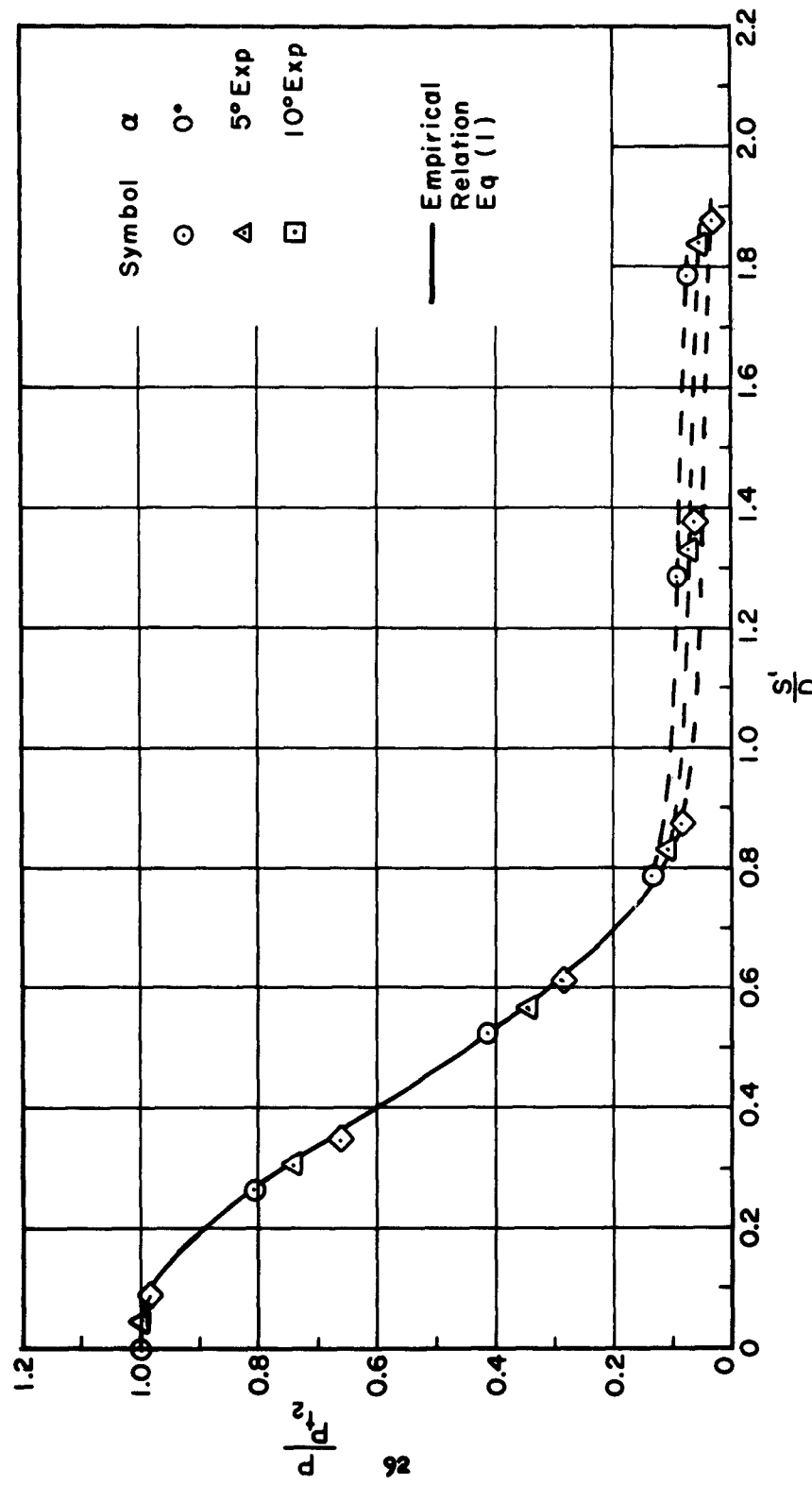


Figure 29 Pressure Distribution On The Nose Of The Flat Plate —  $M = 12$ ,  $Re_D = 9000$

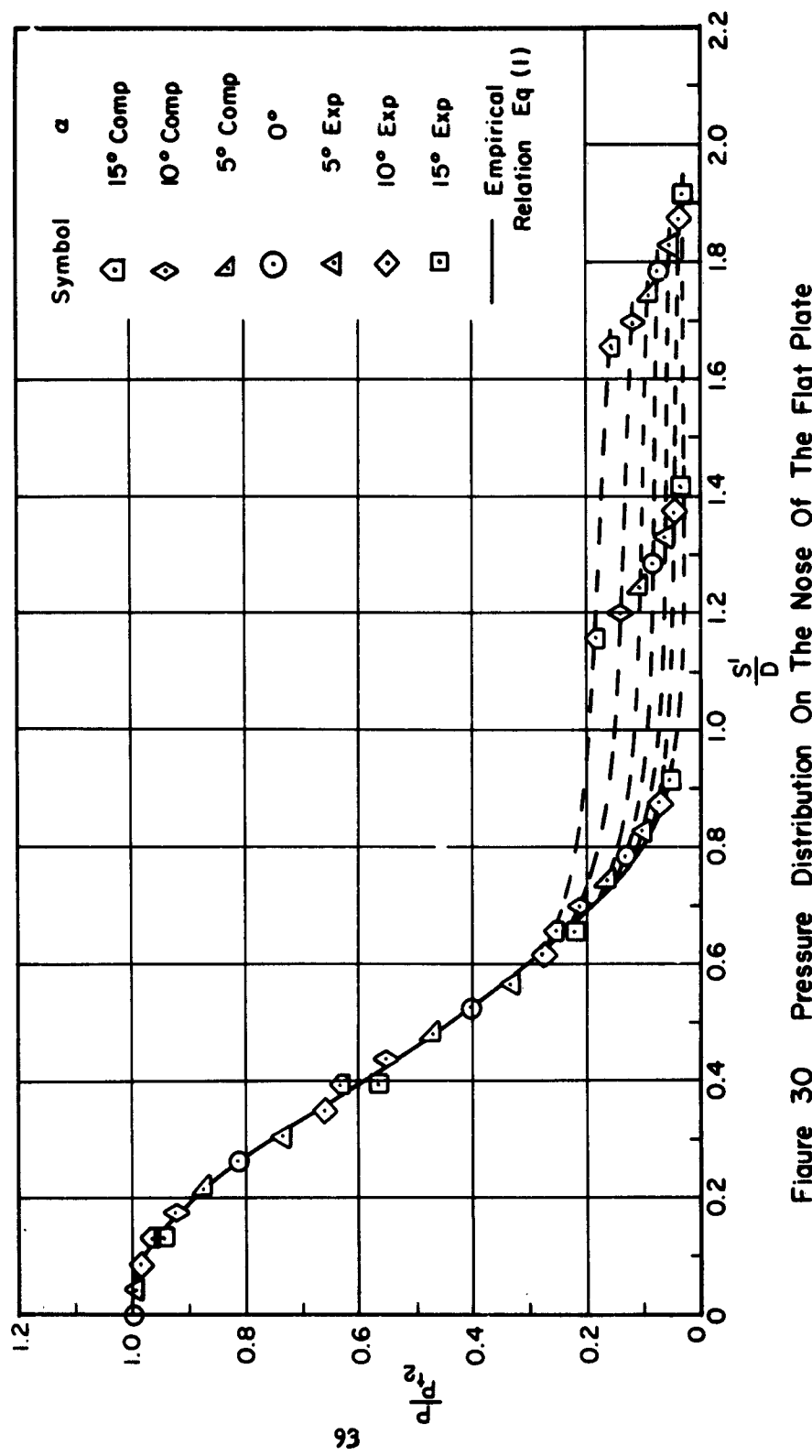


Figure 30 Pressure Distribution On The Nose Of The Flat Plate  
 $M = 12$ ,  $Re_D = 13,700$

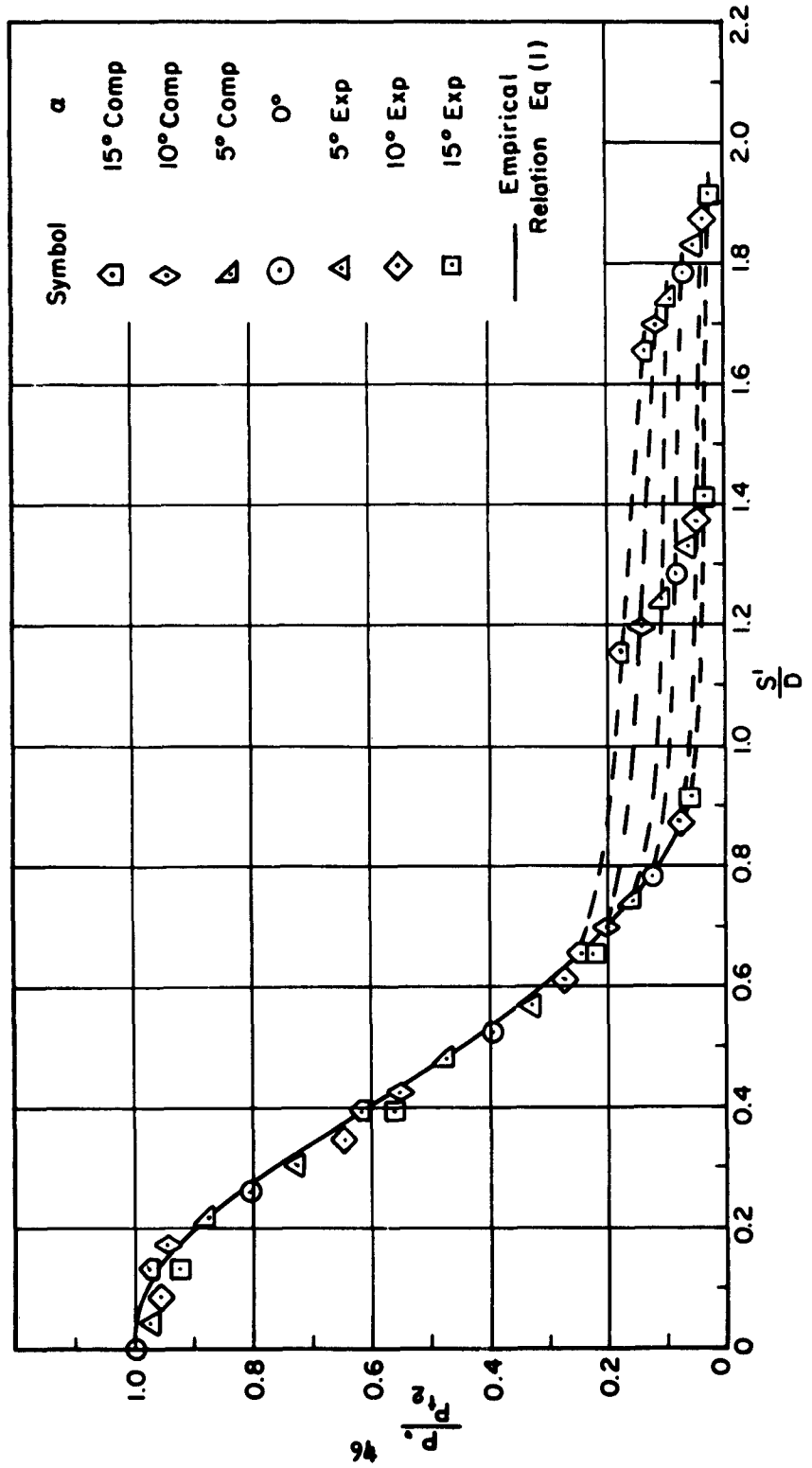


Figure 31 Pressure Distribution On The Nose Of The Flat Plate —  $M=12$ ,  $Re_0=21,300$

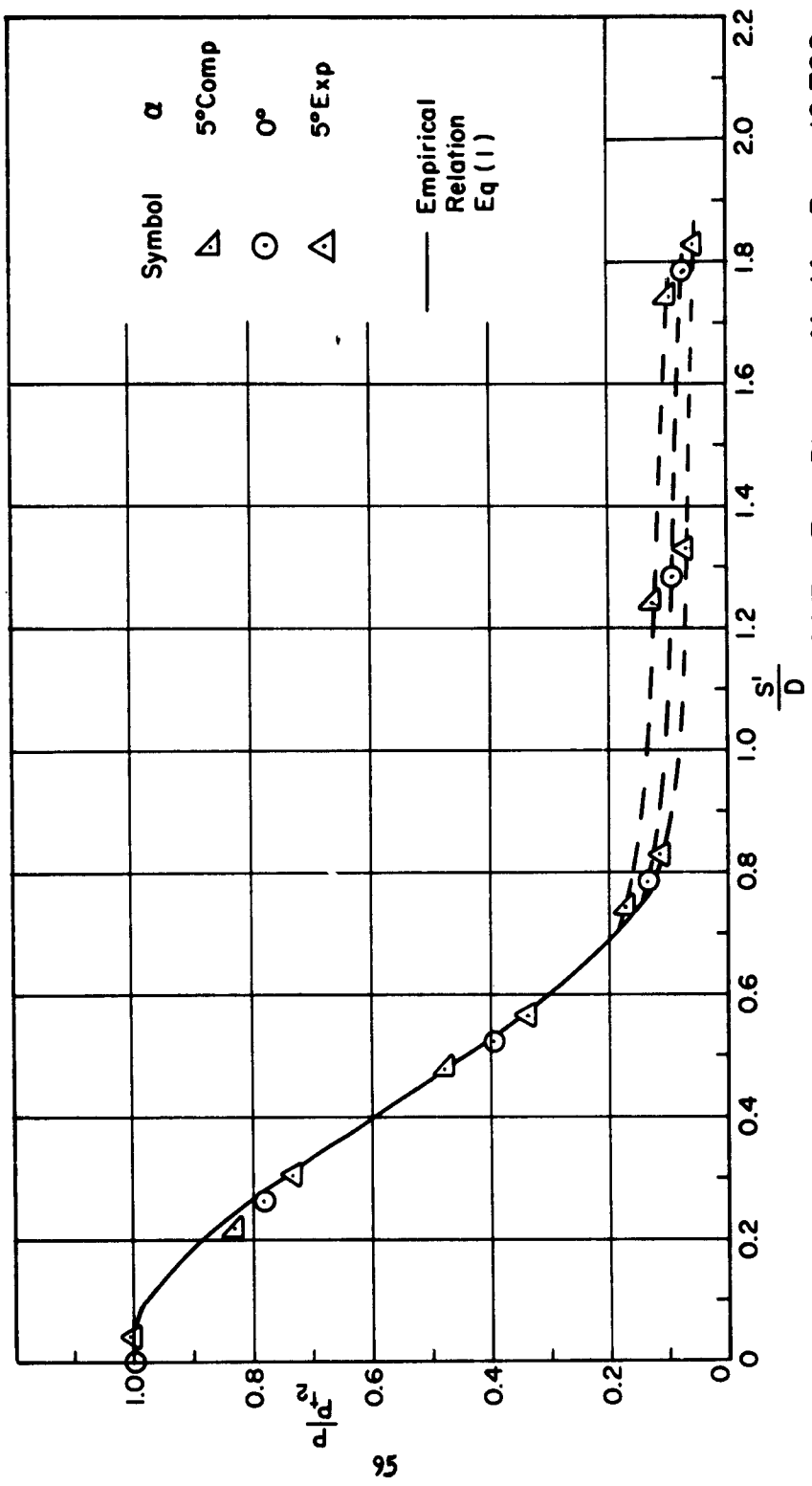


Figure 32 Pressure Distribution On The Nose Of The Flat Plate —  $M = 14$  ,  $Re_D = 12,700$

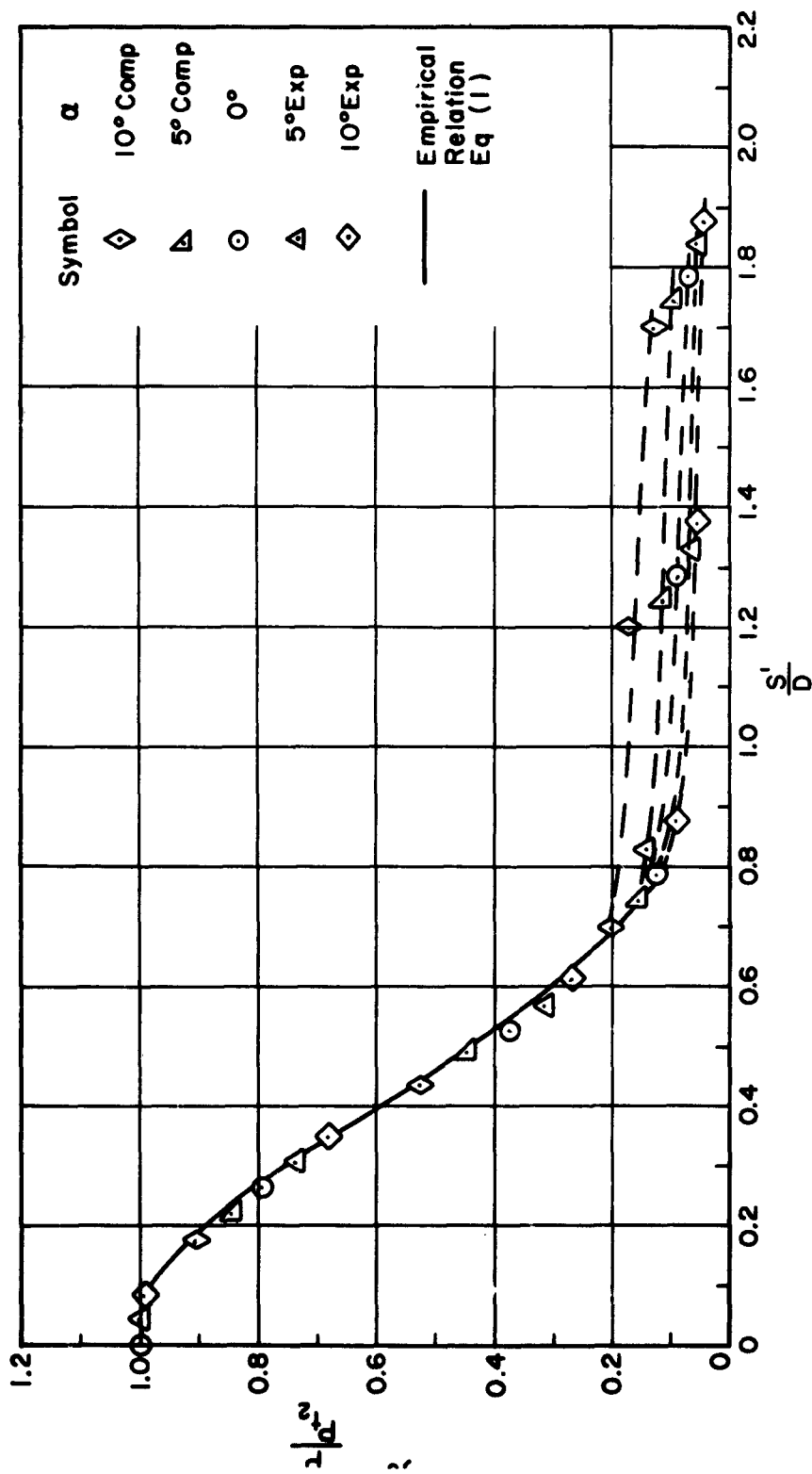


Figure 33 Pressure Distribution On The Nose Of The Flat Plate —  $M = 14$ ,  $Re_D = 16,000$

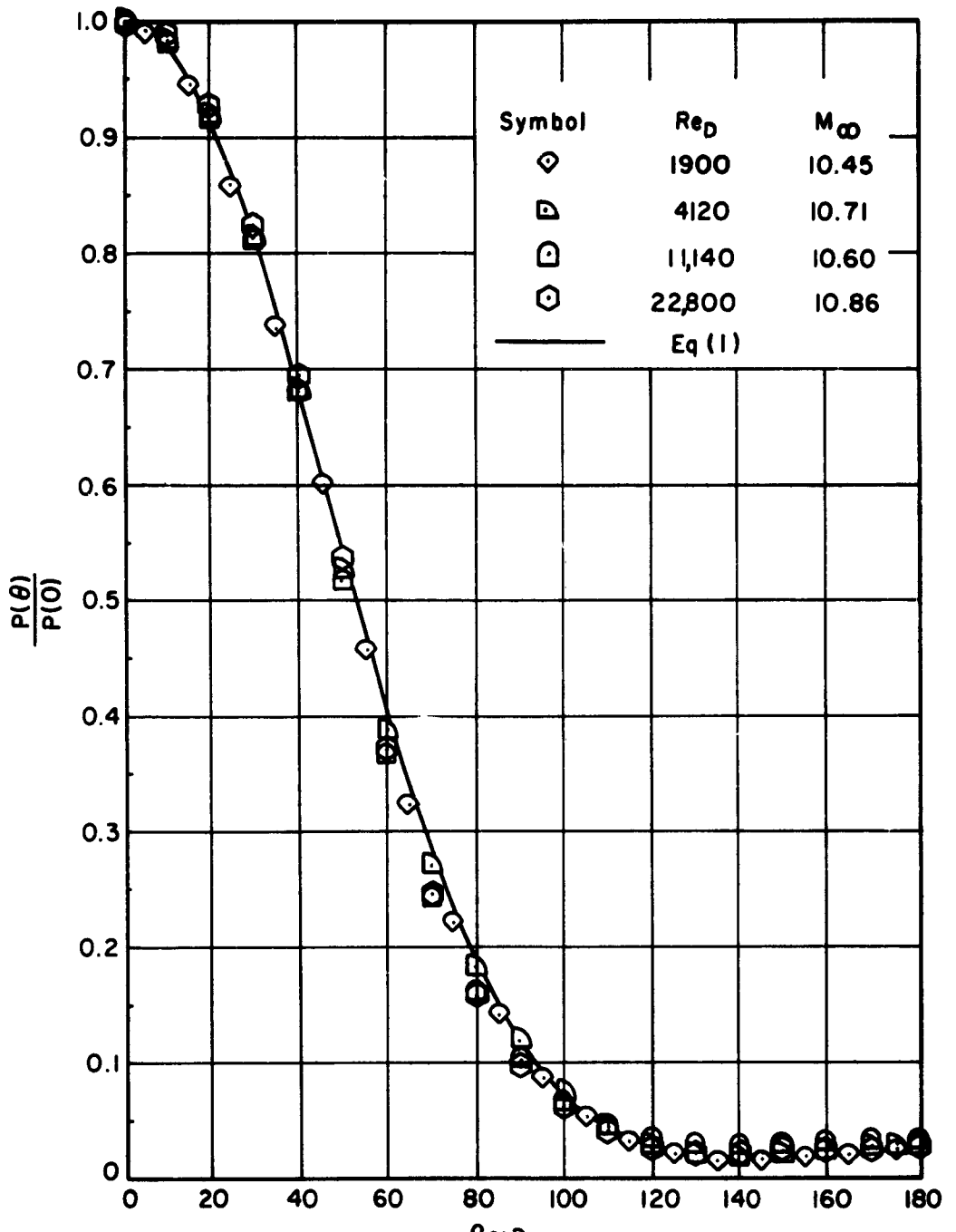


Figure 34 Pressure Distribution About Cylinder  
 $M=10$

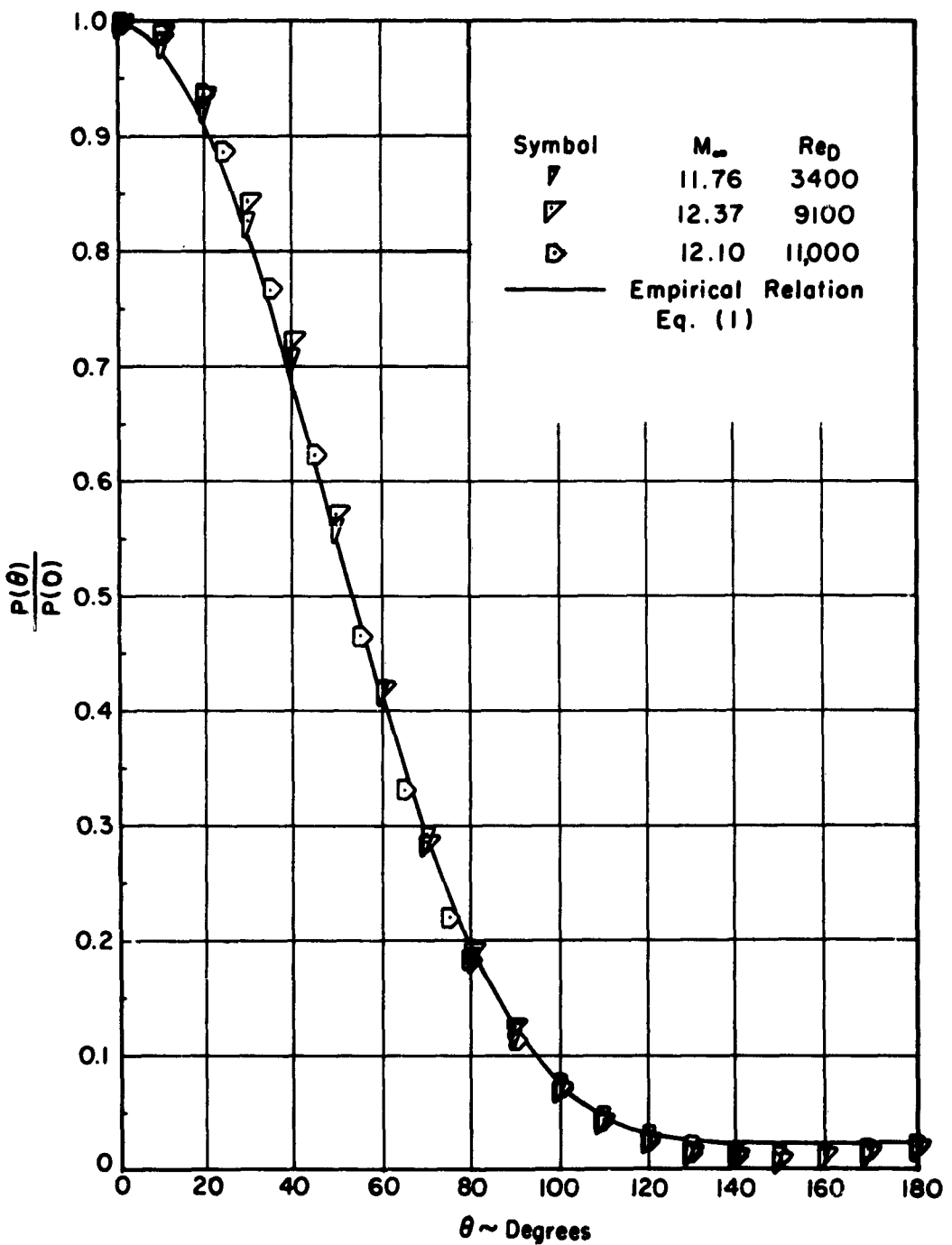


Figure 35 Pressure Distribution About Cylinder —  $M = 12$

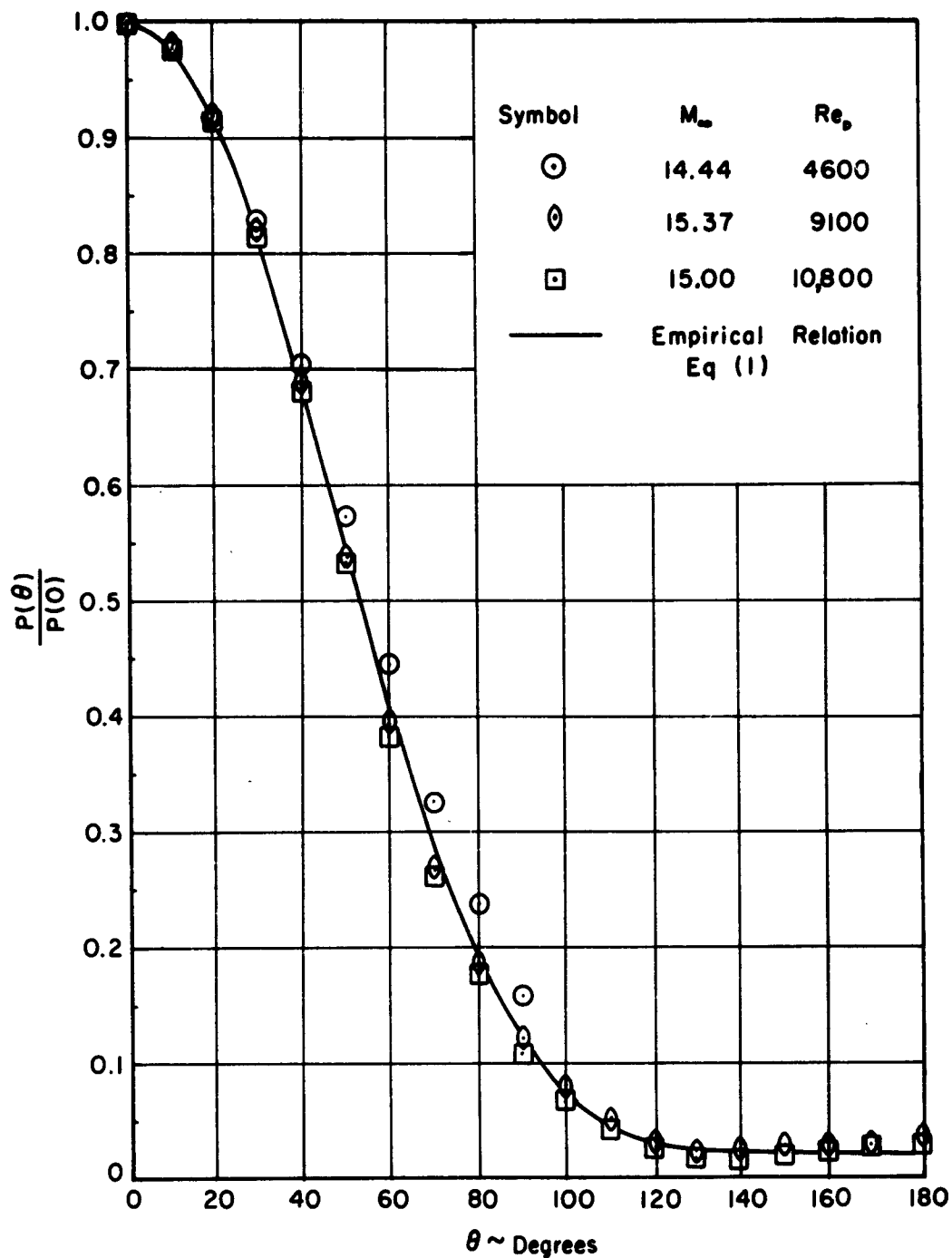


Figure 36 Pressure Distribution About Cylinder  
 $M = 15$

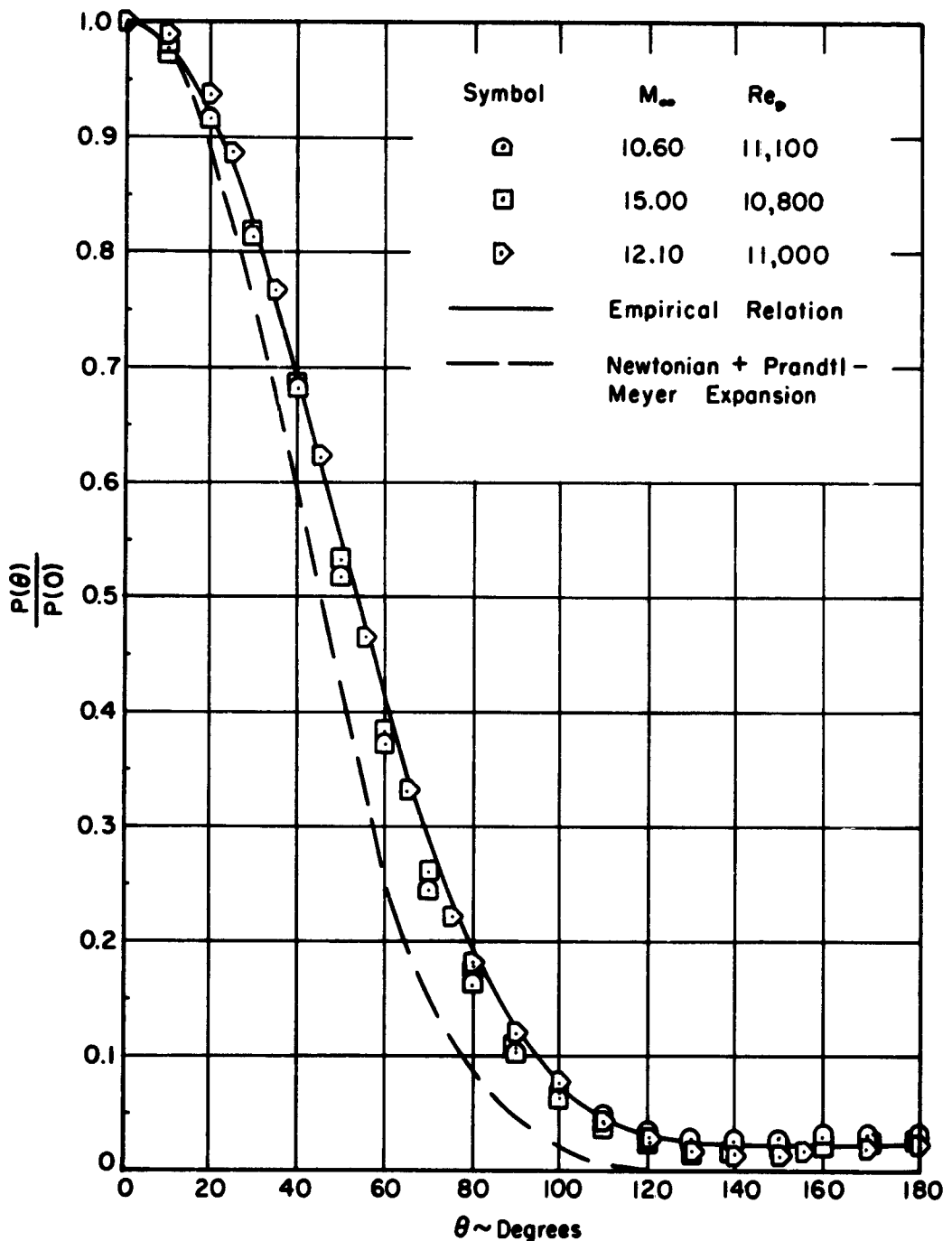


Figure 37 Effect Of Mach Number On Pressure Distribution About Cylinder —  $Re_\theta = 11,000$

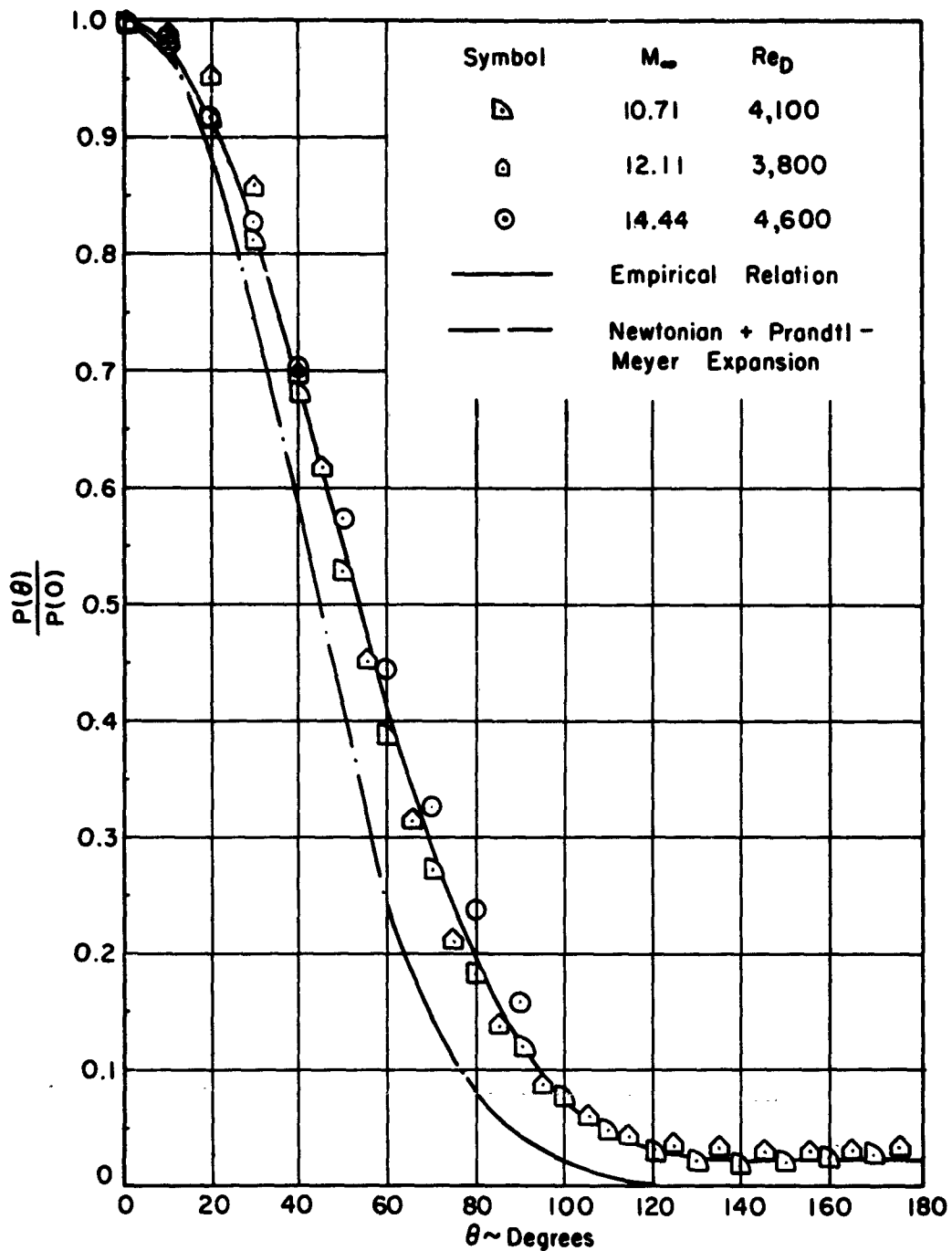


Figure 38 Effect Of Mach Number On Pressure Distribution About A Cylinder,  $Re_D = 4000$

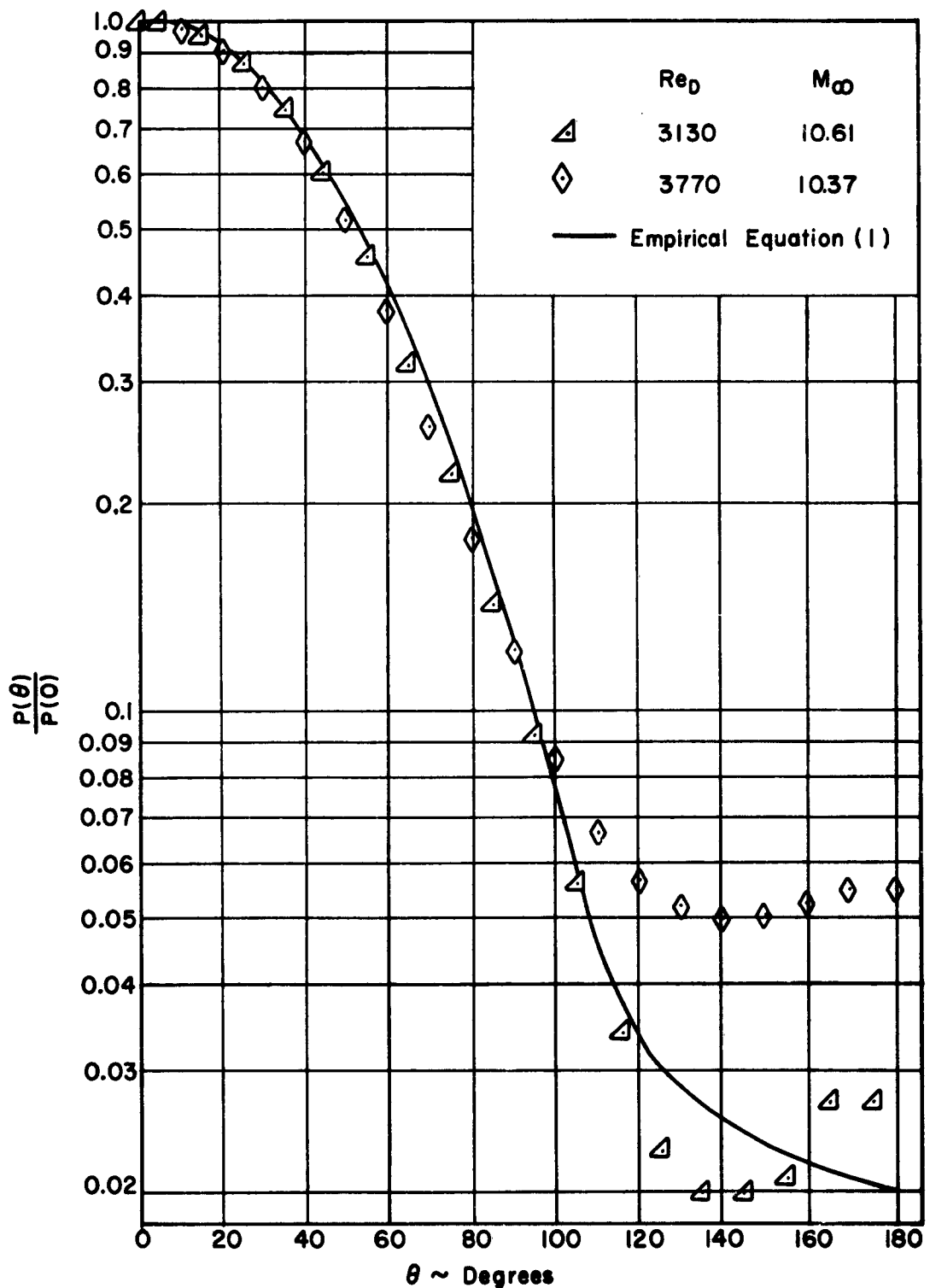


Figure 39 Tunnel Interference On Cylinder Distributions

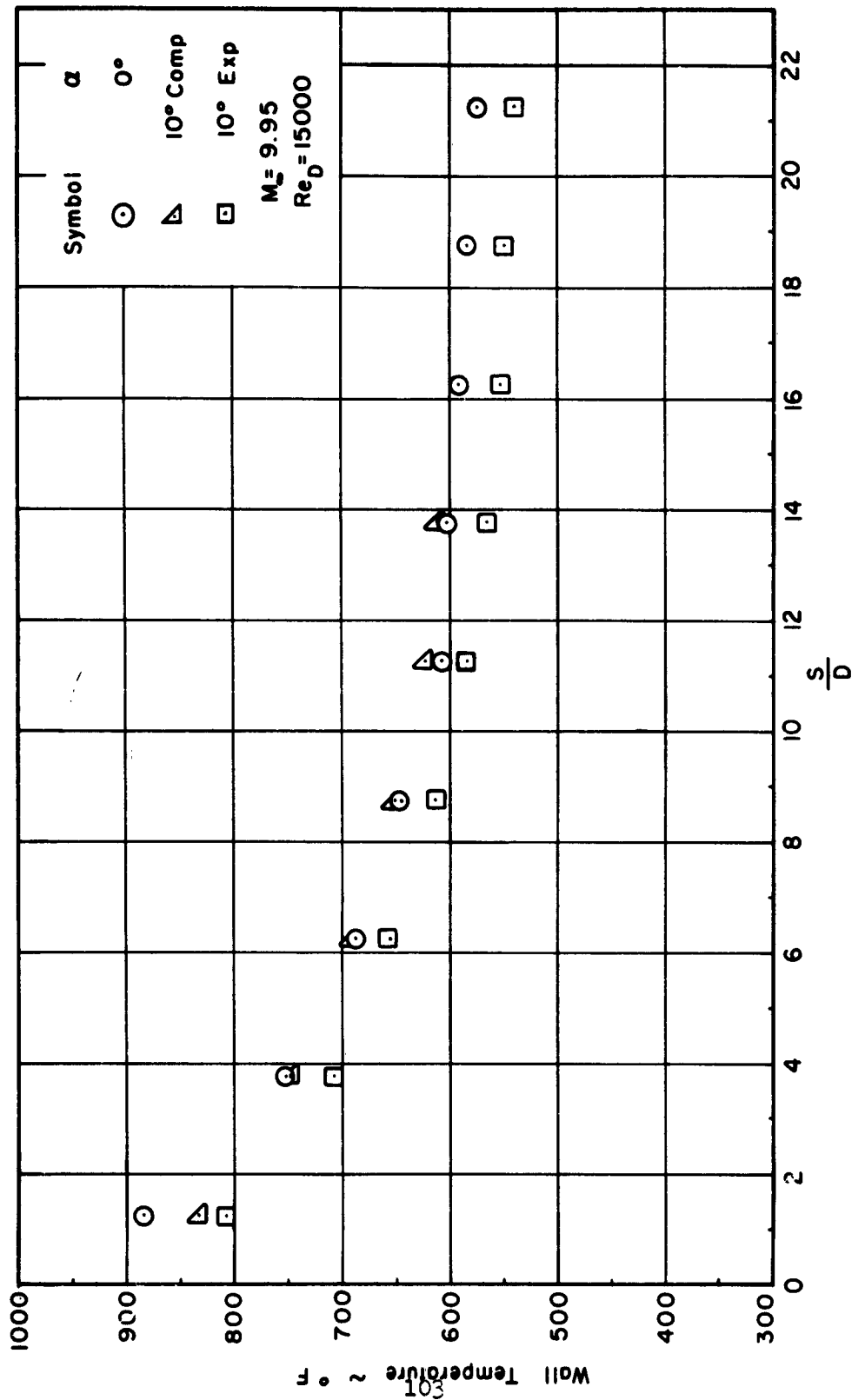


Figure 40 Typical Temperature Distribution On The Flat Plate

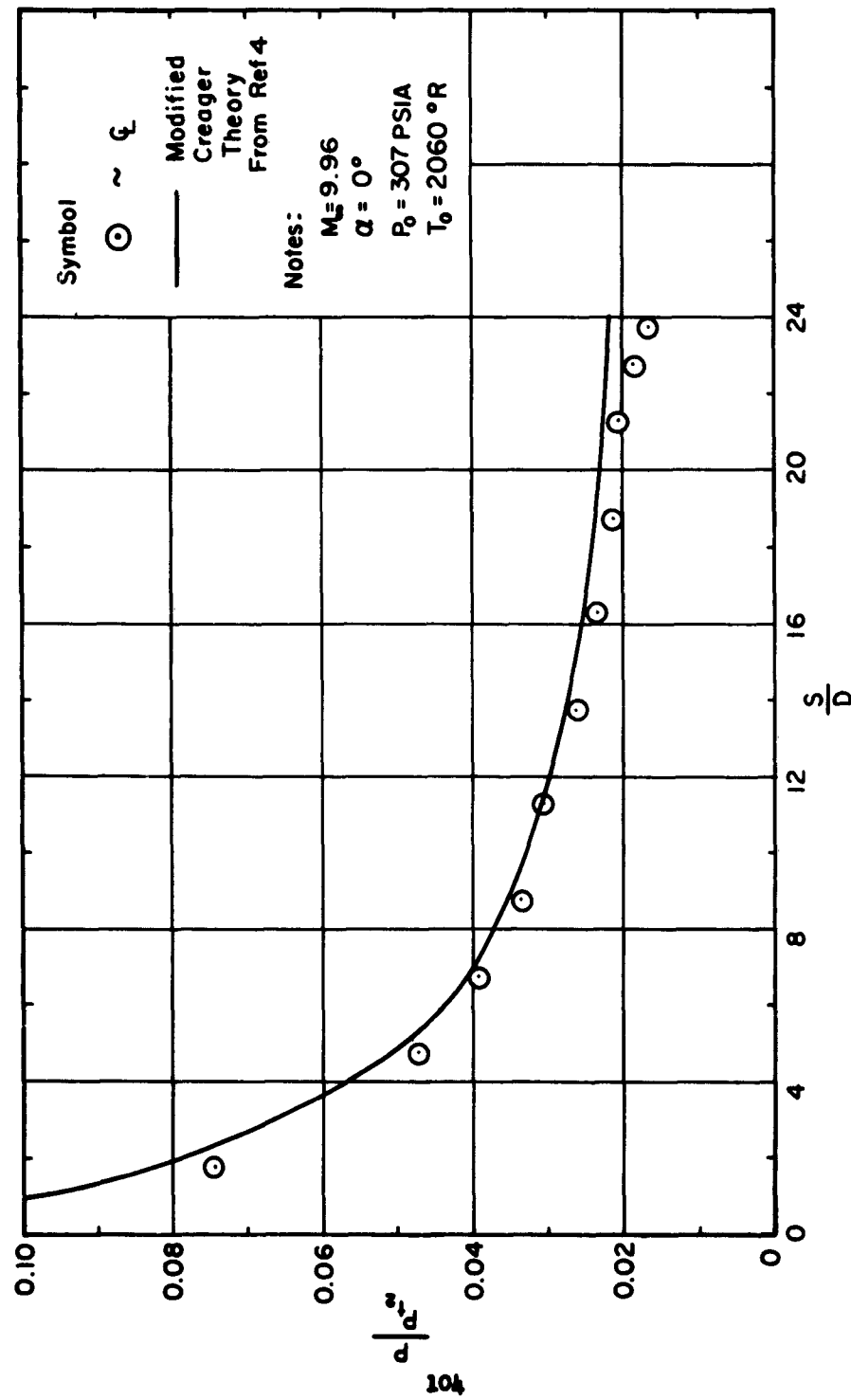


Figure 4 | Comparison Of Modified Creager Theory With Experiment

1. Boundary layer  
 2. Hypersonic flow  
 3. Laminar boundary layer  
 4. Compressible flow  
 5. Hypersonic wind tunnels

I. AEDC Project 1366,  
 Task 13666  
 II. Contract AF 33(616)-7827

III. Ohio State University,  
 Columbus, Ohio

IV. G. M. Gregorek, T. C.  
 Hart, J. D. Lee

V. Avail fr ORS  
 VI. In ASTIA collection

N = 7	7500	$\leq$	Reynolds	$\leq$	20,600	Angle-of-attack $15^\circ \leq \alpha \leq -15^\circ$
N = 10	8500	$\leq$	Reynolds	$\leq$	15,000	
N = 12	9000	$\leq$	Reynolds	$\leq$	21,300	
N = 14	12700	$\leq$	Reynolds	$\leq$	16,000	

Pressures were measured over the surface of an un-swept blunt flat plate having a cylindrical leading edge 1/2-inch in diameter under the following conditions:

I over )

Pressures were measured over the surface of an un-swept blunt flat plate having a cylindrical leading edge 1/2-inch in diameter under the following conditions:

I. Boundary layer  
 2. Hypersonic flow  
 3. Laminar boundary layer  
 4. Compressible flow  
 5. Hypersonic wind tunnels

I. AEDC Project 1366, Final report, Mar 63 10sp. incl illus., tables, 5 refs.

II. Contract AF 33(616)-7827

III. Ohio State University, Columbus, Ohio

IV. G. M. Gregorek, T. C. Hart, J. D. Lee

V. Avail fr ORS

VI. In ASTIA collection

N = 7	7500	$\leq$	Reynolds	$\leq$	20,600	Angle-of-attack $15^\circ \leq \alpha \leq -15^\circ$
N = 10	8500	$\leq$	Reynolds	$\leq$	15,000	
N = 12	9000	$\leq$	Reynolds	$\leq$	21,300	
N = 14	12700	$\leq$	Reynolds	$\leq$	16,000	

Unclassified Report

Pressures were measured over the surface of an un-swept blunt flat plate having a cylindrical leading edge 1/2-inch in diameter under the following conditions:

I. Boundary layer  
 2. Hypersonic flow  
 3. Laminar boundary layer  
 4. Compressible flow  
 5. Hypersonic wind tunnels

I. AEDC Project 1366, Final report, Mar 63 10sp. incl illus., tables, 5 refs.

II. Contract AF 33(616)-7827

III. Ohio State University, Columbus, Ohio

IV. G. M. Gregorek, T. C. Hart, J. D. Lee

V. Avail fr ORS

VI. In ASTIA collection

N = 7	7500	$\leq$	Reynolds	$\leq$	20,600	Angle-of-attack $15^\circ \leq \alpha \leq -15^\circ$
N = 10	8500	$\leq$	Reynolds	$\leq$	15,000	
N = 12	9000	$\leq$	Reynolds	$\leq$	21,300	
N = 14	12700	$\leq$	Reynolds	$\leq$	16,000	

Unclassified Report

The flat plate was side-mounted in the AEDC 12-inch continuous hypersonic wind tunnel. Separate tests were conducted with cylinders in order to obtain detailed data for the leading-edge. Stagnation temperatures were sufficiently high to eliminate condensation effects. The leading-edge and cylinder pressure ratios were noted to be independent of both Mach number and Reynolds number. The flat plate pressure ratios show a small dependence on Mach number. Reynolds number effects on the plate pressure ratios were small except at the lower levels of Reynolds number where the interaction of the thickened boundary layer caused increases in pressure. Boundary layer profiles, obtained during the same program, are reported in Volume II of this report.

The flat plate was side-mounted in the AEDC 12-inch continuous hypersonic wind tunnel. Separate tests were conducted with cylinders in order to obtain detailed data for the leading-edge. Stagnation temperatures were sufficiently high to eliminate condensation effects. The leading-edge and cylinder pressure ratios were noted to be independent of both Mach number and Reynolds number. The flat plate pressure ratios show a small dependence on Mach number. Reynolds number effects on the plate pressure ratios were small except at the lower levels of Reynolds number where the interaction of the thickened boundary layer caused increases in pressure. Boundary layer profiles, obtained during the same program, are reported in Volume II of this report.

( over )